BEHAVIOR AND MODELING OF CFRP RETROFITTED SANDSTONE BLOCK MASONRY WALLS

BY

AMR ABUBAKER BARAHIM

A Thesis Presented to the
DEANSHIP OF GRADUATE STUDIES

KING FAHD UNIVERSITY OF PETROLEUM & MINERALS

DHAHRAN, SAUDI ARABIA

In Partial Fulfillment of the
Requirements for the Degree of

MASTER OF SCIENCE

In

CIVIL ENGINEERING

FEBRAURY, 2015

KING FAHD UNIVERSITY OF PETROLEUM & MINERALS

DHAHRAN- 31261, SAUDI ARABIA

DEANSHIP OF GRADUATE STUDIES

This thesis, written by **AMR ABUBAKER BARAHIM** under the direction his thesis advisor and approved by his thesis committee, has been presented and accepted by the Dean of Graduate Studies, in partial fulfillment of the requirements for the degree of **MASTER OF SCIENCE IN CIVIL ENGINEERING**.

Dr. Mohammed H. Baluch
(Advisor)

Dr. Omar A. Al-Swailem
Department Chairman (A)

Dr. Muhammad K. Rahman
(Member)

Dr. Salam A. Zummo
Dean of Graduate Studies

Dr. Ali H. Al-Gadhib
(Member)

30/6/15

Date

DEDICATED TO

ADEN & THEIR PEOPLE

AND

MY BELOVED PARENTS

AND

MY BROTHERS & SISTER

AND

MY LOVELY WIFE

ACKNOWLEDGMENTS

First of all I thank Allah, the Sustainer, the Opener, the Knower of all for giving me strength, patience and knowledge to complete this work.

The Prophet, peace and blessings be upon him, said, “He has not thanked Allah who has not thanked people.” In this regard, I would like to express my deepest gratitude to Dr. Mohammed Baluch my supervisor for his continuous guidance, valuable support and motivated encouragement. Actually, his wisdom and passion about research inspired me and improve my skills as a junior researcher. Also, I am deeply grateful to my committee member, Dr. Mohammad K. Rahman, for his continuous support, and personal involvement in all phases of this research. I am also grateful to my other committee member, Dr. Ali Al-Gadhib, for their constructive guidance, valuable advice and cooperation.

I would like to offer my acknowledgement to Dr. basheer Algohi who helped and trained me in preparing the experimental set-up and doing the FEM using ABAQUS. In fact, the first step on my research has been climbed under his guidance. Also, I would like to offer my deepest thanks to my brothers Khaled Muneef and Abdullah Basaleh who gave me a tremendous help and support in preparing the experimental set-up. It’s my pleasure and honor to share these unforgettable memories with you.

Also, I would like to express my sincere gratitude to technical staff of the structural laboratory for their patience and cooperation in all phases of the experimental work. Great thanks to Eng. Omer, Eng. Imran, Eng. Mukkaram and Eng. Najamuddin. It was my privilege to work with you all.

This research was financially funded by the Deanship of Scientific Research (DSR) of King Fahd of Petroleum and Minerals which is gratefully acknowledged. Also, great thanks are due to ULTIMATE SOLUTIONS for their cooperation and technical support regarding ABAQUS software.

I would like send my appreciation and gratitude to Hadhramout Establishment for Human Development (HEHD) for giving me the scholarship, especially to Eng. Abdullah Bugshan who always standing by my side and supporting me during my Master Program from the beginning until the end and in the future inshallah.

To Dr. Mohammed Al-Osta, Dr. Ibraheem Hakeem and Dr. Abdul Samee Halahla, who helped me during all phases of my research, thank for your valuable support. Also, thanks are due to my colleagues at the University for spending great times and sharing unforgettable memories during my graduate studies.

Lastly, I would like to express my love and appreciation to my mother, father, sister, brothers, wife and all family members for their valuable prayers and motivated encouragement throughout my master program.

TABLE OF CONTENTS

LIST OF TABLES

LIST OF FIGURES

LIST OF ABBREVIATIONS

URM	:	Unreinforced Masonry
CFRP	:	Carbon Fiber Reinforced Polymer
FEM	:	Finite Element Modeling
UNESCO	:	United Nations Educational, Scientific and Cultural Organization
USGS	:	United States Geological Survey
CATDAT	:	Damaging Earthquakes Database
FRP	:	Fiber Reinforced Polymer
CMU	:	Concrete Masonry Unit
ASTM	:	American Society for Testing and Materials
DMC	:	Dry Mortar Company
EN	:	European Standard
LVDT	:	Linear Variable Differential Transformer
CDP	:	Concrete Damage Plasticity
HPC	:	High Performance Computing
ITC	:	Information Technology Center

LIST OF SYMBOLS

(w/m)	:	Water to mortar ratio
U1	:	Displacement in X-direction
U2	:	Displacement in Y-direction
U3	:	Displacement in Z-direction
ψ	:	Dilation Angle in Degree
ε	:	Eccentricity
f_{b0}/f_{c0}	:	Biaxial compressive stress to uniaxial compressive stress
K	:	Ratio of the second stress invariant on the tensile meridian

ABSTRACT

Full Name : [Amr Abubaker Mohammed Barahim]

Thesis Title : [BEHAVIOR AND MODELING OF CFRP RETROFITTED SANDSTONE BLOCK MASONRY WALLS]

Major Field : [CIVIL & ENVIRONMENTAL ENGINEERING]

Date of Degree : [Febraury-2015]

Stone block wall is considered as the oldest building construction member that has lasted until today, being built all over the world, mostly in remarkable heritage regions as a trace of what our ancestors had achieved in the ancient history. In fact, the majority of existing historical buildings were constructed without taking into account the earthquake hazard. These buildings consequently do not have enough capacity to dissipate the energy resulted from the excitation action during earthquake event. It is visible that most of the heritage buildings constructed in early nineteenth century and before are unreinforced masonry (URM) structures. As a result, an urgent desire has emerged in the direction of retrofitting these buildings to improve their ability to withstand potential seismic damage and thereby reserving the heritage buildings which reflected by many investigations carried out in this area. Application of CFRP (Carbon Fiber Reinforced Polymers) is one of the techniques used for strengthening of URM structures. Saudi Arabia possesses unique historical buildings that have been made using sandstone blocks. However, research into seismic retrofitting of these structures using CFRP is rather scarce, leading to this research into the use of CFRP as a retrofit technique in order to avoid the possibility of serious damage to such historical treasures in a seismic event.

Experimental and numerical investigation has been carried out to comprehend the behavior of retrofitted sandstone block wall subjected to cyclic loading. The experimental part of this work has been conducted in Reaction Floor Lab at Bldg. 26 KFUPM involving cyclic load testing of three sandstone block walls; one of them being unreinforced (control), while the others are strengthened with CFRP using different configurations. The strength, energy dissipation, cracking pattern and failure mode of the walls and performance of the walls under different orientations of CFRP sheets are investigated. In terms of the numerical part, finite element modeling has been carried out in order to get a full knowledge of how the sandstone masonry wall will perform when subjected to cyclic simulation. FEM of Masonry wall retrofitted with different configurations has been conducted in the ABAQUS environment using a Plastic-Damage model developed by Lubliner et al (1989) and further expanded by Lee and Fenves (1998).

CFRP strengthening has been shown to be reliable and effective option in rehabilitation and strengthening the masonry walls. Also, FEM analysis yielded a good matching with the experimental results which confirms that FEM can be used as a vital tool to predict the behavior of retrofitted and non-retrofitted masonry structures under simulated seismic loading.

ملخص الرسالة

الاسم الكامل:عمرو أبوبكر محمد بارحيم

عنوان الرسالة: سلوك ومحاكاة لجدران الحجر الرملي معززة ببوليمرات ألياف الكربون المقوى

التخصص: هندسة مدنية وبيئية

تاريخ الدرجة العلمية: فبراير 2015

تعتبر الجدران الحجرية من أقدم العناصر الانشائية التي ظلت مستمرة حتى يومنا هاذا في جميع أنحاء العالم. معظمها منتشر في المناطق الأثرية البارزة كدليل عن ما انجزه اجدادنا خلال العصور القديمة. في الواقع، معظم المباني التاريخية القائمة شيدت من دون الأخذ بعين الاعتبار مخاطر الزلازل. لهذا لا تمتلك هذه المباني القدرة الكافية لتبديد الطاقة الناجمة من الحركة الاهتزازية للزلازل. من الواضح أن معظم المباني التراثية التي شيدت إلى أوائل القرن التاسع عشر هي مباني ذو هياكل بنائية غير مقواة (URM) . ونتيجة لذلك، ظهرت هناك رغبة ملحة في اتجاه تقوية وترميم هذه المباني لتحسين قدرتها على تحمل الاضرار الزلزالية المحتملة, وبالتالي الاحتفاظ بهذه المباني التراثية, انعكس ذلك من خلال العديد من الابحاث التي أجريت في هذا المجال. إستخدام CFRP (البوليمرات المقواة من ألياف الكربون) هي واحدة من التقنيات المستخدمة لتقوية هياكل URM. المملكة العربية السعودية تمتلك مزيجاً فريداً من المباني التاريخية التي شيدت باستخدام طوب من الحجر الرملي. رغم ذلك، الابحاث التي اجريت في مجال تعزيز وتقوية الهياكل البنائية المبنية من هذا النوع من الحجر باستخدام CFRP نادرة إلى حد ما، مما دفع بنا الى تقديم هذا المشروع البحثي في استخدام CFRP كتقنية تعزيز وتقوية من أجل تجنب احتمال حدوث اضرار جسيمة لهذه المباني التي تمثل ارث تاريخي للمجتمع السعودي في حال وقوع حدث زلزالي لاسمح الله.

في هذا المشروع البحثي , تم تنفيذ دراسة مختبرية وتحليلية وذلك لفهم سلوك الجدار المعزز المبني من الحجر الرملي عندما يتعرض لتحميل دوري. التجارب المعملية التي تم تنفيذها في مختبر المنشآت الثقيلة في جامعة الملك فهد للبترول والمعادن (KFUPM), اشتملت على فحص واختبار ثلاثة عينات من الجدران المبنية من الحجر الرملي بحيث أن كل عينة تم تحميلها محورياً ومن ثم جانبياً. أحد هذه العينات غير مقواة (بحالتها الطبيعية) بينما بقية العينات مقواة ومعززة بالياف الكربون CFRP بتركيبات مختلفة. القوة وتبديد الطاقة وانماط الشقوق والصدوع وانواع انهيار الجدران وأداء الجدران المعززة بتركيبات مختلفة لCFRP. كل هذه الخصائص تم دراستها والبحث فيها استناداً على

نتائج التجارب المعملية على عينات الجدران. في جانب الدراسة التحليلية العددية، تنفيذ طريقة العناصر المتناهية باستخدام برنامج ABAQUS من أجل الحصول على معرفة شاملة عن سلوك الجدران المبنية من الحجر الرملي معززة بتركيبات مختلفة لCFRPعندما تتعرض لأحمال دورية محاكية للواقع.

ثبت من خلال هذه الدراسة البحثية أن CFRP يعتبر خيار موثوق وفعال في إعادة تأهيل وتقوية جدران البناء. أيضاً أسفرت هذه الدراسة البحثية عن تطابق جيد بين نتائج الدراسة التحليلية العددية FEM ونتائج التجارب المعملية مؤكدةً أن FEM يمكن استخدامه كطريقة فعالة للتنبؤ بسلوك هياكل البناء سواء كانت معززة او غير معززة تحت تأثير الحمل الزلزالي المحاكي للواقع.

CHAPTER 1

INTRODUCTION

1.1 General

Heritage structures include castles, palaces, monumental buildings, religious places of worship, etc. All of these structures are considered as invaluable treasures worldwide. Some of them are nominated by UNESCO as world historical sites whereas the others are highly recognized by their region's governments. These structures have become an essential part of humanity culture since the humankind creation. Some countries like Spain, Italy, Egypt, Greece and Turkey are taking these structures into account as one of the main sources of their income budget because it brings millions of tourists annually.

It is well-known that heritage structures are constructed mainly of unreinforced masonry walls (URM) due to its vital function in supporting the whole structure, low cost, beauty and ease of construction. According to the architectural researches in the history of URM, the stone is considered as the most material used in constructing the URM because of its availability in the nature as a main supply.

Despite the advantages of URM, they behave badly when subjected to earthquakes due to weak energy dissipation, deficient flexural and shear strength and inadequate ductility and in-plane stiffness. However, the stability of the residual structure remaining after the earthquake is mainly credited to the URM. URM, which is a composite material, is

regarded as anisotropic in terms of elastic properties as well as failure criteria. Orthogonal planes of weakness are attributed to the mortar joints. Failure modes for URM components are based on geometry and loading types. In particular, walls having an aspect ratio (ratio of height to weight) close to one possibly fail in the following modes: (i) compressive crushing, (ii) diagonal tensile splitting of units, (iii) tensile cracking along head and bed joints, (iv) the sliding shear failure of bed joints, and (v) rocking failure.

USGS has reported that 293767 earthquake events occurred worldwide between 2000 and 2012 and around 813 856 people have passed away [1]. Also, it has been stated by CATDAT that the total economic loss due to earthquakes worldwide has been reached 2.258 trillion USD approximately since 1900 up to 2012, 16% of it taking place in 2011 [2].Consequently, earthquake is considered as the major hazard should be taken into account when dealing with preserving and maintaining the URM structures.

Based on that, many investigations have been examining and presenting in the area of preservation and maintenance of URM structures against seismic events during the last decades. The most common one is using CFRP (Carbon Fiber Reinforced Polymers) in reinforcing and retrofitting URM structures. The trend of using CFRP in strengthening the URM system is being considered as the most feasible retrofitting techniques all around the world .by virtue of their outstanding combination of properties including high strength-to-weight ratio that results in ease of installation, invulnerability to chemical and

environmental corrosion, high fatigue resistance, and excellent mechanical strength and stiffness in the direction of fibers.

Considerable research on the behavior of URM walls strengthened with FRP has been carried out by Saadatmanesh (1994), Ehsani (1995), Ehsani et a1. (1997) and Triantafillou (1998). Schwegler (1994) was one of the pioneers to conduct an experimental study on the use of CFRP laminates that were epoxy-bonded to the masonry surface as seismic reinforcing elements of URM wall. The laminates worked as the tensile reinforcement and test results proved that using CFRP laminates is an effective retrofitting technique for masonry walls subjected to in-plane and out-of-plane cyclic testing loading.

1.2 Research Significance

As any country, Kingdom of Saudi Arabia possesses unique historical buildings all around the area especially in Diriyah, Northwest of Riyadh and mostly they consist of URM walls. URM systems constructed in Saudi Arabia are mostly considered as load bearing type, designed only to sustain gravity loading. They have not been originally designed to withstand seismic loading.

As stated by the Saudi Geological Survey [3], Saudi Arabia is subjected to a range of earthquake activity from low to moderate. Damaging earthquakes have been recorded in Yemen (1982), Egypt (1992) and the Gulf of Aqaba (1995) where the newest event, of magnitude 6.3 in Richter scale, was followed by over 7000 aftershocks and caused significant structural destruction in the Haql town located in North-West of Saudi Arabia.

According to this survey, most of the historical buildings are located in regions prone to seismic activity. Therefore, there is a movement by some private and governmental sectors in the Kingdom to strengthen significant heritage buildings in order to avoid destruction of national heritage. As a retrofit measure to protect such URM structures from damage, CFRP sheets are commonly being used to reinforce these structures especially in Jeddah western region of Saudi Arabia.

URM walls of historical buildings in Saudi Arabia were distinctively built using rocks as a block and lime mortar as a joint. One type of the rock used in constructing these heritage structures is sandstone blocks. Therefore, extensive study should be carried out with sandstone block walls retrofitted with CFRP experimentally and analytically in order to understand its behavior when subjected to cyclic loading exerted by the earthquake and verify the effectiveness of CFRP in enhancing the lateral resistance of URM system. Consequently, we can develop design guidelines which would predict how these retrofitted blocks would respond to robust ground motion leading us to protect this invaluable treasure.

1.3 Objective and Scope

The fundamental objective of this research is to evaluate the performance of architecturally unique historical masonry structures under simulated cyclic loading anticipated in the case of low or moderate earthquake events. Enhancement of lateral resistance of a representative wall system would be carried out through using CFRP. The effect of the number of CFRP sheets and their alignment geometry on the strength and ductility will be investigated.

The following items constitute the main objectives of the research:

1. To estimate the seismic performance of CFRP retrofitted sandstone block masonry based on indices of ductility and strength.

2. To simulate behaviour of the wall system selected subjected to seismic loading using mechanistic and finite element modeling.

3. To conduct parametric studies on seismic response of CFRP reinforced walls including the influence of different CFRP alignment geometry.

4. To suggest recommendations for development of seismic resistance of heritage structures.

The scope of this investigation included testing and analyzing three full-scale sandstone block walls; one of them was unreinforced one (control) while the others were reinforced with CFRP with different configurations. Also, Non-linear finite element simulation in an

ABAQUS environment will be conducted to simulate the behavior of wall system for both unreinforced & reinforced.

1.4 Thesis Organization

The following provides the outline of the current thesis, and the content of each chapter:

Chapter 1: This chapter introduces the specific research area adopted for the thesis. It discusses research needs and areas that require further research and development. The objectives are identified and the steps followed in the research project are itemized as the scope.

Chapter 2: Chapter 2 provides literature review. Previous research in the area of seismic retrofit of masonry walls is discussed. Application of CFRP on stone masonry URM is mainly considered.

Chapter 3: In this chapter, the properties and configuration of the materials used, details of the specimens including their strengthening, description of the test setup, loading system and testing procedure are discussed.

Chapter 4: This chapter presents the results obtained from the wall tests. Both the observations made during testing, and the relationships obtained by processing recorded numerical data, are presented to assess the performance of walls and the strengthening techniques adopted.

Chapter 5: In this chapter, forming the model step by step has been highlighted. Additionally, the FEM analysis results including stress and plastic strain contours are presented. Also, the generated lateral load-displacement hysteresis loop diagrams are displayed and compared with that experimentally obtained.

Chapter 6: This chapter presents summary and conclusions of the research project des. It also provides recommendations for use in practice.

CHAPTER 2

LITERATURE REVIEW

2.1 Introduction

In the last decades, several investigations have been carried out in order to comprehend the behaviour of the masonry wall before and after the retrofitting process. In terms of experimental aspect, a number of loading types such as in-plane loading, out-of- plane loading and cyclic loading were exerted on the wall specimens. On the other hand, analytical research has been undertaken so as to get a full knowledge of how the masonry wall will perform whether retrofitted or not under such loads, although not on the same rate as the experimental aspect.

External reinforcement, surface treatments (ferrocement, shotcrete, etc.), grout injections, and center core are considered as the first trials in the retrofitting of the masonry wall .However, many disadvantages have been discovered in these conventional techniques [4,5] involving: wasting time, taking much space, discomforting the occupancy, disturb the beauty of the façade , etc… In addition, this result in an increase in the earthquake induced inertia forces because of the additional mass. Owing to these drawbacks of using conventional techniques, using FRP opens an optimistic vision in the efforts to reduce the vulnerability of the masonry wall against the excitation action exerted by earthquake.

FRP (Fiber Reinforced Polymers) have been considered as one of the innovative materials used in the manufacture of the airplanes, cars and sports fittings for long time.

Utilizing these materials in the construction industry was started in the end of the 20th century. by virtue of their outstanding combination of properties including high strength-to-weight ratio that results in ease of installation, invulnerability to chemical and environmental corrosion, high fatigue resistance, and excellent mechanical strength and stiffness in the direction of fibers. As a result of these valuable advantages, FRP materials are being used in the structures' reinforcing replacing the ordinary reinforcement, structures' strengthening to improve its strength and structures' retrofitting to rehabilitate the damaged structural elements in order to sustain the design load without considering the damage.

Figure 2. 1 Various types of FRP

In this chapter, a literature survey of the experimental and analytical efforts on strengthened and retrofitted masonry wall is presented .After that, a brief review of cyclic loading types is introduced.

2.2 Literature Survey

Tomaževiˇc et al.[6] studied the structure when confined with CFRP laminate strips utilizing the seismic isolation in order to enhance the effectiveness of the ancient masonry building against the seismic action. They tested five representative brick masonry building of two-story where the floors were wooden and ties were excluded using shaking table platform. Tomaževiˇc et al. stated based on the experimental results that the representative buildings behavior against the shaking table loading is remarkably improved.

Santa Maria et al.[7] examined 24 un-retrofitted masonry (URM) panels externally retrofitted with bonded carbon fiber reinforced polymer (CFRP) sheets subjected to in plane shear load. Five of them were URM panels and the others were externally bonded: 14 panels were tested under monotonic loading and 10 in cyclic loading .Two configurations of the retrofitting were investigated in this test. Santa Maria et al [7] reported a sharp increase in the shear strength and decrease of the crack's width of URM walls retrofitted by externally bonded CFRP. Finally, they concluded that the diagonal configuration performs better than the horizontal configuration in terms of strength and stiffness.

Saatcioglu et al. [8] conducted an experimental study on reinforced concrete frames designed against the gravity load, infilled with concrete block masonry, to establish a seismic retrofit strategy that includes the use of (CFRP) carbon fiber reinforced polymer sheets. Two concrete frames of half-scale, infilled with masonry walls, were exposed to incrementally increasing horizontal load in cyclic mode under constant axial load with and without CFRP. Saatcioglu et al. [8]stated that in-filled frames without CFRP develop extensive cracking in the walls and frame elements as well

while the retrofitted specimens tested showed approximately 300% increase in lateral force resistance.

Shrive [9] has extensively inspected the use of fiber reinforced polymers (FRPs) for masonry rehabilitation and strengthening. Making use of their light weight, Shrive assured that they do not alter the mass of a structure and thus the effect of inertial forces resulting from seismic excitation will not increase. Also, he proved that they can improve the load deformation response considerably due to their strength as well as their toughness. Finally, Shrive observed that using FRP opens a promising new era of possibilities for using in seismic retrofitting of masonry.

ElGawady et al.[10] investigated the effect of fibre-reinforced polymers (FRP) on URM walls before and after applying it in terms of in-plane seismic behaviour. Five URM walls of different aspect ratios using half-scale brick units and considered as a reference samples are subjected to Dynamic in-plane tests. Then, these reference samples were retrofitted by applying different FRP's types and variable FRP's layouts on a single side and retested. ElGawady et al. [10] found that parameters of URM walls including in-plane strength, stiffness, and deformability have significantly increased because of the noticeable effect of FRP retrofitting technique. In addition, they observed that all samples have kept the fundamental frequency and the initial stiffness approximately unchangeable whether retrofitted or not. During this investigation, they noticed that there is an approximate linear strain distribution along the samples' cross-sections even it fails in flexure. Consequently, the flexural strengths of the samples could be computed using linear elastic approach. Finally, they concluded that the variation takes place between the measured and the computed

lateral strength is credited to the difference between the real and nominal ultimate strains of FRPs.

Vandergrift et al. [11] were interested in the seismic retrofit on unreinforced hollow concrete masonry (CMU) area .For this purpose, six CMU walls retrofitted by carbon fiber reinforced polymer (CFRP) composites were tested before and after applying the retrofitting composite. Three of the walls were subjected to in-plane shear forces while the others were subjected to out-of-plane bending. All walls were retrofitted with three diverse composite laminates structures. Vandergrift et al. [11] observed that the FRP laminates considerably improved the in-plane shear and out-of-plane bending capacity of pre-cracked unreinforced hollow masonry walls. Moreover, they recognized that the masonry controls the experiment results since the stress level in the FRP material covered both faces of the wall was well below its ultimate values. Additionally, they developed an analytical procedure in order to predict the behaviour of masonry walls retrofitted with composite laminates.

The Improving capacity of unreinforced masonry (URM) walls against the in-plane shear when retrofitted externally by fiber reinforced polymer (FRP) composites were studied and evaluated experimentally by Mosallam & Banerjee [12]. They tested six representative wall samples of aspect ratio 1:1 under fixed axial load and incrementally increasing cyclic lateral load. Various retrofiring systems were externally applied on four samples. Mosallam & Banerjee reported that the ultimate capacity of the wall is highly improved when FRP composite laminates are applied on its faces. Also, they proved that the brittle nature of the failure criteria of walls was moved to ductile one due to the application of FRP composites. Moreover, they

executed a comprehensive investigation in the analytical methods whether a code-based or research-based and validate it with experimental findings. As a result of this investigation, they concluded that these methods will not bring a good prediction when used for several retrofit materials and structures. Consequently, they recommended that extensive research on analytical models should be taken place in near future in order to become valid models used for a wide range of FRP retrofitted URM walls.

Triantafillou [13] investigated the effect of the uni-directional CFRP fabric strips on the behaviour of the representative clay URM walls by conducting a sequence of tests. Out-of-plane bending with gravity load, in-plane bending with gravity load, and in-plane shear with gravity load are all applied on the specimens. According to his experimental results, Triantafillou observed that the strengthening technique increases significantly the capacity of URM walls against the in-plane shear load combined with low axial load. Also, he illustrated that the shearing takes place underneath the bond has a vital role of FRP failure.

Chuang et al. [14] carried out an experimental investigation of three unreinforced clay brick masonry walls retrofitted with FRP strips. All walls were subjected to incrementally increased in-plane lateral displacement reversals combining with constant gravity load. The results proved that both the strength and ductility of tested samples were remarkably improved with this technique. Consequently, he argued that this technique is trustworthy alternative of strengthening unreinforced masonry walls.

Zhao et al. [15] conducted an experimental investigation on three concrete block masonry walls under constant gravity load with lateral load reversals, one of them

designated as a control wall, while the others were retrofitted with carbon fiber sheets externally bonded on both sides, having configuration of X shape . One of the strengthened walls was repaired with FRP after cracking has been taken place; the other wall was retrofitted before cracking with the same amount of FRP applied to the first wall. Zhao et al. [15] studied the parameters of the retrofitted walls including the cracking load, the ultimate load and the deformation capacity. They reported that all these parameters were considerably increased. Finally, they showed that the maximum resistance of the second retrofitted wall is more than the first repaired wall by 20%.

As previously seen in this survey, most research investigations aimed to study the behaviour of retrofitted masonry were focused on concrete or clay brick or block masonry walls. On the other hand, few efforts spent on experimental investigation of the seismic retrofitting features of masonry walls constructed mainly of stones which motivates us to contribute in this scarce research trend.

G. Vasconcelos and P. B. Lourenço[16] studied 23 representative walls simulating the typology of typical walls of various bond arrangements. These walls were subjected to variable vertical normal stress level. The investigation revealed that the in-plane behavior of stone masonry walls is mainly influenced by energy dissipation and ductility. In fact, these two factors rely substantially on the textural patterns of the stones. In addition, it showed that the high capacity of nonlinear deformation with reasonable damage levels is attributed to the good quality of stone masonry walls. Finally, it proved that there is a good agreement between the horizontal resistance of

stone walls experimentally measured and the computed one using simplified analytical means.

Marcari et al.[17] investigated the in-plane behavior of full scale tuff masonry walls with variable FRP retrofitting strategies in terms of FRP's type, FRP's density and FRP's configuration under monotonic shear-compression loading in quasi-static test set-up. Tuff rocks were largely used in Italy, Turkey, Japan and America due to its feasible properties. They reported that the retrofitted wall with FRP exhibits significantly improved shear strength. Moreover, they noted that the original failure mode of the strengthened wall altered its failure mode because of the large effective axial stiffness of the FRP strips. Also, they proved that the elastic stiffness of FRP retrofitted walls as well as the inelastic deformation was not greatly modified by the external retrofitting.

Demir [18] carried out a research on the response of walls which resembles the walls used in the monumental structures in Istanbul under cyclic loading. In his investigation, Demir studied the effect of cyclic loading on a multi-leaf masonry wall used in the heritage Bayezid II Mosque located in Istanbul. Demir has observed different types of failure of the walls consistent with the level of exerted axial load. He noticed that the walls are likely to be stiffer as the axial stress becomes higher.

Al-Gohi[19] carried out an experimental and numerical investigation on sandstone masonry wall widely has been used in the heritage structures in Riyadh. Al-Gohi examined three walls under a combination of axial load and horizontal load; two of them were unretrofitted while the third one was CFRP retrofitted .Also, he conducted an extensive effort on simulating the behaviour of the walls when subjected to this

loading combination. He observed that walls with an aspect ratio approximately equal to one possess mostly conformable interaction relationship between lateral strength and the axial force applied to the wall. Furthermore, he showed that using CFRP, considering the bonding strength between CFRP and masonry wall, boosted the lateral strength as well as lateral stiffness of the wall. In addition of that, the author noticed that CFRP aids to prevent premature rocking failure of the wall, and allows for the mobilization of the wall as a one body which contributes to the resistance against the applied forces.

2.2 Cyclic Loading Types

The masonry structures behaviour against the seismic loading has been studied by using various testing systems. Those systems differ from each other by the loading nature such as dynamic shaking table loading, pseudo-dynamic loading and quasi-static monotonic or cyclic loading. The most accurate loading simulating the seismic loading is the dynamic shaking table loading according to the Gerardin and Negro [20]. Also, they stated that there are similar features between the pseudo-dynamic and shaking table loading. Gerardin and Negro argued that quasi-static loading is the most common system used to investigate the masonry walls behaviour despite the low rate of loading due to number of features summarized by them in the following points:

1- Simple test compared to other testing systems in terms of installation and operation.
2- Forces and displacements measurements can be more accurate.
3- Damage development can be clearly recorded.

4- Results can be more conservative in contrast with the dynamic tests in which the inertia effect adds more resistance to the wall.

5- The lateral loading can be extracted from real seismic loading.

CHAPTER 3

EXPERIMENTAL PROGRAM

3.1 Introduction

Many experimental investigations on masonry walls subjected to both axial and lateral cyclic loading have been carried out as indicated in Chapter 2. The purpose of these investigations is to fully understand the behaviour of these walls subjected to such loads so as to evaluate the effectiveness of using FRP as retrofitting technique on such walls.

The experimental phase of this study consisted mainly of testing three full-scale Sandstone block masonry walls; one of them was un-strengthened one (control) while the others were strengthened with CFRP with different configurations. These walls were subjected to cyclic lateral load applied incrementally under a constant axial load. In addition, a number of tests have been carried out on the related materials in order to extract as much data as possible on the mechanical properties of such materials. As a result, it can be used as input data in the modelling aspect.

In this chapter, the properties and configuration of the materials used, details of the specimens including their strengthening, description of the test setup, loading system and testing procedure are discussed.

3.2 Materials

As we know masonry wall is a composite structure consists of different materials having its own properties. Therefore, a clear description of these properties will be presented in

order to have better understanding of the structural behavior of the masonry wall specimens. This description often needs to perform supplementary tests to extract some properties which will be highlighted hereafter.

3.2.1 Sandstone

The sandstone used in this study is the product of hotat bani-tamim quarry in Riyadh, Saudi Arabia. It is nearly resembles the sandstone used to build the heritage structures in Diriyah, Northwest of Riyadh. Two typical sizes of sandstone blocks have been used in this study. The larger block had a dimension of 300x100x200mm while the smaller one had a dimension of 150x100x200mm.

Two main categories of supplementary tests have been conducted to sandstone material in order to extract its mechanical properties needed in the modeling aspect. Those tests are Compression tests and Tension tests.

3.2.1.1 Compression tests:

For compression test, cylindrical specimens were used to find the compressive behavior of the sandstone material. Specimens have been prepared according to the ASTM D 4543. According to ASTM, the ratio of height to diameter should be less than 2.5 and more than 2.0. For that, the dimensions of the specimens were chosen (Figure 3.1).

Cylindrical specimens have been prepared by coring from a sandstone block using a coring machine (Figure 3.2). Due to the nature of coring process, the outer surfaces of the cylinders were not perfectly smooth. Because of that, a capping process has been done to get flat surfaces (Figures 3.3 & 3.4).

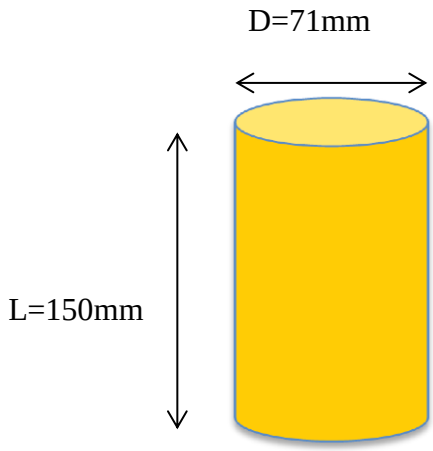

Figure 3. 1 Dimensions of cylindrical specimens

Figure 3. 2 Coring processes of cylindrical specimens

Figure 3. 3 Capping processes of cylindrical specimens

Figure 3. 4 cylindrical specimens after capping

After preparing the cylindrical specimens for testing, two types of compression tests were conducted:

i. Compression test to find the ultimate strength of the material.

ii. Compression test to find all mechanical properties (ultimate strength, stress strain curve, Young Modulus and Poisson's ratio).

In the first type (i), the purpose is to find the ultimate strength of the specimen so we can choose the best machine that would be fit for these specimens in the second type of the compression test. This test was conducted using ELE compression testing machine (Figure 3.5). Table 3.1 shows the compression test result of the specimens

Figure 3. 5 Cylinder under compression test in ELE compression testing machine

Table 3. 1 Ultimate strength of the sandstone cylindrical specimens

Name	Strength, MPa
SCTS1	39.1
SCTS2	42.76
SCTS3	50.53
SCTS4	52.43
SCTS5	55.72
SCTS6	45.52
SCTS7	38.05
SCTS8	53.58

The test result of the compression test reveals that, the average capacity of the sandstone was about 47.21 MPa with standard deviation of 6.8.

In the second type (ii), complete stress strain curve (including the softening branch) was targeted because it is essential to be used in the numerical simulation. For that, Two PLC-60-11 cross type; strain gauges, connected to Data logger, were used in two opposite sides of the cylinders to efficiently capture the behavior of the cylinders

under test and to find Young modulus, and Poisson's ratio (Figure 3.6). The test was conducted using LLOYD LR 300 K testing machine (Figure 3.7). The failure with shattering happened to one of the specimens is shown in the Figure 3.8.

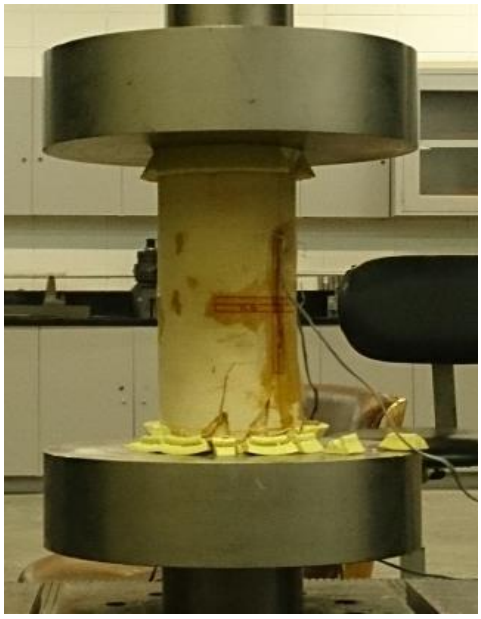

Figure 3. 6 PLC-60-11 cross type; strain gauges attached to cylinder under uniaxial compression test

Figure 3. 7 Compression test set-up

Figure 3. 8 Result of sudden failure of sandstone specimen

Stress strain curves were plotted as shows in Fig 3.9. Due to the nature of the strain gauges, it is not possible to capture the stress-strain curve in the softening branch. For that, this branch can be found using the displacement between the end loading plates (Fig 3.9).

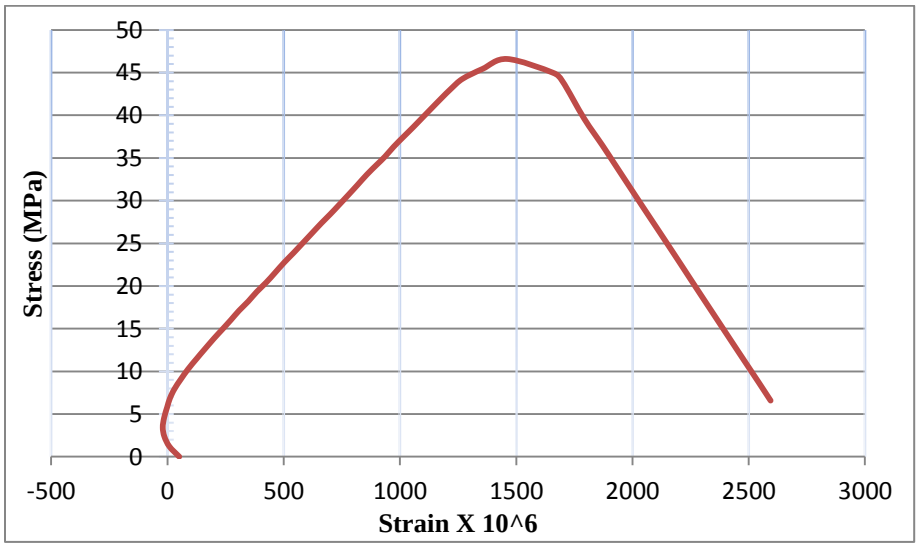

Figure 3. 9 Typical curve of Stress Strain of Sandstone compression test.

From the results, the modulus of elasticity was in the range of 36442 MPa. Poisson's ratio result for the test was in the range of 0.3. The density of sandstone material was also found. Table 3.2 shows the measured density of the samples. The density of sandstone material was in the range of 2256.0 Kg/m^3.

Table 3. 2 Destiny of sandstone material

Name	Density, Kg/m^3
SCTS1	2234.301
SCTS2	2292.738
SCTS3	2253.872
SCTS4	2242.524
SCTS5	2252.746
SCTS6	2258.456
SCTS7	2256.706

3.2.1.2 Tension tests:

In this category, two types of tests have been carried out namely:

i. Split test.

ii. Direct tension test.

In the first type (i), the purpose of the test is to find indirectly the tensile strength of Intact Rock Core Specimens. Following ASTM D 3967 and C 496, specimen preparation, and testing procedures have been adopted. According to ASTM, the ratio of thickness to diameter should be less than or equal to 0.75 and more than or equal to 0.2. For that, the dimensions of the specimens were chosen (Figure 3.10).

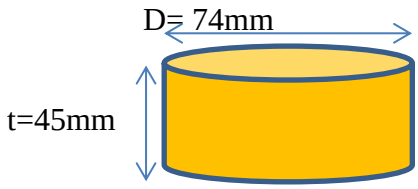

Figure 3. 10 Dimension of sandstone samples tested in split test

Sandstone samples have been prepared by coring from a sandstone block using a coring machine. Due to the nature of coring process, the surfaces of the sandstone samples were not perfectly smooth. Because of that, a polishing process has been done to get flat surfaces as much as possible (Figure 3.11).

Figure 3. 11 Sandstone samples after coring and polishing.

After preparing the samples, the split test has been conducted using Toni compression testing machine. Figs 3.12 and 3.13 show the samples under test and also show the texture of the fractured surfaces.

Figure 3. 12 Sandstone sample under split test

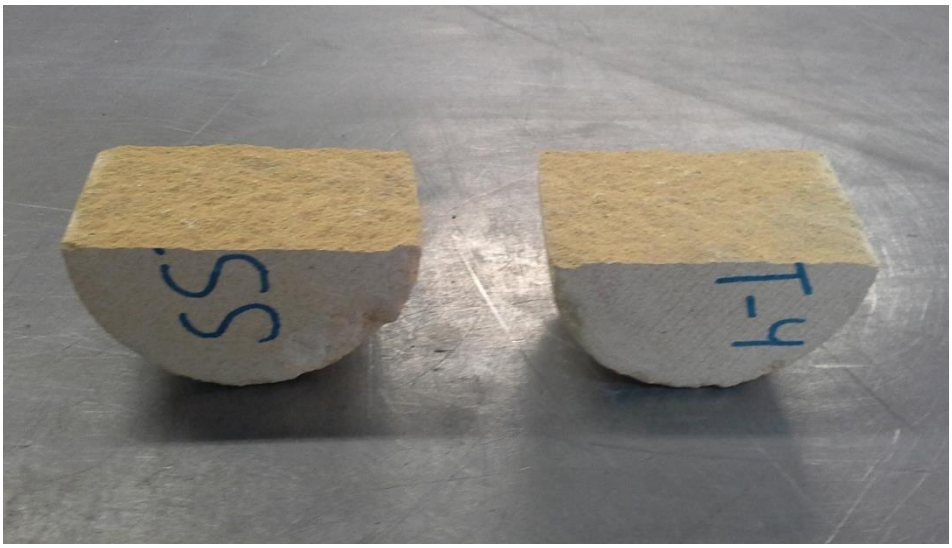

Figure 3. 13 Sandstone sample after split test

Table 3.3 shows the split test result of the samples. The test result of the split test reveals that, the average split tensile strength of the sandstone was about 2.459 MPa with standard deviation of 0.42.

Table 3. 3 Split tension test results of sandstone samples

Name	Split Tensile Strength, MPa
SSPT-1	2.86
SSPT-2	2.27
SSPT-3	2.61
SSPT-4	2.86
SSPT-5	2.59
SSPT-6	2.87
SSPT-7	1.71
SSPT-8	2.44
SSPT-9	1.92

In the second type (ii), the purpose of the test is to capture the correct behavior specially the softening branch of the stress strain curve in the uniaxial tension test which will be

utilized in the modeling aspect as a vital input data. According to Vasconcelos [21], the samples were prismatic shape of 80mm height, 50mm length and 40mm width (Figure 3.14). To capture the behavior of the cracked surfaces, notches have been introduced to the prisms in two opposite faced so that the crack will happen in the targeted area (Figure 3.15). The top and bottoms faces of the prisms were prepared to be rough so that good adhesion is achieved between the specimen and the epoxy that will glue the specimen to the loading plates (Figure 3.16). The testing procedure was conducted in according to ASTM D 2936.

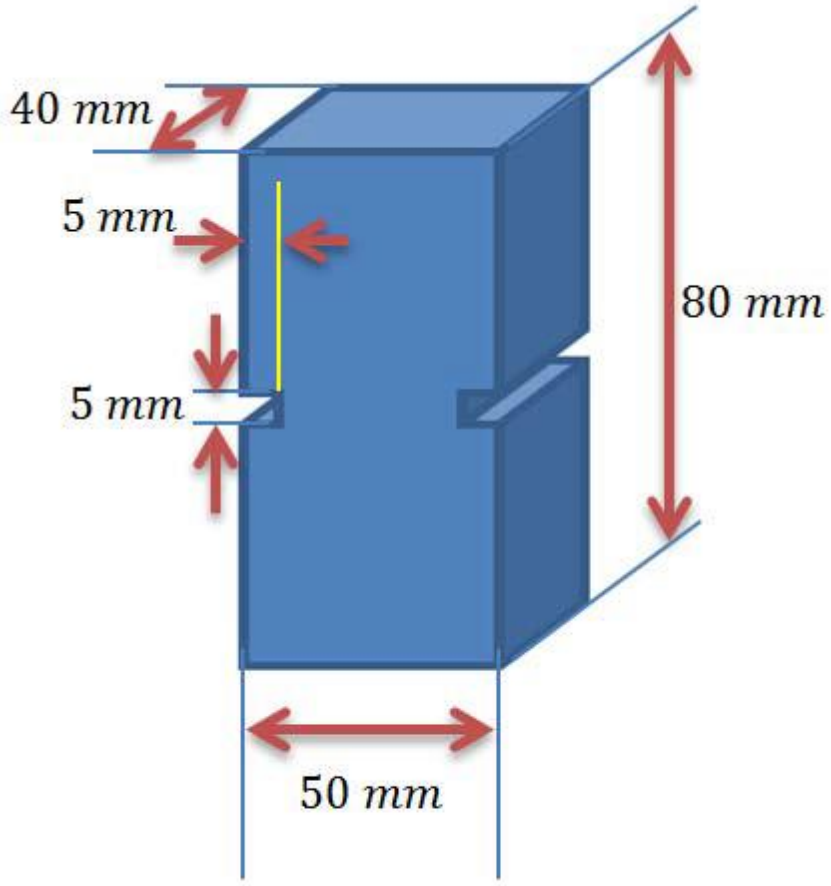

Figure 3. 14 Sandstone samples dimension

Figure 3. 15 Sandstone samples with introduced notches

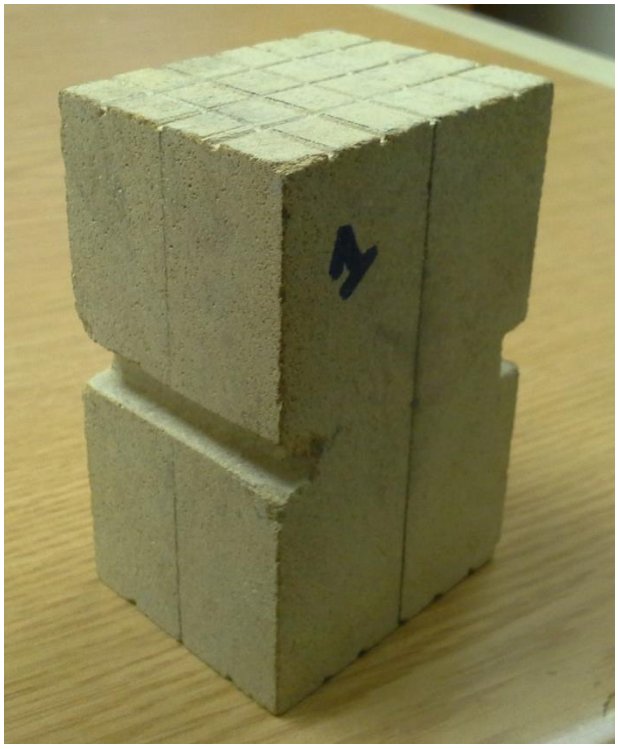

Figure 3. 16 Rough surface of sandstone sample for better adhesion

Two strain gauges where attached to the un-notched faces of the specimen and two PI-shape Displacement Transducer (PI-5) were attached to the specimen on the notched faces to measure the displacement through the notch. A sample under loading is shown in Figures 3.17&3.18.

Figure 3. 17 sandstone sample in direct tension test

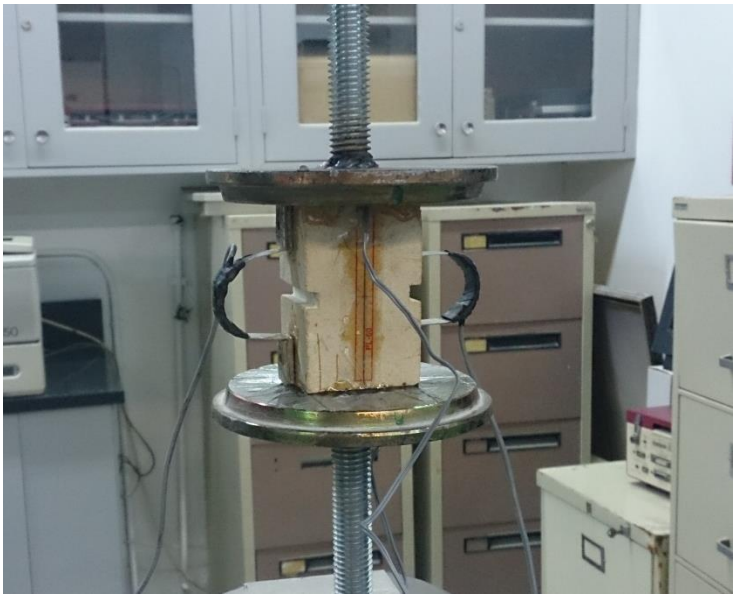

Figure 3. 18 Configuration of Direct tension test

Failure of the sandstone sample through notches and the texture of the fractured surfaces is shown in Figure 3.19.

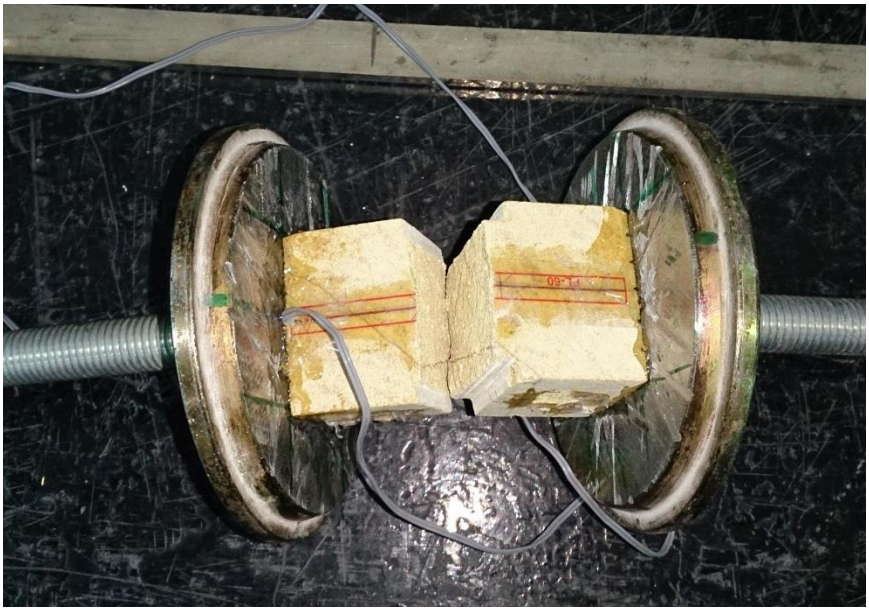

Figure 3. 19 Sandstone sample after Direct tension test

Typical result of direct tension test is shown in Figure 3.20.

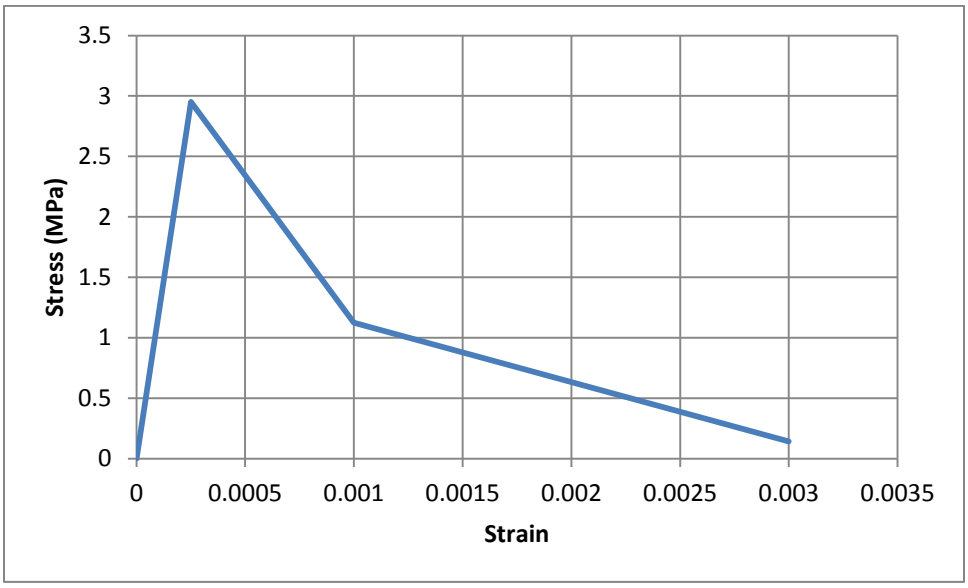

Figure 3. 20 Typical curve of Stress Strain under Direct tension test.

3.2.2 Lime Mortar

Mortar is the second component after sandstone that constitutes the masonry wall which mainly affects the behavior of the masonry structures according to Edgell and Haseltine [22]. In this study, ready mixed Lime Mortar LM70 from Dry Mortar Company (DMC LM70 Technical details.) was used to build the wall specimens and the prisms as well Figure 3.21.

Figure 3. 21 Ready mixed Lime Mortar LM70

The lime ready mixed lime mortar consists of hydrated lime and white cement and also some other additives. This lime mortar is manufactured in according to M5, EN 998-2,

ASTM C270 type N; ASTM C150, and ASTM C144. The water mix ratio specified by the manufacturer (w/m) is 0.3. This type of lime mortar was used in order to simulate approximately the behavior of the real mortar used in the heritage masonry structures located in the historical city (Diriyah).

The Lime mortar used in this study was from the same batch used by B.Algohi who reported the main mechanical properties utilized as input data in FEM aspect [19]. According to Algohi, the average compressive strength was in the range of 1.8 MPa while the average split tensile strength was in the range of 0.24 MPa.

3.2.3 Masonry Prisms

In this study, response of masonry walls subjected to pure compression force is needed especially when doing the numerical analysis and choosing the constant axial load in the full-scale cyclic test. However, it is difficult to conduct the compression test of full scale wall due to lacking of high capacity machine. This obstruction leads to make use of prism that gives the same behavior of the full scale wall. In this study, compression test was conducted to prisms representing the sandstone masonry wall. Specifications and description of the test are according to ASTM C 1314 and European Standard EN1052 1(1999). The prisms were constructed using the same materials as those in full scale walls during constructing the sandstone masonry wall specimens. A total of two masonry prisms were constructed for the purpose of testing under pure compression load. Shape and configurations of prism are shown in Figures 3.22&3.23. These prisms subjected to continuous curing for 28 days (Figure 3.24).

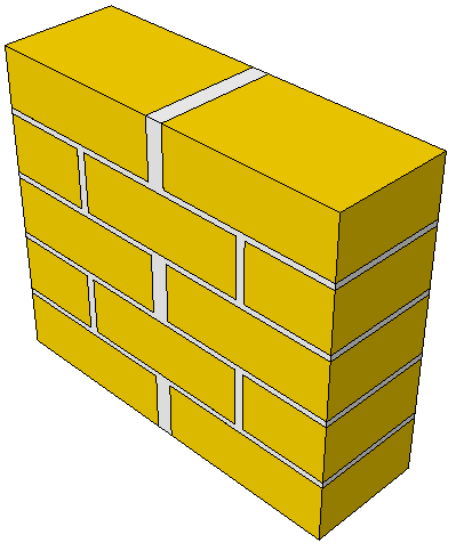

Figure 3. 22 Isometric view of the sandstone prism

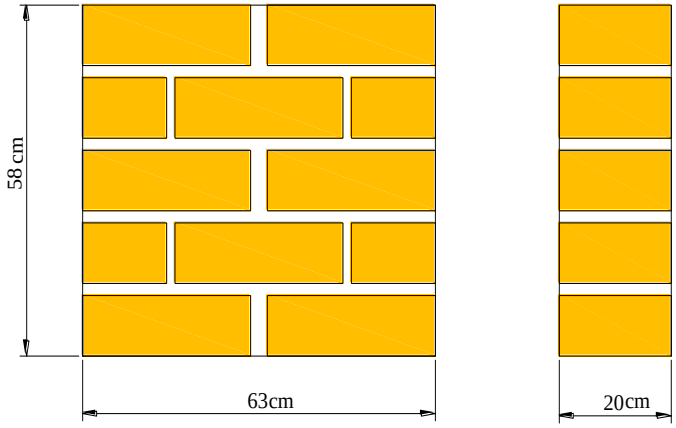

Figure 3. 23 Dimensions and configuration of the sandstone prism

Figure 3. 24 Sandstone Prisms under curing period

This test was carried out using Enerpac hydraulic jack fixed in a steel frame available in the reaction floor lab. Due to the nature of prims construction, the top side of the prism was not perfectly flat. Because of this, a thick layer of high strength mortar EMACO S88 CT was placed at the top of the prism so that the stress is uniformly distributed on the top side of the wall without any stress localization or concentration. Two steel beams were placed at top and bottom sides of the prims so that a uniform stress is exerted on the prism (Figure 3.25). For each prism, four vertical CDP-25 LVDTs and two horizontal CDP-25 LVDTs were used to capture the horizontal as well as the vertical displacement of the prism. Figures 3.26&3.27 show the configuration of the instrumentation on the prism body.

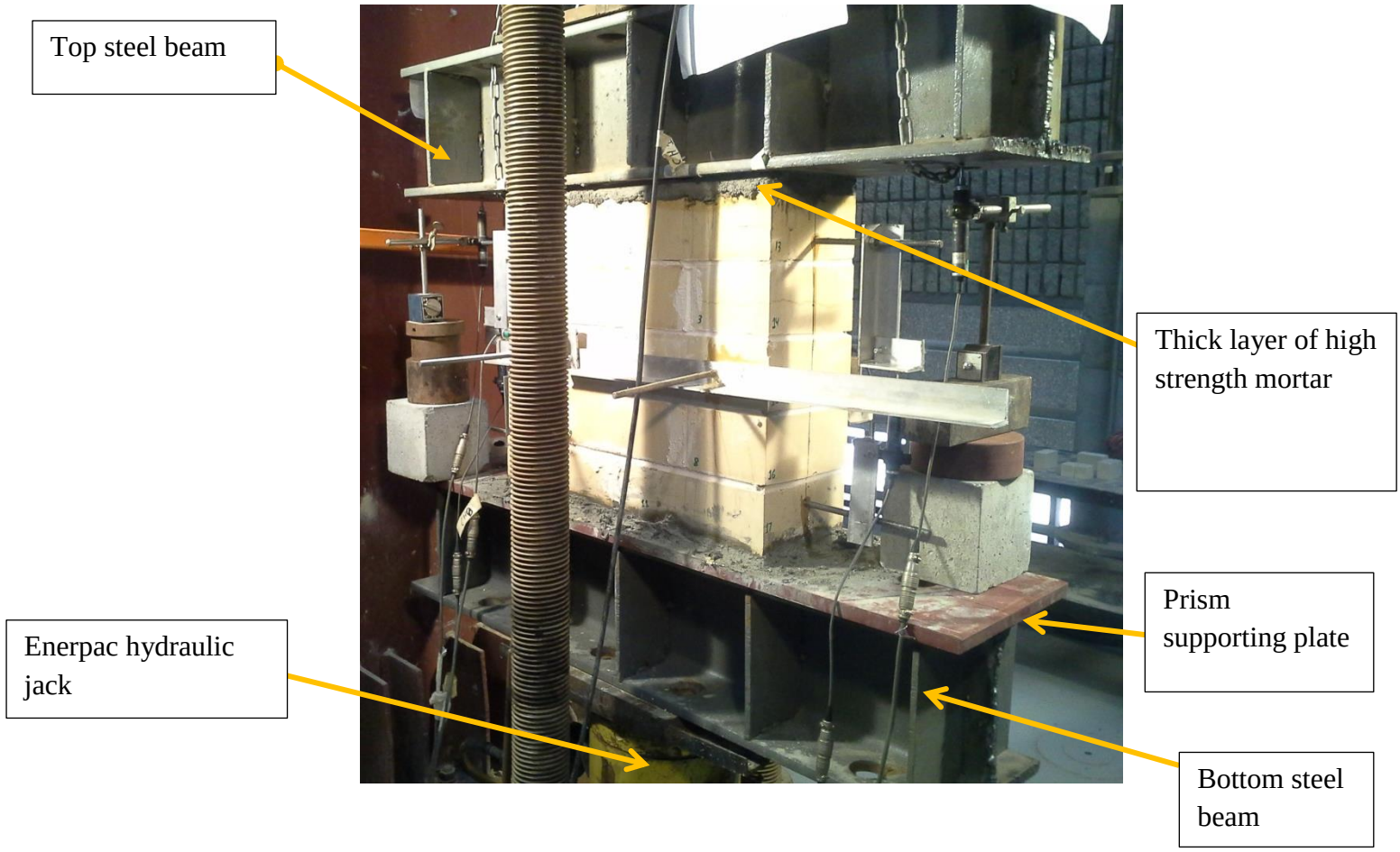

Figure 3. 25 Setup of the Sandstone prism in the steel frame

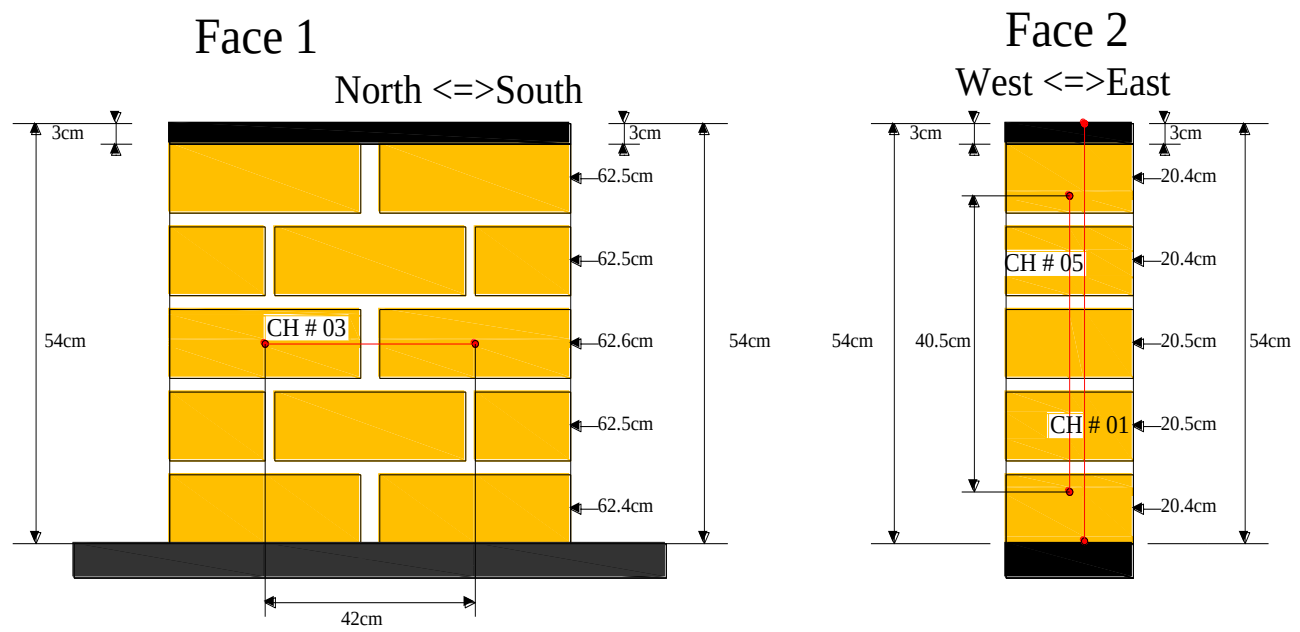

Figure 3. 26 Dimensions and LVDTs configuration of prism (face 1&2)

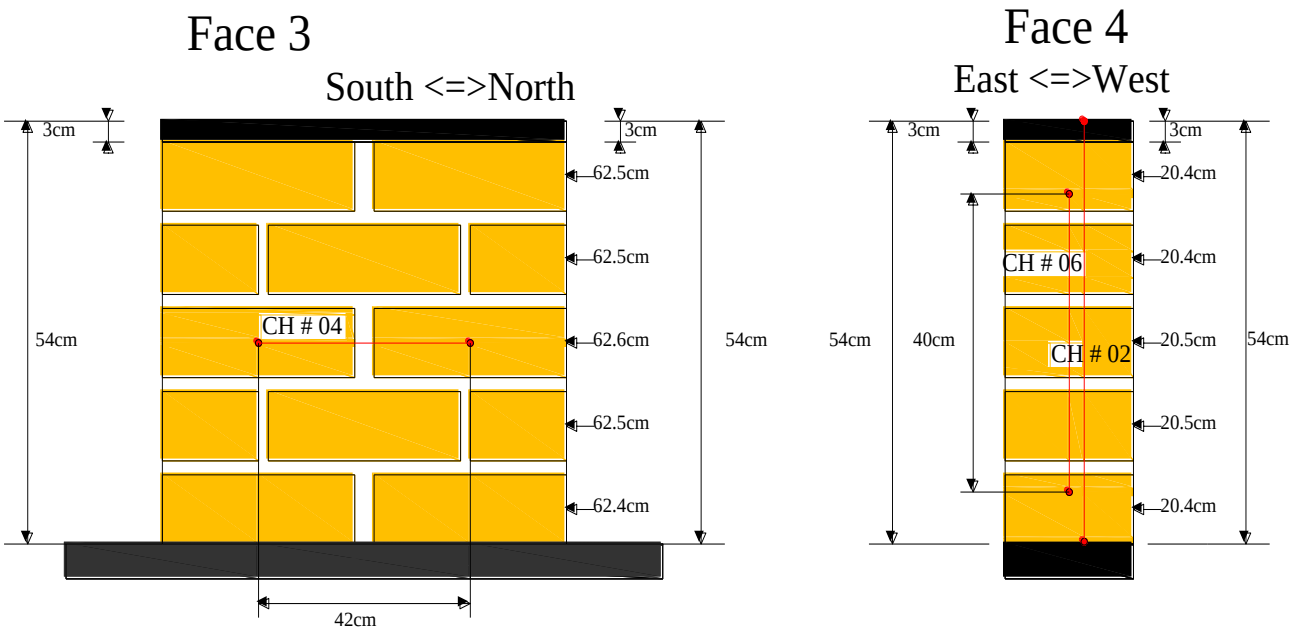

Figure 3. 27 Dimensions and LVDTs configuration of prism (face 3&4)

Axial force was applied on the prism though a strong steel frame attached firmly to the reaction floor. The axial load was recorded though a load cell of 2000 KN capacity placed between the prism and the steel frame. The data was gained using TOKYO SOKKI data logger. Table 3.4 shows the total number of channels used in the experiment. Figure 3.28 shows the setup configuration ready for compression test.

Table 3. 4 Channels used in the prism compression test

Channel Type	Channels	Number
Load Cell	0	1
CDP-25	1,2,3,4,5,6	6
Total		7

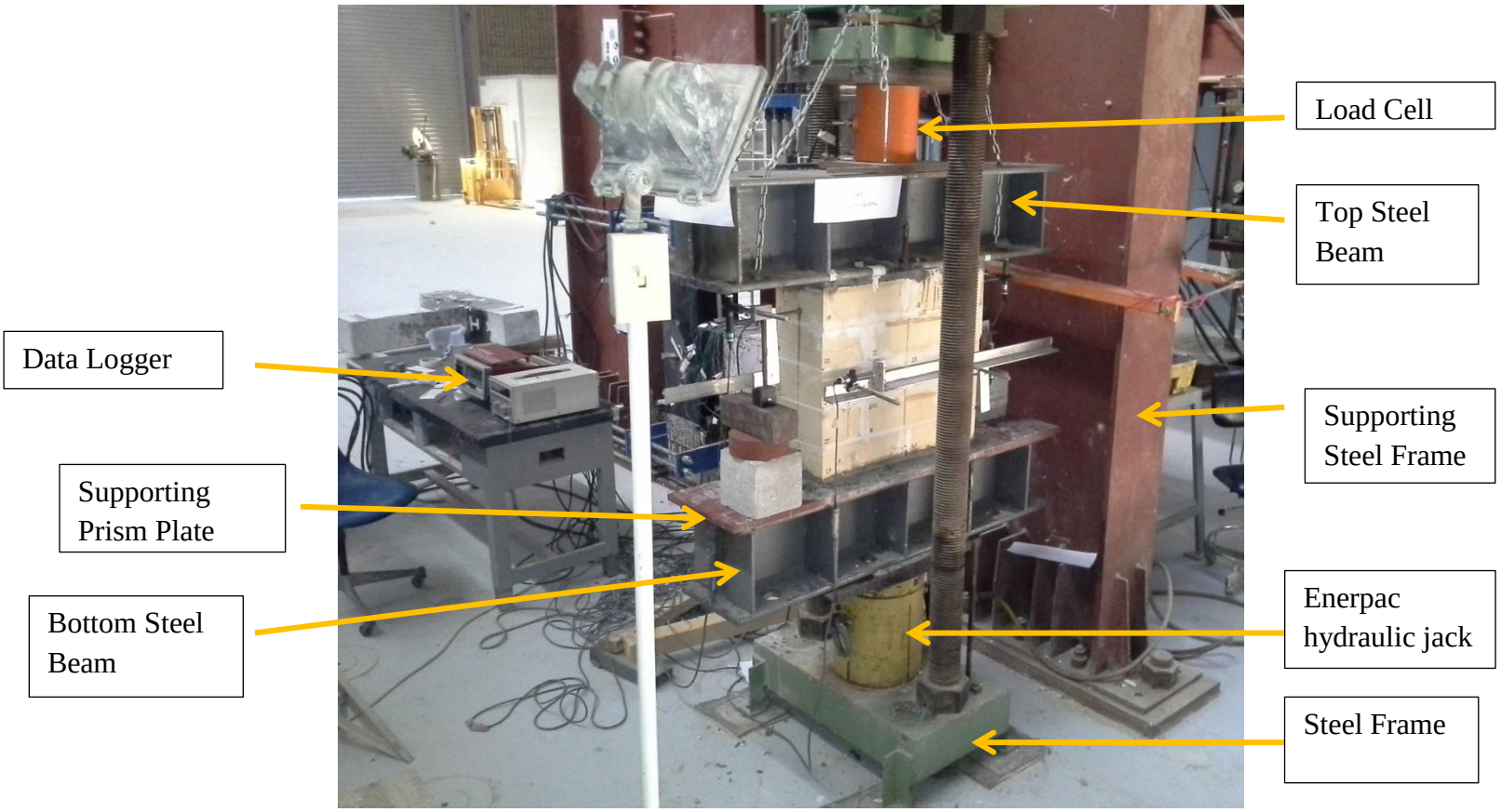

Figure 3. 28 Setup configuration of the sandstone prism compression test

The Experiment period was approximately 30 minutes. While the load was increasing, the cracks started longitudinally accompanying with spalling of lime mortar from the joints then diagonal cracks started to appear which was associated with crushing of some joints. This failure mechanism continued uniformly until the collapse happened. Prism during and after collapsing are illustrated in Figures 3.29&3.30.

Figure 3. 29 Sandstone prim during collapse

Figure 3. 30 Sandstone prism after collapse

The axial strength of the two prisms is shown in Table 3.5.

Table 3. 5 Axial compression strength of the prisms

Prism	Average Width mm	Average Thickness mm	Max. Force kN	Stress MPa
Prism-1	625	204	1949	15.29
Prism-2	630	205	1995	15.45

3.2.4 Carbon Fiber Reinforced Polymer (CFRP)

CFRP (Carbon Fiber Reinforced Polymer), which has a high tensile strength capacity, is a structural strengthening material. In this study, SikaWrap Hex 230C Carbon fiber fabric will be used in strengthening the masonry walls which will be attached to the surface by using Sika-Dur 300 Epoxy (Figure 3.31).

Figure 3. 31 , SikaWrap Hex 230C CFRP with Sika-Dur330 Epoxy

This CFRP is a unidirectional black fiber sheets supplied in 600mm wide and 50m long roll. According to the manufacture's provided data, The CFRP sheets used for wall strengthening had carbon fibers with tensile strength of 4300 MPa and elastic modulus of 238 GPa. The tensile rupturing strain was 1.8% while density of the fiber material was 1.76 gm/cm3. The Sika-Dur 330 epoxy had 55 MPa strength with a tensile modulus of 1,724 MPa, resulting in 3% elongation at break. The composite laminate thickness was 1.0 mm with a tensile strength of 350 MPa and elastic modulus of 28 GPa.

3.3 Specimens

The sandstone block masonry walls constructed for the purpose of the experimental investigation are intended to represent the typical sandstone masonry wall of heritage buildings located in Diriyah, Northwest of Riyadh. Three sandstone masonry walls (1 m long × 1m high), were built using the materials described above. All the specimens had the same geometrical dimensions and configuration and were built by the same mason in order to avoid any limitations regarding the geometry and workmanship. These specimens are single-wythe sandstone masonry consisting of 9 courses of 20cm thickness. Shape and configuration of the specimens are illustrated in the following figures 3.32&3.33. These specimens had an aspect ratio (ratio of height to length) close to one in order to insure that the shear behavior of the tested wall under cyclic loading will be dominated [12].

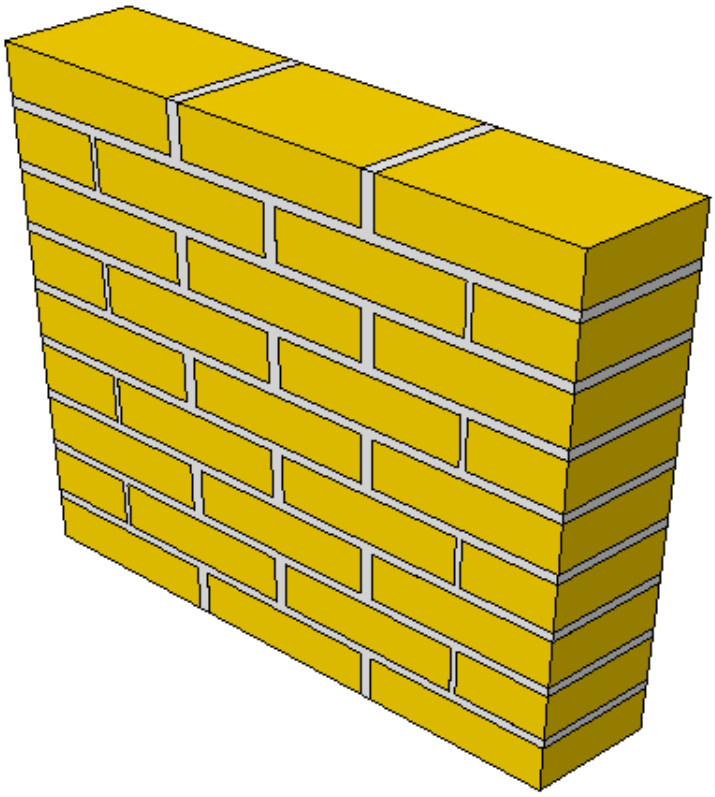

Figure 3. 32 Isometric view of the sandstone masonry wall sample

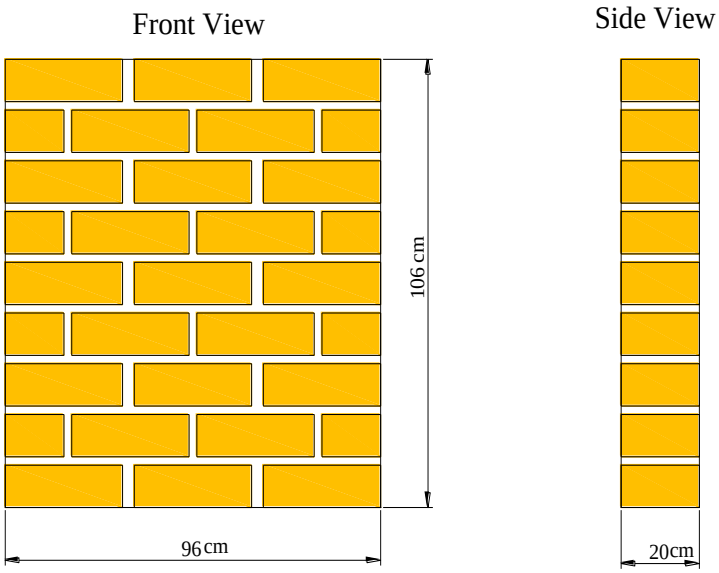

Figure 3. 33 Dimensions and configuration of the sandstone masonry wall sample

Hiring a professional mason, a steel base beam having a U-channel was used to build the walls upon it (Figure 3.34). In addition, this base beam was used to facilitate the transportation of the specimens without any damage and to fix them firmly to the loading frame connected to the strong reaction floor by using threaded bolts.

Figure 3. 34 U-channel base beam

These specimens were constructed in Reaction Floor Lab at Bldg. 26 KFUPM and take approximately one hour to complete for each one (Figure 3.35). After constructing these specimens, they were continuously cured with water three times a day for approximately three weeks. After curing process, the specimens were transported to the testing set-up area using 2.2 ton trolley then they were lifted to the loading frame using 15 Ton crane and connected to the strong reaction floor using threaded bolts. (Figure 3.36).

Figure 3. 35 Specimens under curing process

Figure 3. 36 Specimen placed connected to the reaction floor

The first wall was considered as a control wall for the purpose of comparison while the other walls were strengthened with CFRP in different configurations for parametric purpose.

3.4 Retrofitting

As mentioned before, two masonry specimens were strengthened using non-prestressed CFRP (SikaWrap Hex 230C) with different configurations. One of them was strengthened in a diagonal pattern (X-shape) while the other was in a grid pattern (cross shape). Figure 3.37 illustrates the scheme of the two strengthened masonry walls.

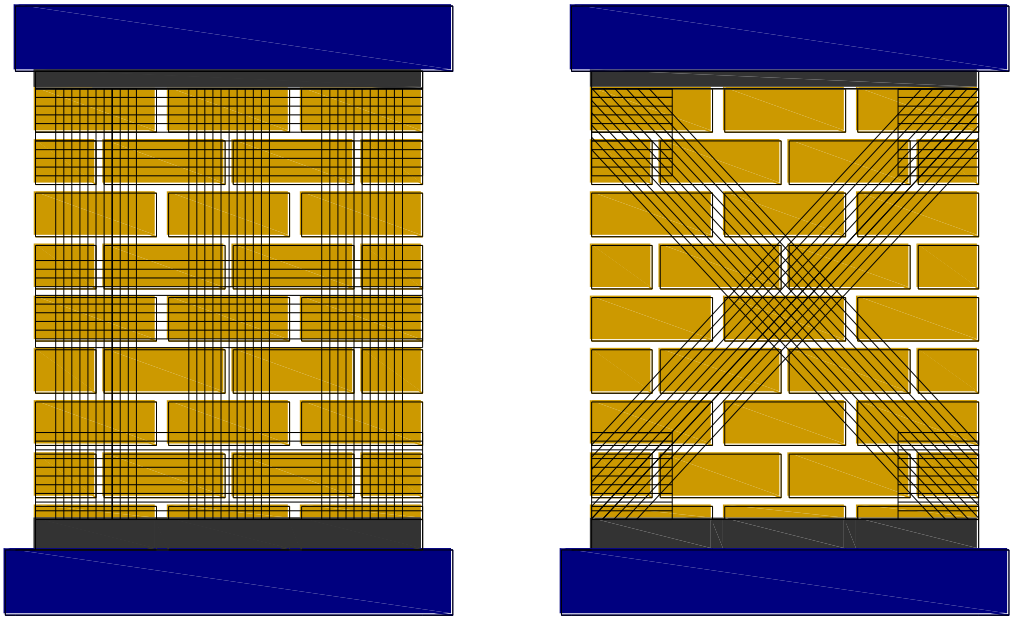

(a) Grid CFRP Pattern **(b) Diagonal CFRP Pattern**

Figure 3. 37 CFRP configurations utilized in this study

Prior to applying the CFRP sheets, the specimen surface was prepared by removing projections by hand girder as well as fine dust and loose mortar by air compressor. Next the CFRP sheets were cut into strips of required length and 20cm bandwidth. After that, a 2-part epoxy resin (Sika-Dur 300) was applied to the targeted surface following the manufacturer's instructions regarding the mixing and applying [27]. Then the strips of one layer were applied on both sides of the specimen by hand in the targeted area. Next the strips were pressed by the epoxy saturated roller in order to insure a full distribution of the epoxy through strip fibers. Last a steel roller was used to press and remove any air bubbles created during the application process (Figures 3.38&3.39).

Figure 3. 38 Applying vertical strips (Retrofitting process)

Figure 3. 39 Applying horizontal strips (Retrofitting Process)

The strengthened composite was subjected to dry curing process for at least 24 hours prior to testing. Figures 3.40and3.41 show the two masonry specimens after strengthening process, respectively.

Figure 3. 40 X-shape strengthened masonry wall

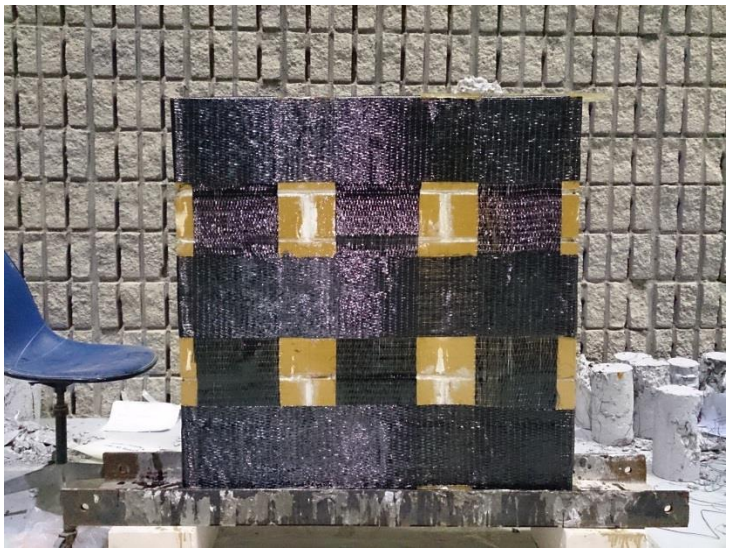

Figure 3. 41 Grid-shape strengthened masonry wall

3.5 Experimental Procedure

In this subsection, all parts constitute the full-scale cyclic test involving test setup, loading system, measuring instrumentation and test sequence will be highlighted here after.

3.5.1 Test Setup and Loading System

The setup used in this study consisted mainly of a steel frame which was constructed on the reaction floor lab at Bldg.26 KFUPM (Figure 3.42). This frame was used to exert the axial as well as lateral load on the specimen. The axial load was exerted on the specimen using Enerpac hydraulic jack which has a capacity of 2000 KN (Figure 3.43) while the lateral load was exerted on the wall using specific equipment fabricated for this test. The equipment consisted of hydraulic jack and controller (Figures 3.44&3.45). The vertical as well as horizontal forces were exerted on the wall through a stiff concrete beam connected to the top of the wall. High strength mortar (BASF EMACO S88C) was used to attach the stiff concrete beam to the top of the wall. This high strength mortar distributes the vertical and horizontal force on the wall uniformly without any stress localization.

Figure 3. 42 Constructed steel frame.

Figure 3. 43 Enerpac hydraulic jack

Figure 3. 44 Hydraulic jack Controller

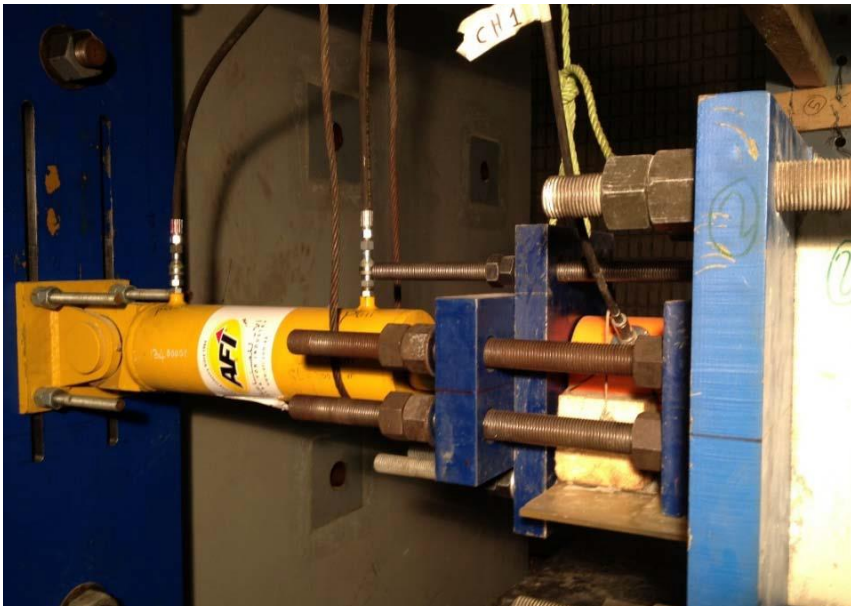

Figure 3. 45 Push Pull hydraulic jack

To complete the experimental setup, firstly the sandstone wall was placed on top of built-up steel section connected firmly to the reaction floor through two high strength big bolts of 5 cm diameter. The wall was then firmly attached to this built-up section. This was achieved by fastening the U base beam supporting the wall to the built-up steel section using two high strength blots. To prevent the wall from sliding in the first course, two L steel sections were used at the two bottom ends of the wall. These two L sections were fastened to the U base beam section using the same bolts used to attach the U base beam to the built-up section. The gap between the L section and the wall was then filled using EMACO S88 CT high strength mortar.

Secondly, the axial force exerted by the Enerpac hydraulic Jack was distributed to the top area of the wall through two beams. One of these beams is a stiff concrete beam fabricated for this purpose. The other beam is a stiff I steel section. At first, the concrete beam was placed and attached to the top side of the wall through a thick layer of high strength mortar EMACO S88 CT. The I steel beam was then placed on top of the concrete beam. The Enerpac hydraulic Jack was then placed on top of the steel I beam. The Enerpac hydraulic jack and the steel beam were stationary in which movements (in-plane and out of plane) was prevented using a set of in-plane and out of plane support using wooden pieces. However, the concrete beam has to move freely in-plane to exert the lateral displacement to the top of the wall. As a result, a set of cylindrical round bars were placed between the steel beam and the concrete beam to allow the stiff concrete beam as well as the top of the wall attached to the concrete beam to move laterally without any obstacles. In addition, in order to prevent the damage of the top side of the concrete beam and also to facilitate the rotation of the round bars, a thick steel plate was

used to cover the top side of the concrete beam. This steel plate was firmly connected to the beam using previously prepared bolts attached to the inner side of the concrete beam at the time of casting.

Finally, the lateral load was transmitted from the horizontal hydraulic Jack to the wall through the concrete beam. One side of the hydraulic Jack was attached to the end of the concrete beam and the other side was reacted against a strong vertical reaction wall. Unfortunately, the horizontal Jack was not designed for recording the exerted load. Due to this limitation, a fabricated setup was prepared and attached to the tip of the horizontal Jack from one side and ending by the stiff concrete beam on the other sided. This fabricated setup allowed recording the lateral load exerted on the wall using only one load cell. The horizontal Jack was then attached to the reaction wall through a thick steel plate and strong hinge that allow only vertical rotation of the hydraulic Jack. The configuration of the whole setup is shown in the following figures (3.46-3.51).

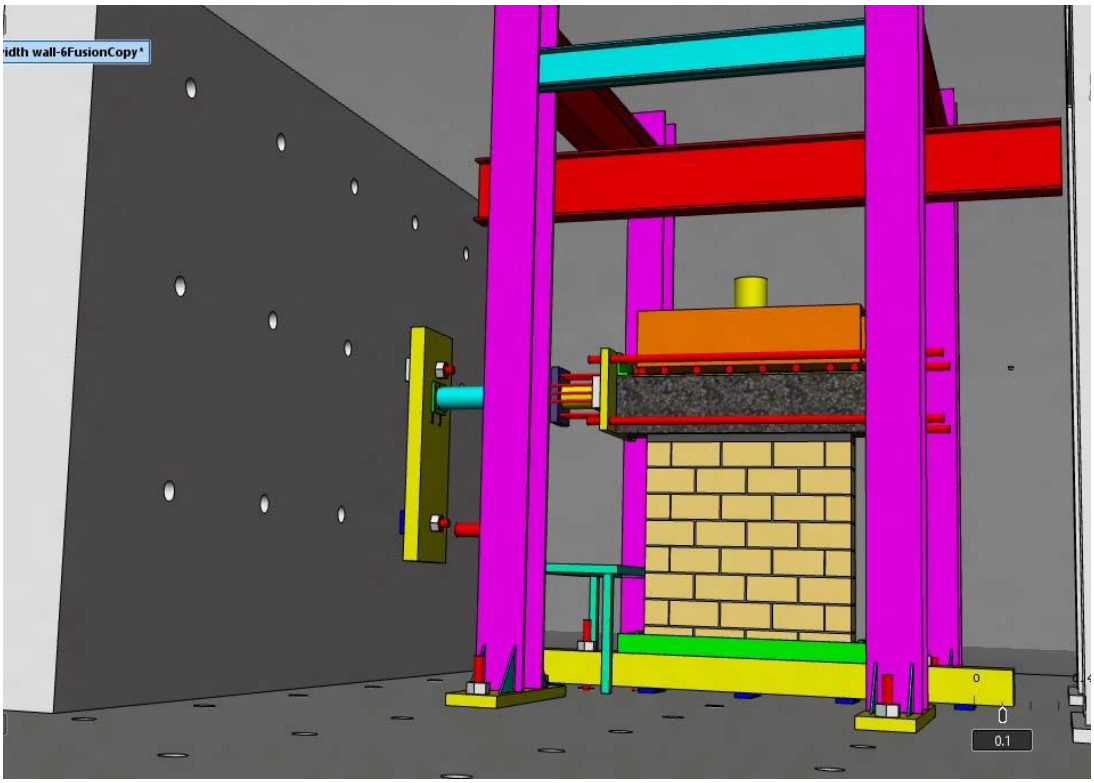

Figure 3. 46 Cyclic test setup (Front view).

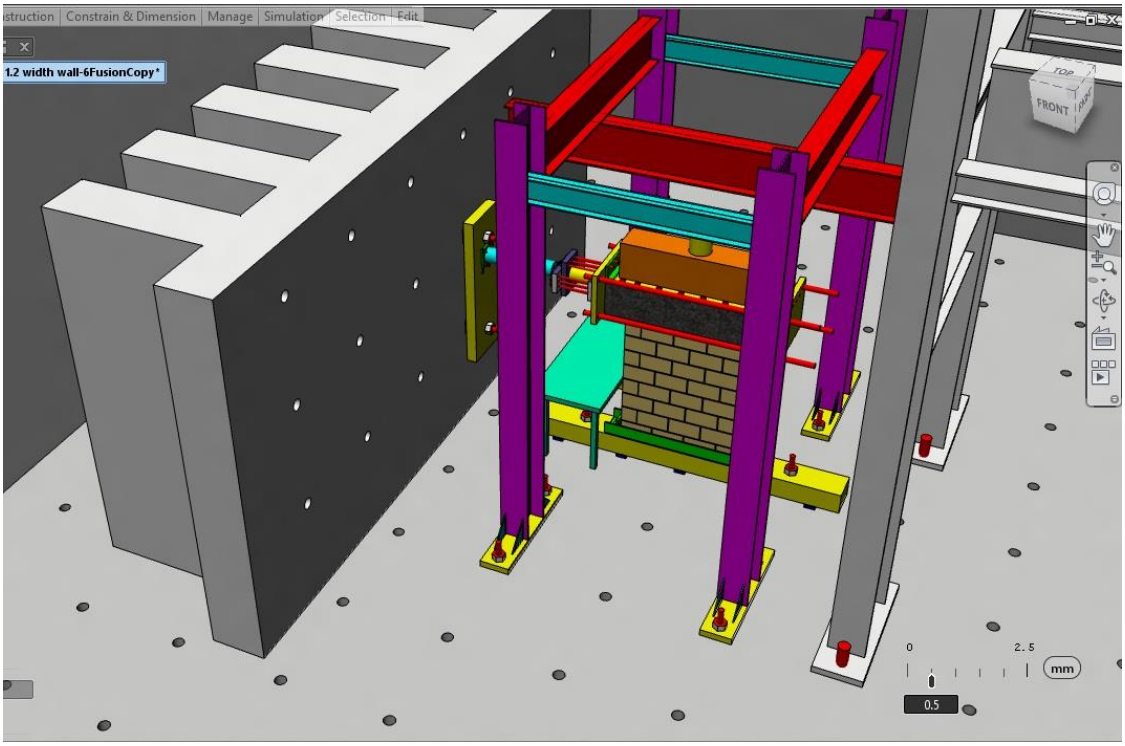

Figure 3. 47 Cyclic test setup (Top view)

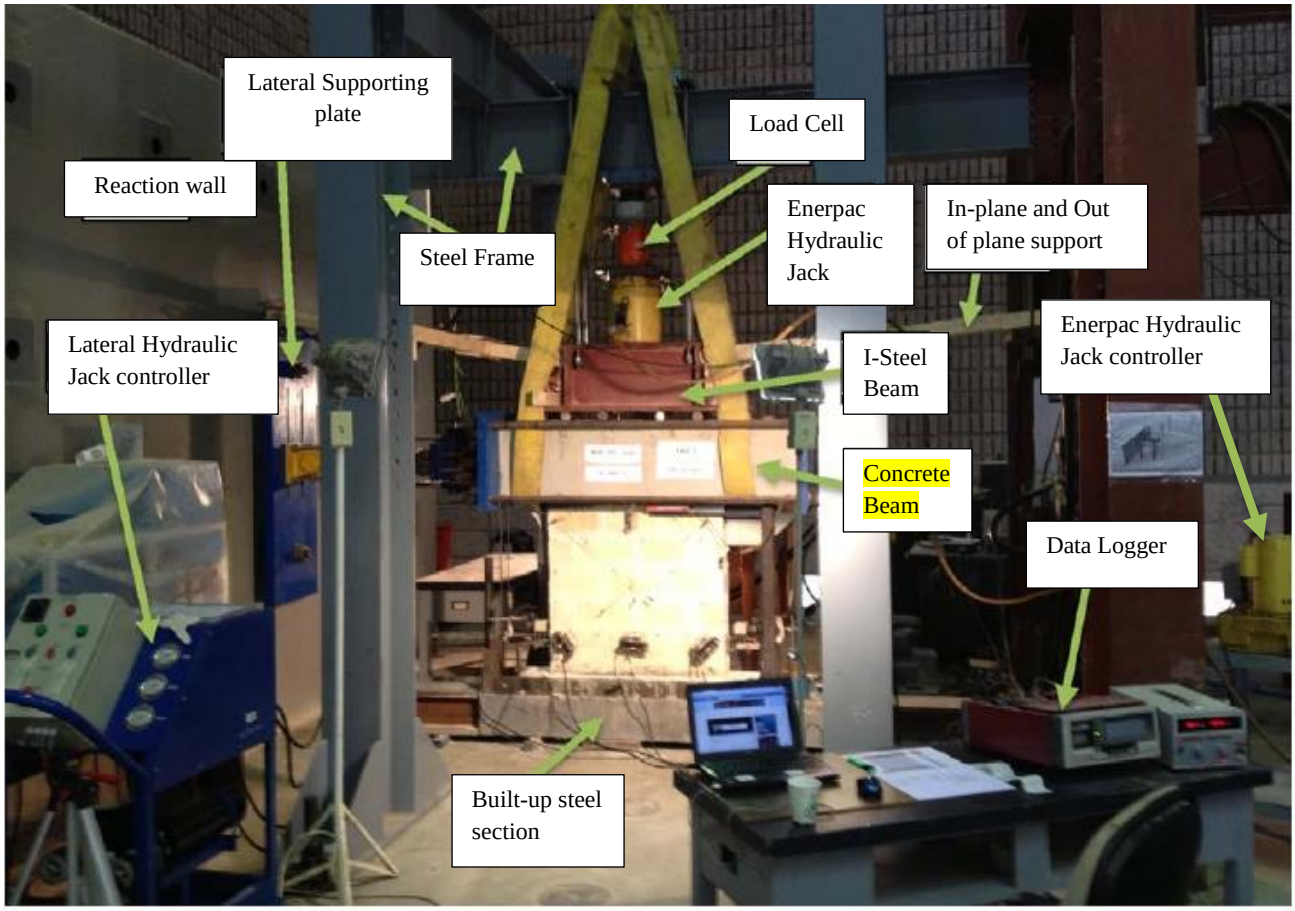

Figure 3. 48 Cyclic test setup of Control wall

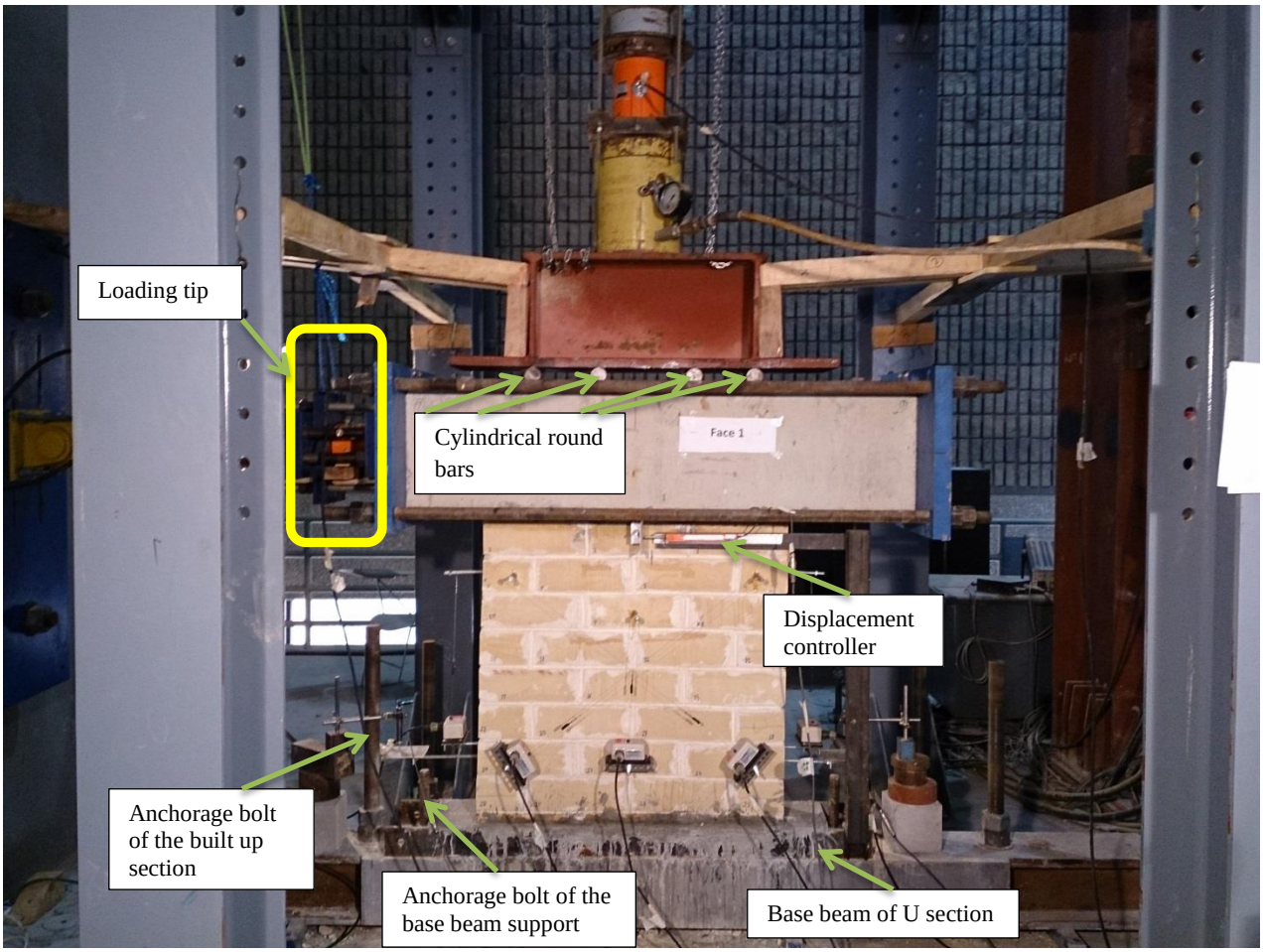

Figure 3. 49 Cyclic test setup of Control wall

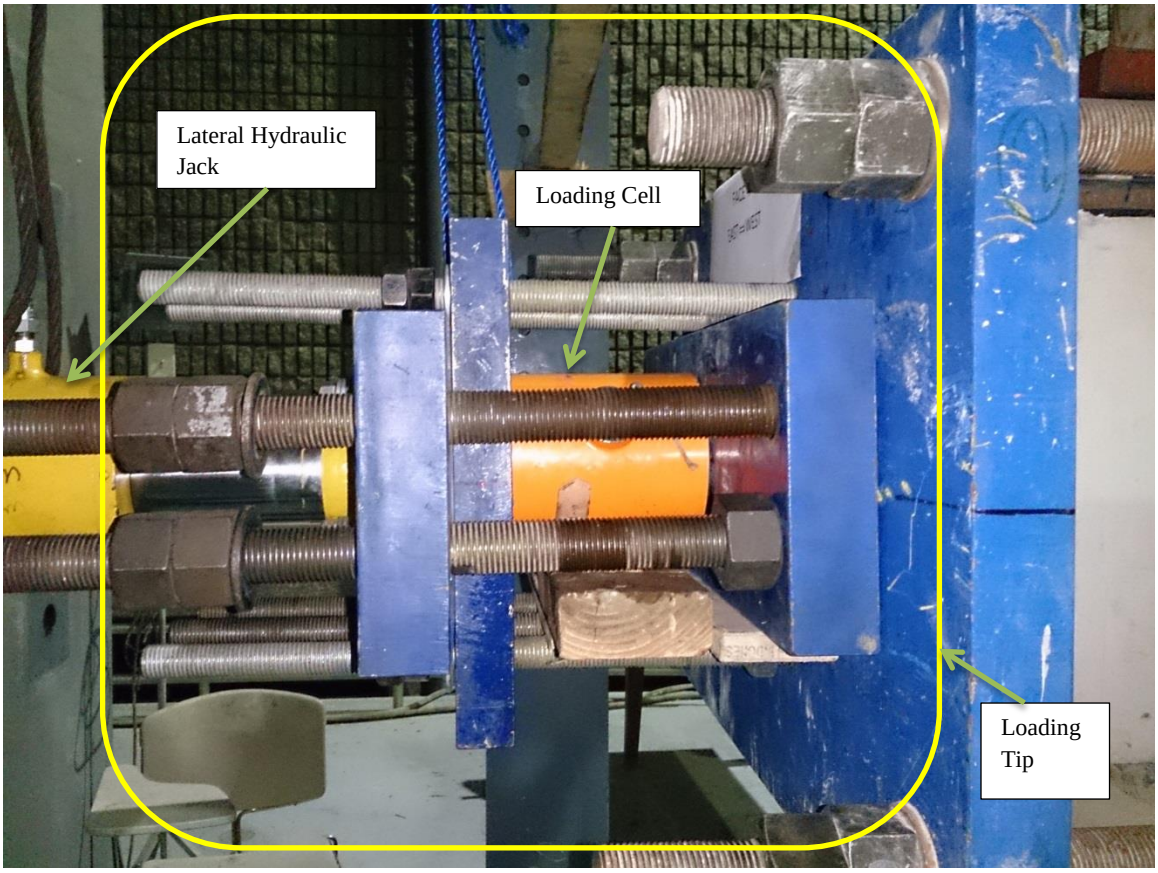

Figure 3. 50 Lateral loading tip

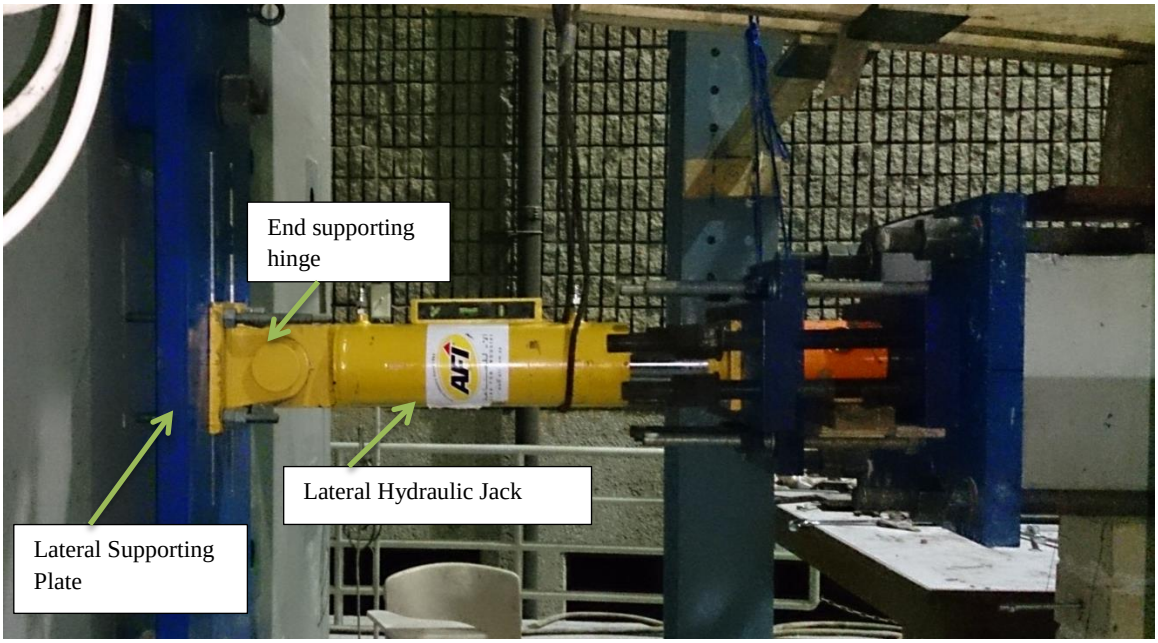

Figure 3. 51 Lateral loading tip

3.5.2 Instrumentation

Instrumentation was used to capture the specimen behavior in the following aspects: i) Applied loads; ii) Overall lateral displacement; iii) masonry and CFRP strips strains. All experimental readings acquired from the measuring instrumentation were recorded through Data Logger. Axial as well as Lateral loading were recorded using load cells. Cable transducer (CDP LVDT-100) was the main instruments for measuring the overall lateral displacement and located at the middle of the top wall. The wall movements and deformations were captured and recorded using several LVDTs attached to the wall at different positions while the CFRP strips strains were captured and measured using strain gauges. Table3.6 clarifies the total number of channels used in the cyclic test and type of those channels based on their readings. Configuration and positions of the measuring instrumentation attached to the wall are shown in figures 3.52 and 3.53.

Table 3. 6 Channels used in the cyclic test

Channel Type	Channel designation	Number
Load Cells	0,1	2
CDP LVDT-100	2	1
PATRIOT LVDT	3,4,5,6,7	5
CDP-25	8,9	2
Total		10

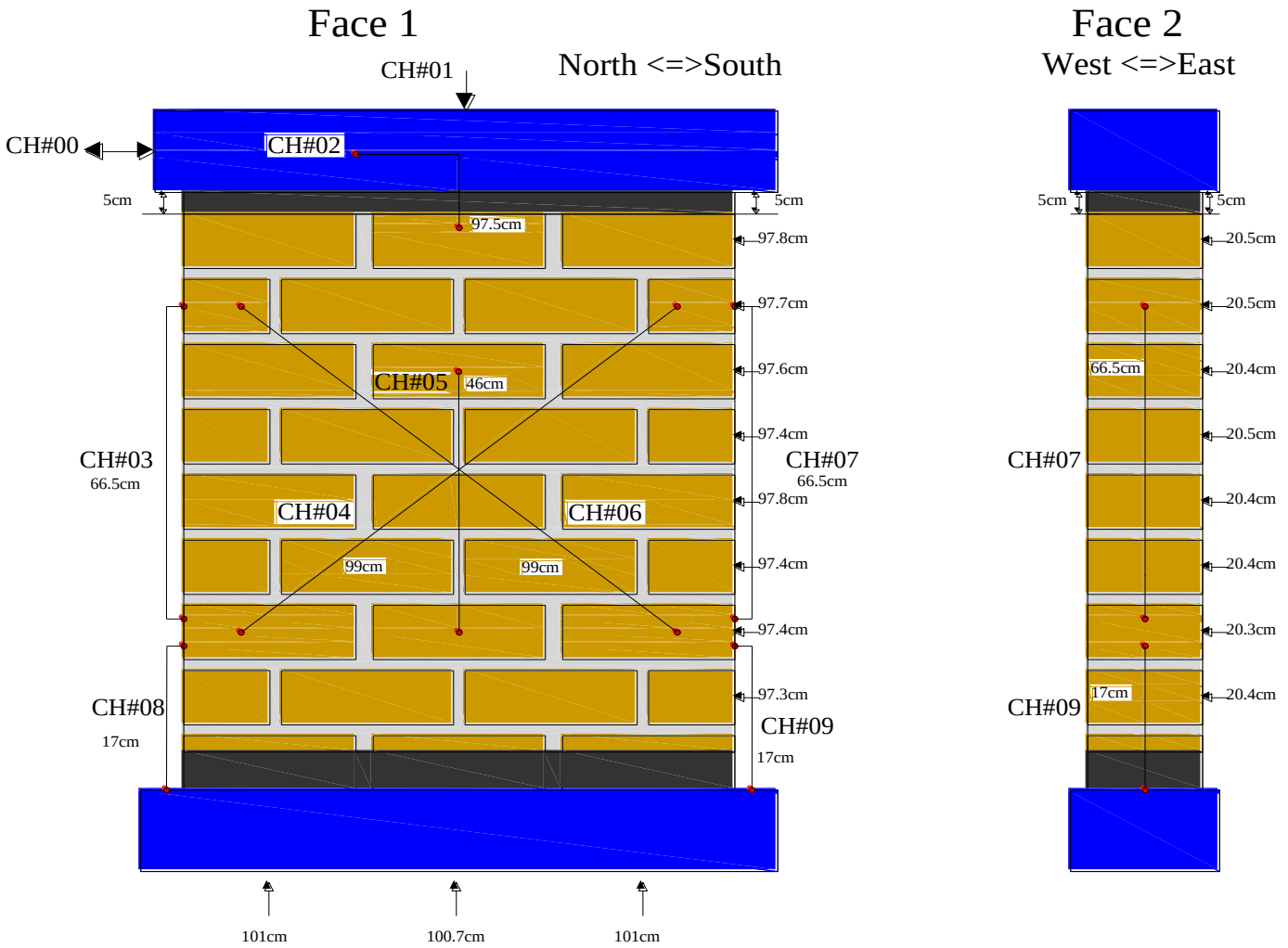

Figure 3. 52 Dimensions and Instrumentation's configuration of the Control specimen

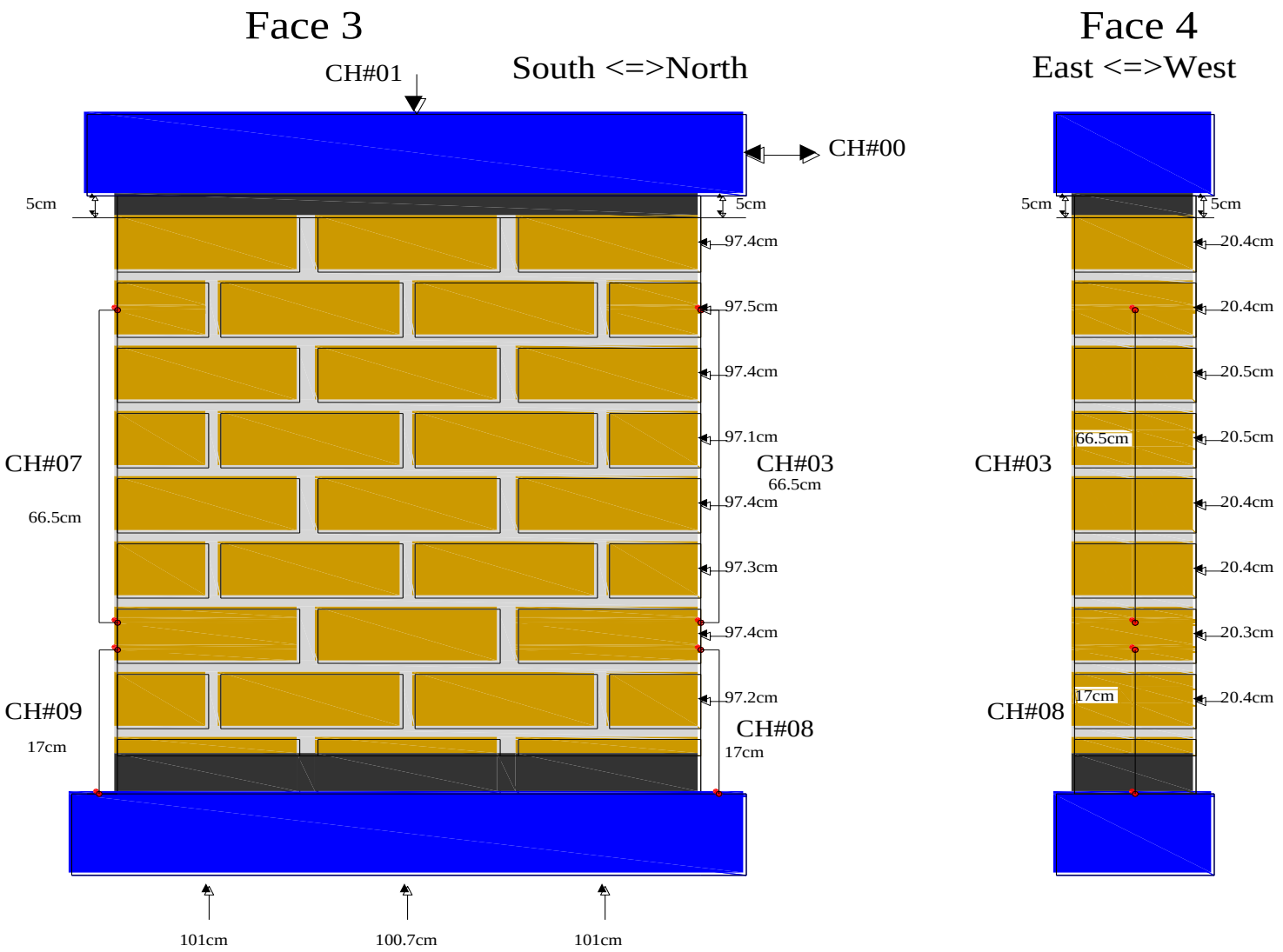

Figure 3. 53 Dimensions and Instrumentation's configuration of the control wall specimen

3.5.3 Testing Sequence

As previously mentioned, a three masonry wall specimens were tested in this study. One of them was unstrengthen (Control wall) while the others were strengthened with different CFRP orientation (X-shape & Grid-shape). During the cyclic test, these specimens were subjected to lateral load increasing incrementally under constant axial load. The axial stresses exerted in this test, varied depending on the specimen. Table 3.7 shows the axial stresses applied on the specimens.

Table 3. 7 Axial stresses exerted in the cyclic test

Name	Axial stress (MPa)
Un-strengthened wall	2
X-shape strengthened wall	2
Grid-Shape strengthened wall	2.55

In the cyclic test carried out on the specimens, firstly the axial loading was exerted slowly with a rate of 1.0 KN/s until it reached to the required axial stress and it was kept constant during the test. The wall was then subjected to a lateral loading in a reversal mode (Push then Pull at each displacement level) using a displacement control load with a loading rate of 0.05 mm/s. The horizontal displacement load was controlled by means of the horizontal CDP LVDT-100 connected to the top central of the wall. The lateral loading adopted in this study was based on the ratio of the top central displacement to the specimen height which called a drift ratio. The amount of the drift ratio exerted on the

wall and the associated lateral displacement levels are illustrated in Table 3.8. The cyclic lateral loading program applied on the specimens is shown in Figure 3.54.

Table 3. 8 Cyclic lateral loading

Cyclic Loading			
No.	Drift ration	Push	Pull
	%	mm	mm
1	0.05%	0.5	-0.5
2	0.10%	1.0	-1.0
3	0.25%	2.5	-2.5
4	0.50%	5.0	-5.0
5	0.75%	7.6	-7.6
6	1.00%	10.1	-10.1
7	1.25%	12.6	-12.6
8	1.50%	15.1	-15.1
9	2.00%	20.2	-20.2

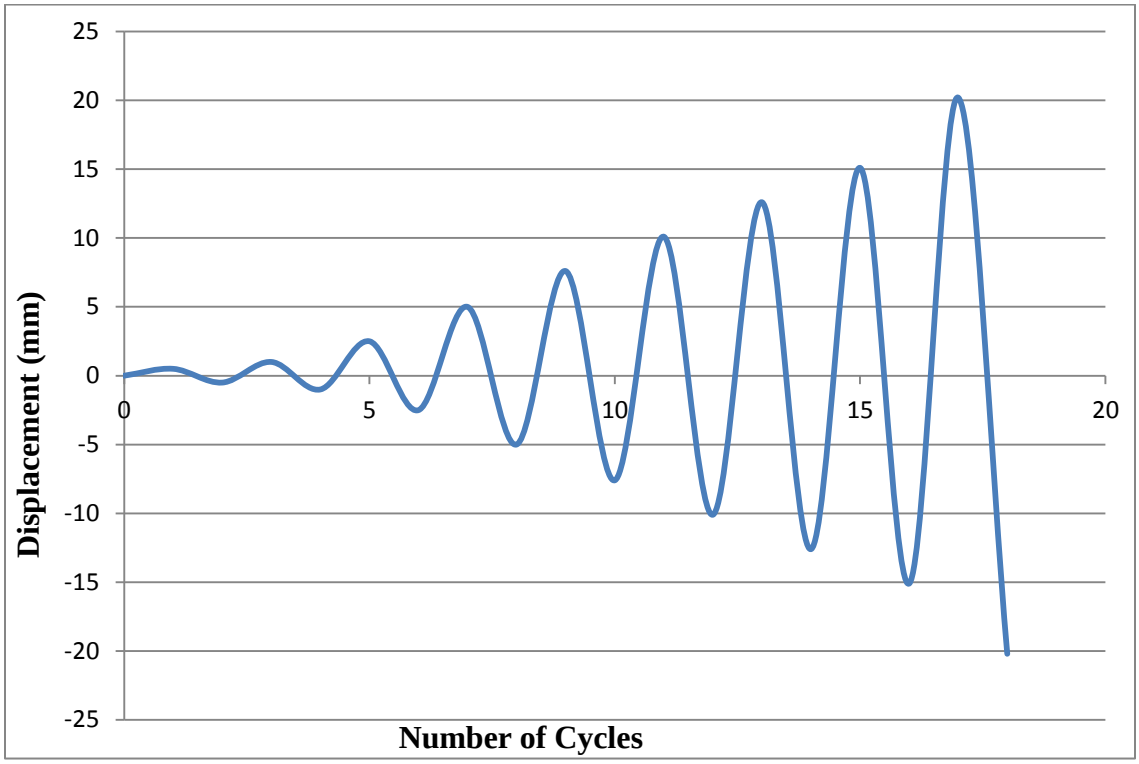

Figure 3. 54 Cyclic Lateral Loading Program

CHAPTER 4

OBSERVATION AND TEST RESULTS

4.1 Introduction

Observed behavior of the cyclic test specimens regarding progressed cracking pattern and failure mode are described in this chapter. These specimens are fully described regarding its dimension, strengthening, test set-up, loading systems and testing procedure in the previous chapter. In addition, cyclic test results in terms of lateral strength, stiffness and energy dissipation are presented hereafter, making use of hysteresis-loop diagrams of relation between the lateral force and the attained displacement. These diagrams are plotted based on the recorded data acquired from the measuring instruments during the cyclic test. Finally, the enhancement gained using CFRP strengthening technique with different configurations is thoroughly discussed by comparing the strengthened specimens with unstrengthened one in terms of the investigated parameters.

4.2 Unstrengthened Wall Specimen

The control specimen was subjected to cyclic loading in order to observe its deficient parameters so as it can be compared with the strengthened ones. This specimen was subjected first to axial load increasing slowly until it reached to the designated value (Table 3.7) and it was kept constant during the test. The specimen was then subjected to cyclic lateral loading. Starting from cycle 3 and through cycle 4, it can be noted that the first cracks were initiated at the bottom left and right corner introducing the rocking failure. These cracks primarily existed in the joints which represent the weaker part of the

masonry system. However, with the consecutive cycles, the cracking pattern took another form and started to initiate within the specimen body in the head and bed joint and the sandstone units itself as well. As the exerted lateral drift was increased, new cracks arose and the existing cracks got wider accompanying with louder noises. As a result, the failure mode can be considered as a combination of rocking and staggered head and bed joint failure. Figures 4.1- 4.6 illustrate the development of the cracking pattern and the associated failure mode throughout the various levels of lateral displacement.

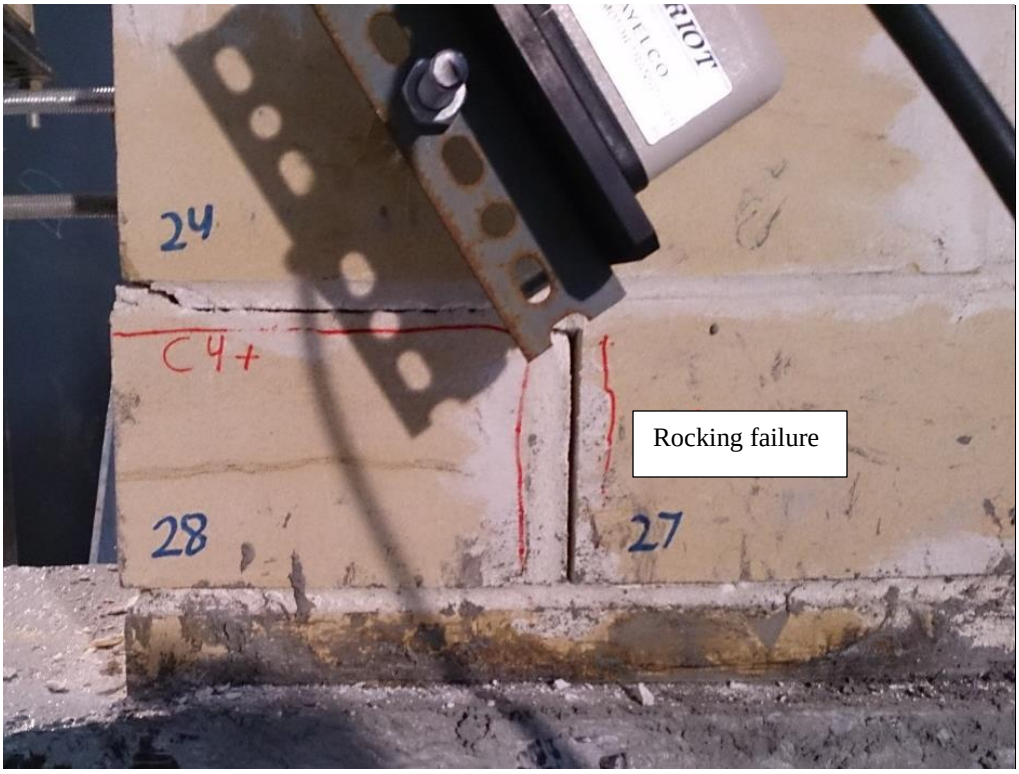

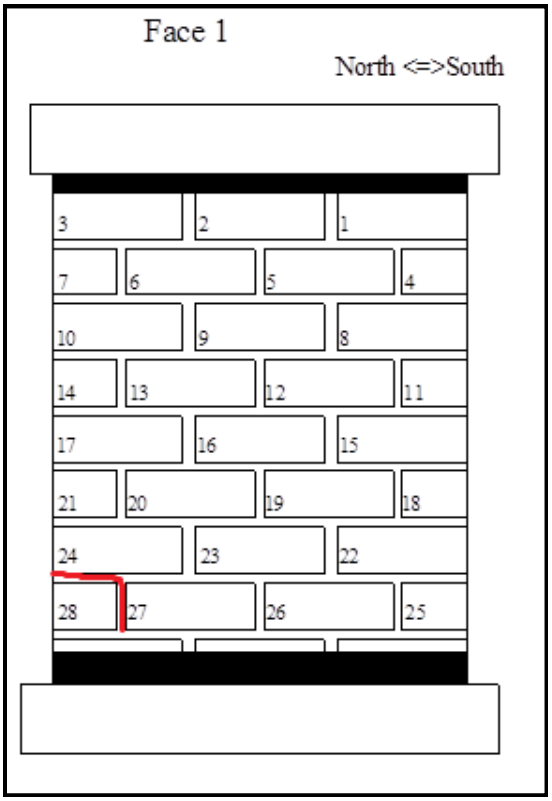

Figure 4. 1 cracking pattern of unstrengthened specimen and its corresponding position

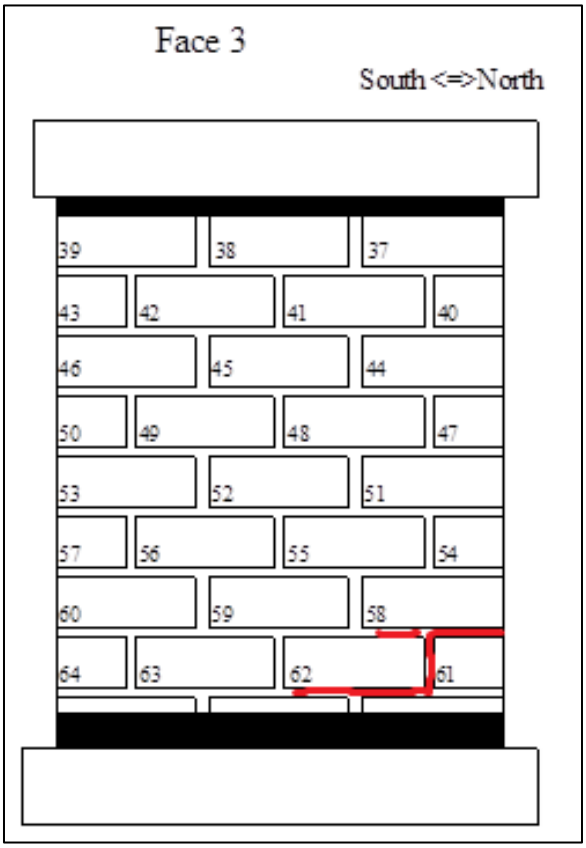

Figure 4. 2 cracking pattern of unstrengthened specimen and its corresponding position

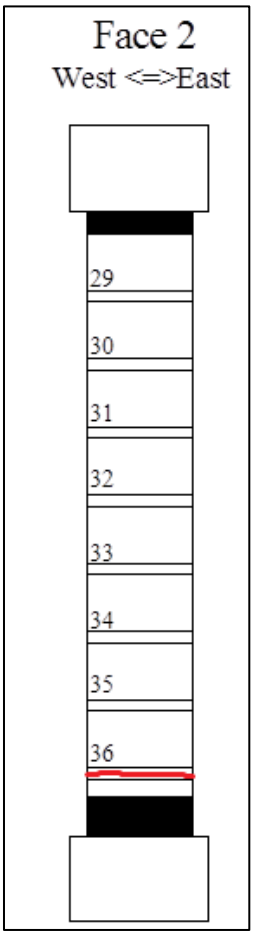

Figure 4. 3 cracking pattern of unstrengthened specimen and its corresponding position

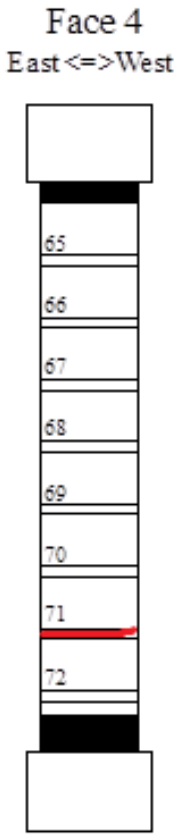

Figure 4. 4 cracking pattern of unstrengthened specimen and its corresponding position

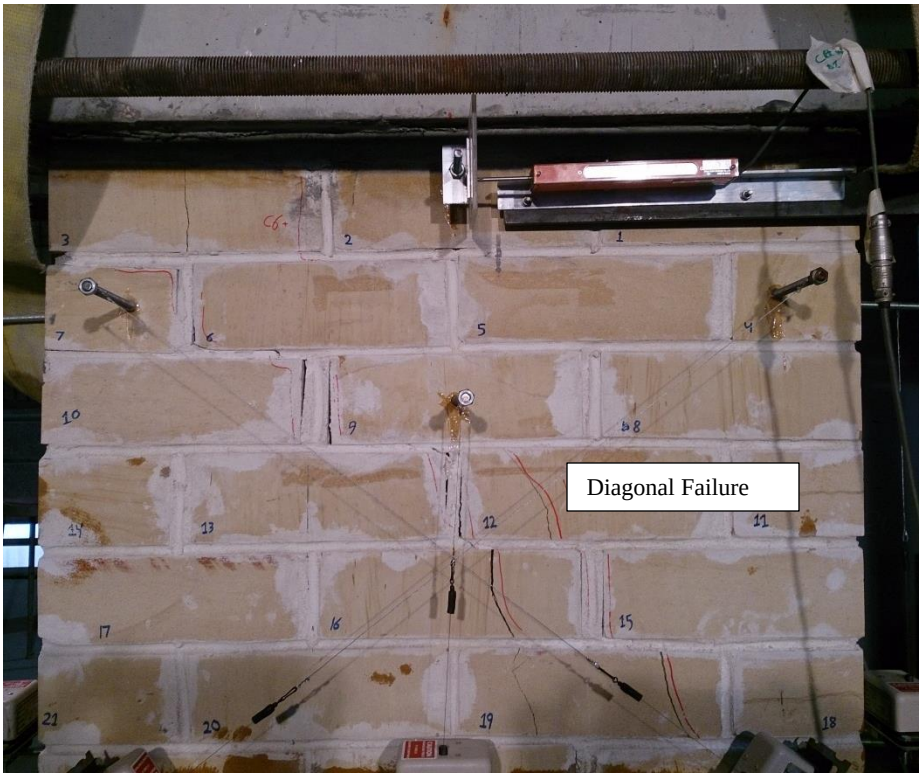

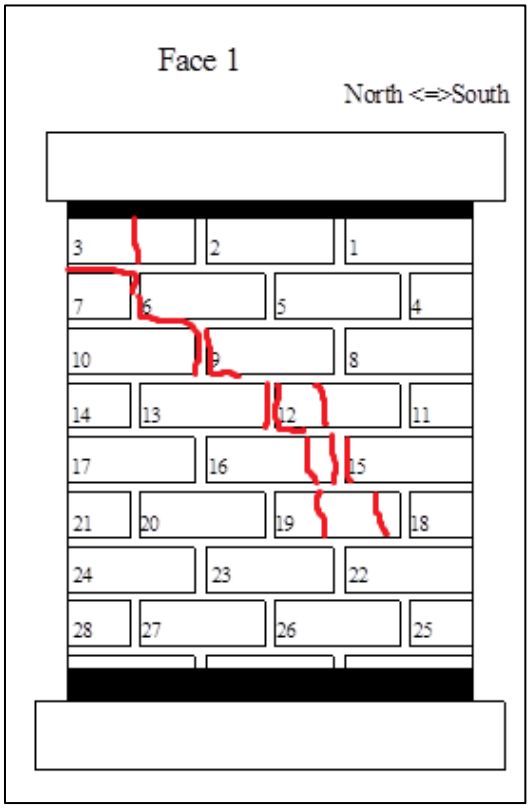

Figure 4. 5 cracking pattern of unstrengthened specimen and its corresponding position

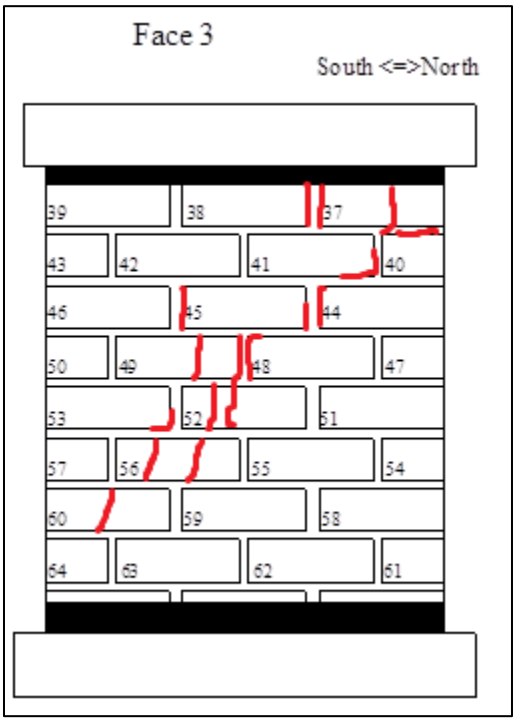

Figure 4. 6 cracking pattern of unstrengthened specimen and its corresponding position

We have to point out that only 6 of 9 cycles (Table 3.8) were completed in this cyclic test due to safety consideration. The complete hysteresis-loop diagram of the test specimen relating the lateral load against the horizontal displacement is shown in Figure 4.7.

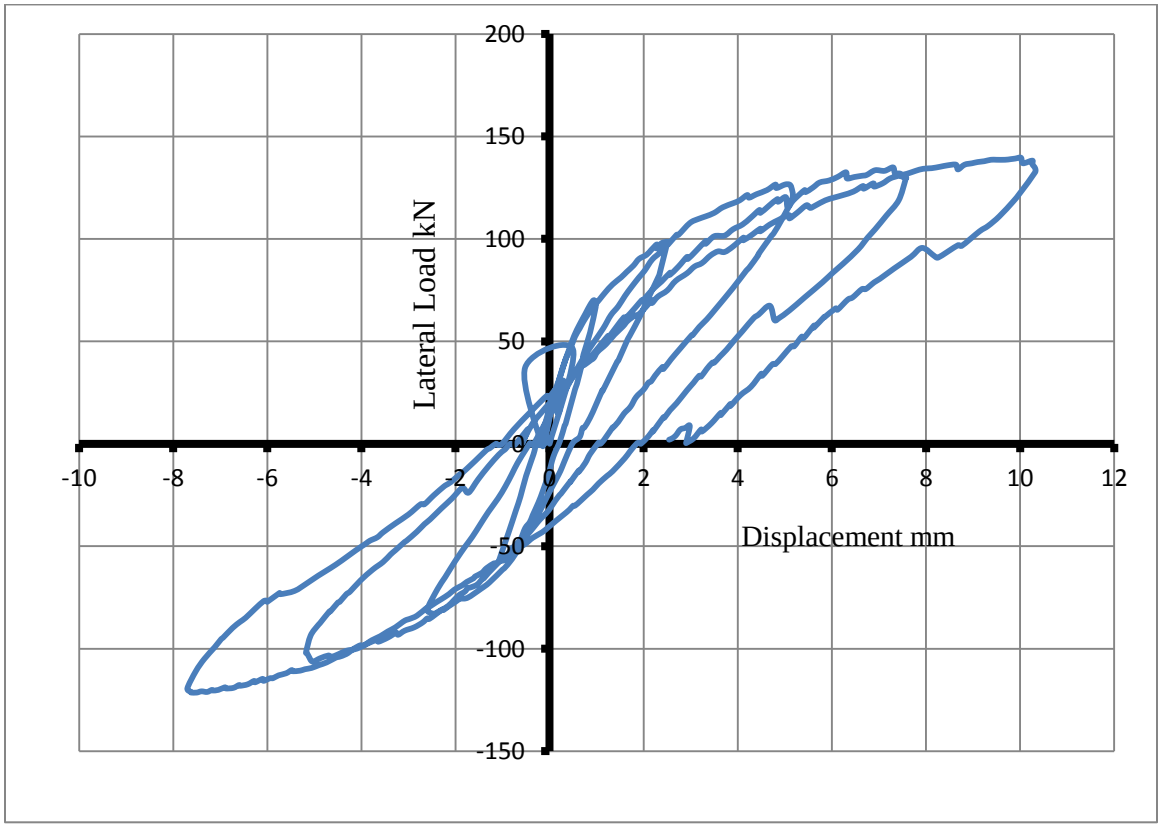

Figure 4. 7 The Lateral Force-Deformation Hysteresis Loop Diagram for Unstrengthened specimen

According to Figure 4.7, it can be observed that the lateral force-deformation curve was increasing linearly up to certain limit confirming that there is a negligible permanent deformation at the first three cycles. Furthermore, it can be noted that the specimen had a high stiffness in these cycles and the lateral strength increased significantly in these cycles. After cycle 3, the curve was noticed to increase slowly comparing with the former cycles as the exerted lateral displacement was increased. As a result, the specimen started to behave nonlinearly and permanent deformation became visible. In addition, the diagram showed noticeable stiffness reduction starting from cycle 4 which referred to the damage happened to the specimen in both sandstone and lime mortar material. Regarding energy dissipation which is the area created under the lateral load – deformation curve, it is evident that the specimen attained high energy dissipation especially after cycle 3 which indicates that the cracks started to initiate from that point. Finally, it can be recognized that the as-built specimen suffers from the stiffness degradation, energy dissipation and combined failure mode when subjected to cyclic loading.

4.3 X-Shape Strengthened Wall Specimen

This specimen was strengthened by a single layer of CFRP on both sides forming X-shape, and then it was subjected to the same loading system exerted to the unstrengthened specimen to evaluate the enhancement gained from this strengthening technique (Figure 4.8). Apart from the small cracks occurred along the lower course of the specimen (Figures 4.9&4.10) due to the excessive rocking behavior during the test, no other cracks were detected within the whole specimen. Also, it was noted that no delamination

happened between CFRP and the specimen and also no fracture of CFRP except at the bottom corners as shown in Figures 4.11-4.13.

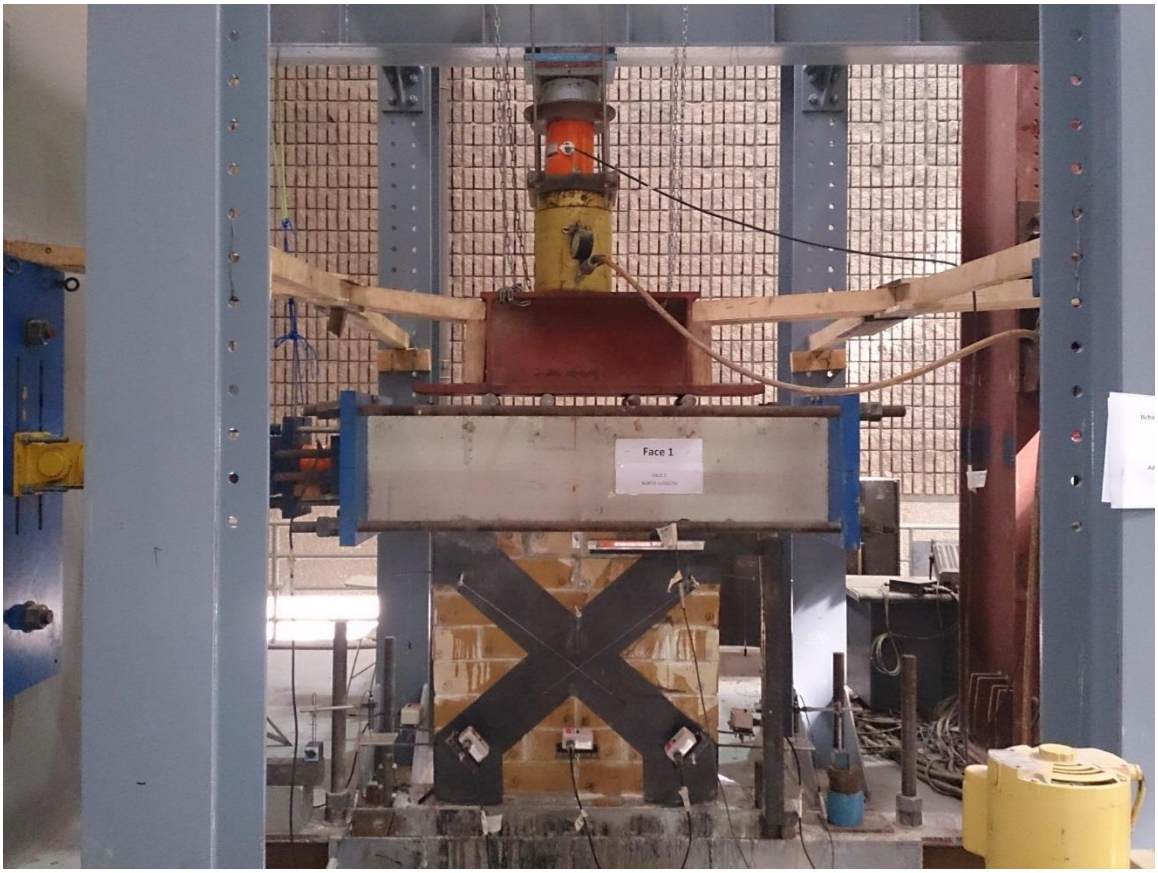

Figure 4. 8 X-Shape Strengthened specimen under test

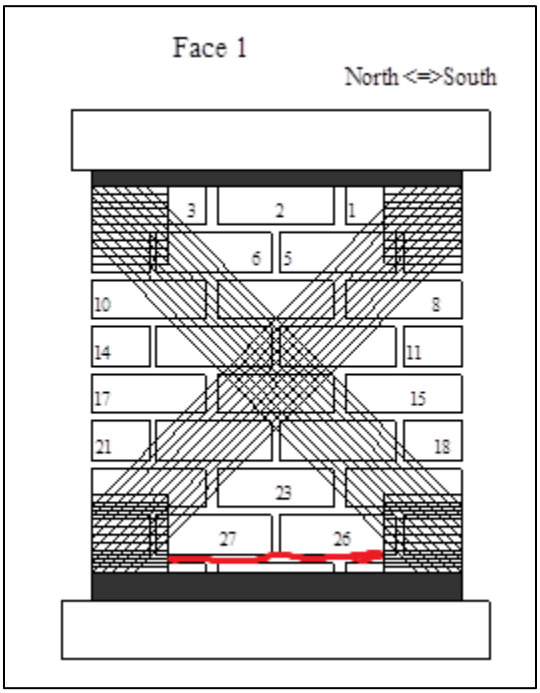

Figure 4. 9 cracking pattern of X-shape strengthened specimen and its corresponding position

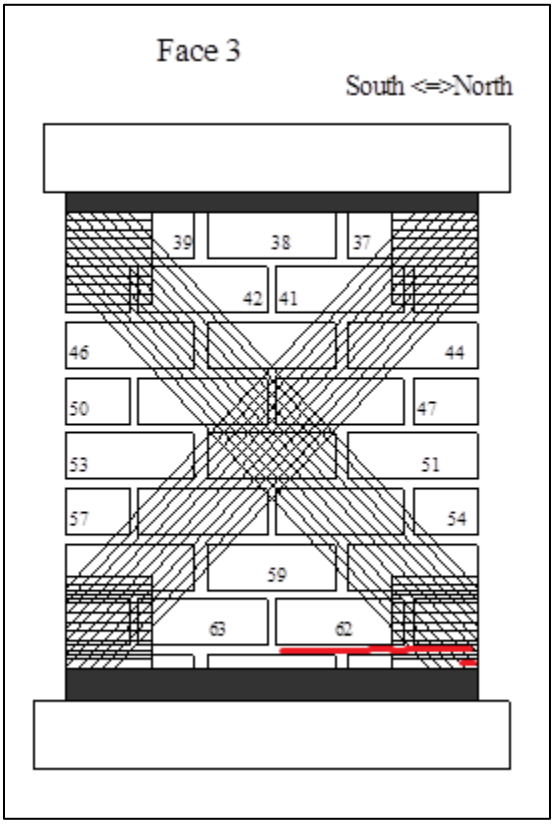

Figure 4. 10 cracking pattern of X-shape strengthened specimen and its corresponding position

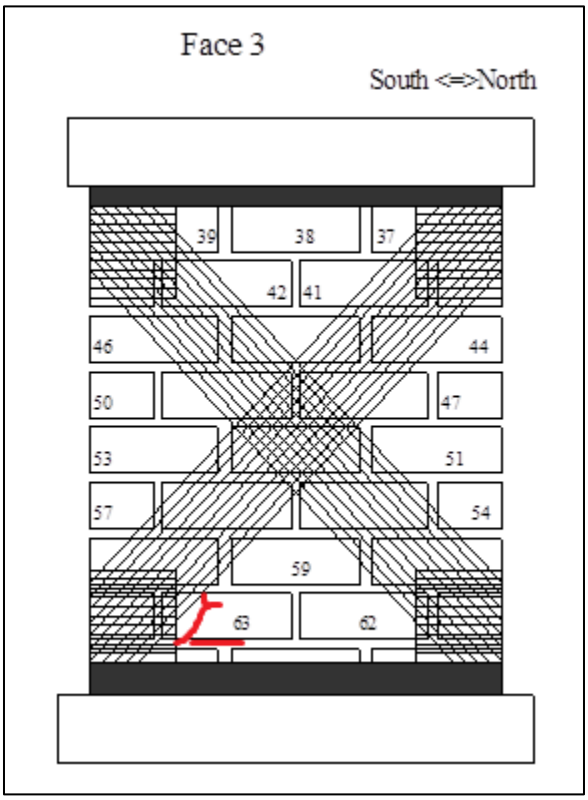

Figure 4. 11 cracking pattern of X-shape strengthened specimen and its corresponding position

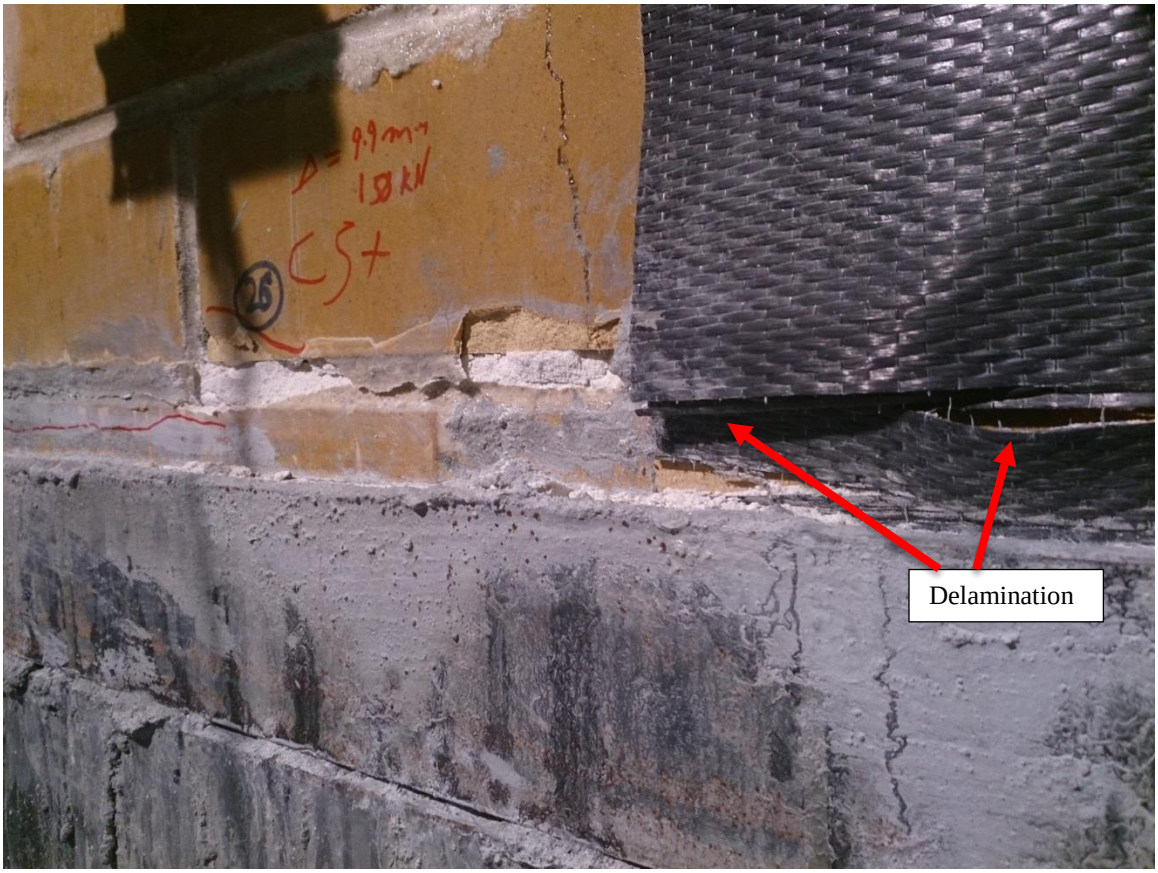

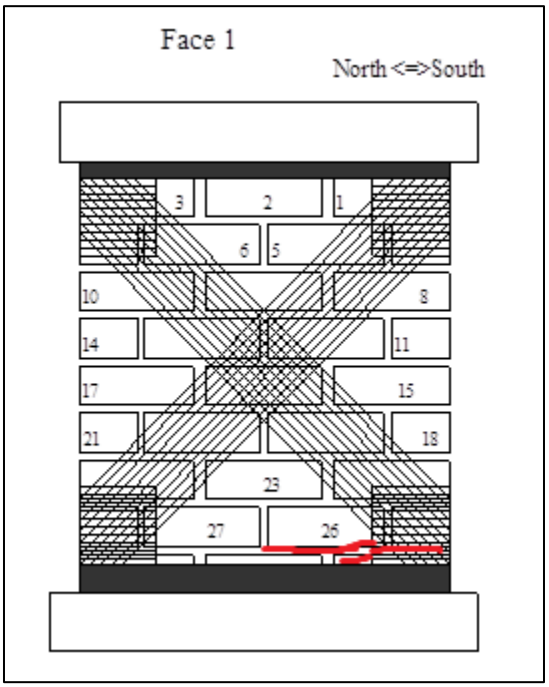

Figure 4. 12 cracking pattern of X-shape strengthened specimen and its corresponding position

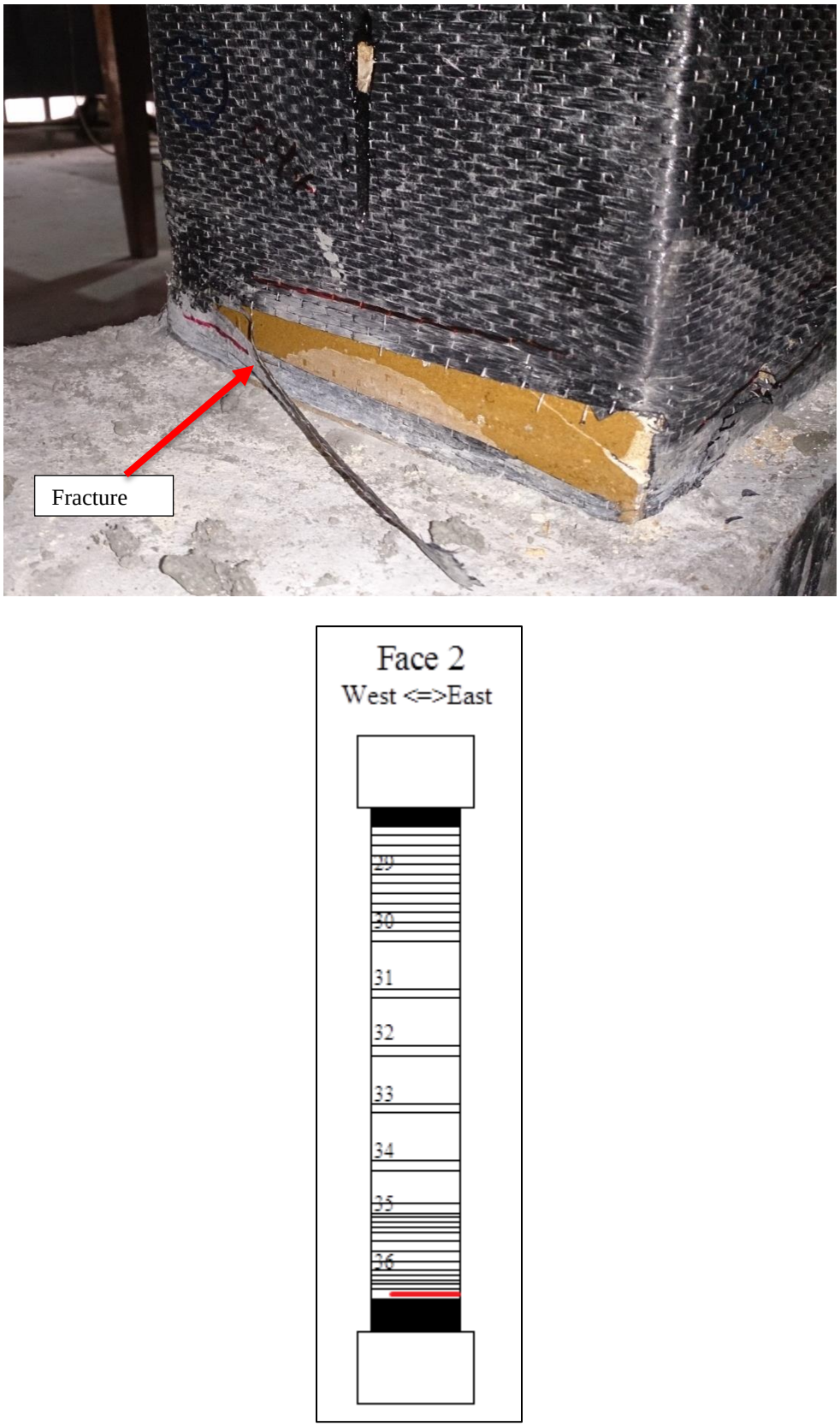

Figure 4. 13 cracking pattern of X-shape strengthened specimen and its corresponding position

It has also to be noted that during the test, some attention-grapping sounds were heard from the test specimen specifically from the CFRP, indicating that it started to work as a strengthening material. Afraid of the excessive rocking behavior of the test specimen, a decision has been made to stop the test at cycle 6 regarding safety considerations. The complete hysteresis-loop diagram of the test specimen relating the lateral load against the horizontal displacement is shown in Figure 4.14.

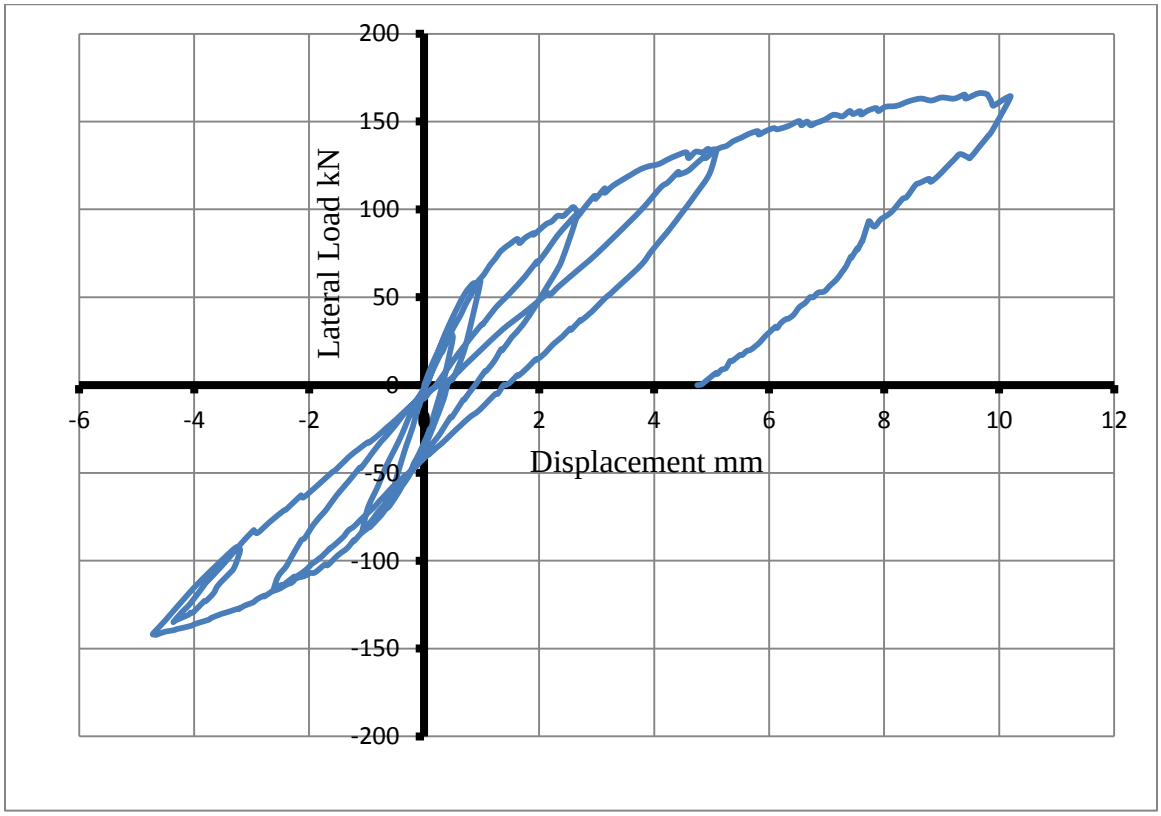

Figure 4. 14 The Lateral Force-Deformation Hysteresis Loop Diagram for X-shape strengthened specimen

According to Figure 4.14, it can be observed that the lateral force-deformation curve was increasing linearly up to certain limit confirming that there is a negligible permanent deformation at the first three cycles similar to the unstrengthened specimen. Furthermore, it can be seen after cycle 3 that the lateral force-deformation curve of the x-shape strengthened specimen developed in a stiff manner a little more compared to the unstrengthened one. However, the specimen experienced a permanent deformation as the lateral load increased due to the tendency of the specimen to overturn as a single body. Also, an improvement in the lateral strength can be noticed from the strengthened specimen compared to the unstrengthened one which confirms the primary purpose of the CFRP strengthening technique. Finally, it is clearly observed that less energy was dissipated during all the displacement levels due to the absence of pronounced cracking initiation within the specimen body.

4.4 Grid-Shape Strengthened Wall Specimen

This specimen was strengthened on both sides with different CFRP layout forming grid pattern and then it was subjected to the same loading system exerted to the X-shape strengthened specimen to evaluate its effectiveness compared with the previous layout (Figure 4.15). It was noted that no visible cracks initiated within the specimen during the cyclic test except a tiny crack occurred at the right bottom corner due to the rocking behavior and an ineffective delamination happened at that spot as well as shown in Figure 4.16. It has also to be noted that during the test, some attention-grapping sounds were heard from the strengthened specimen, indicating that the CFRP started to work as a strengthening material.

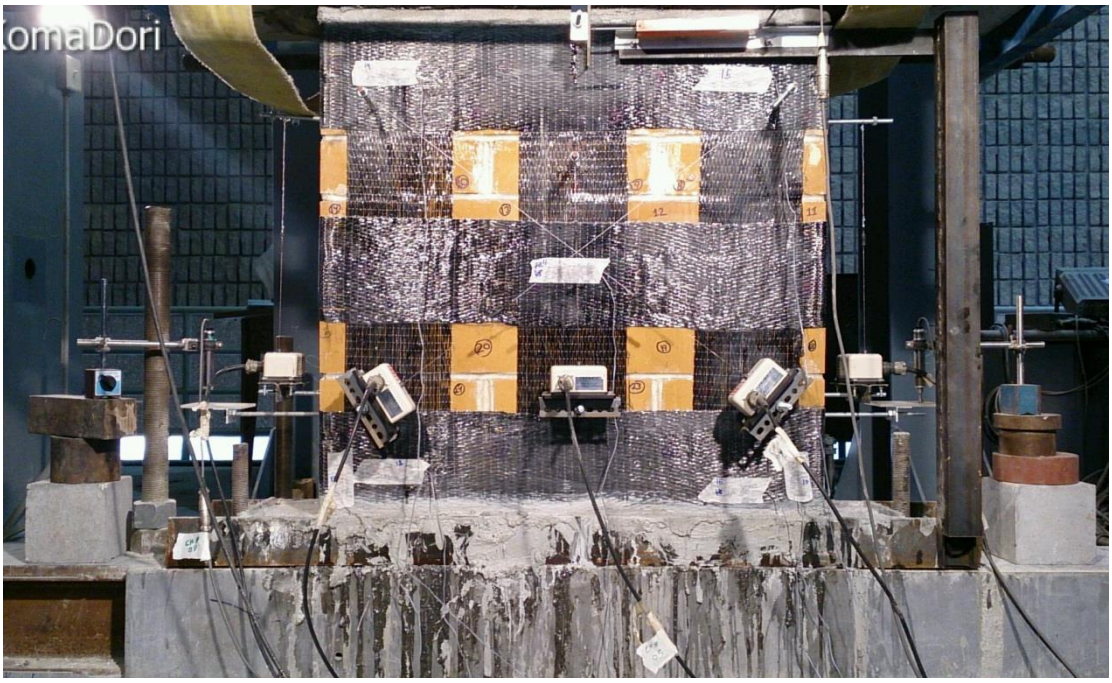

Figure 4. 15 Grid-Shape Strengthened specimen under test

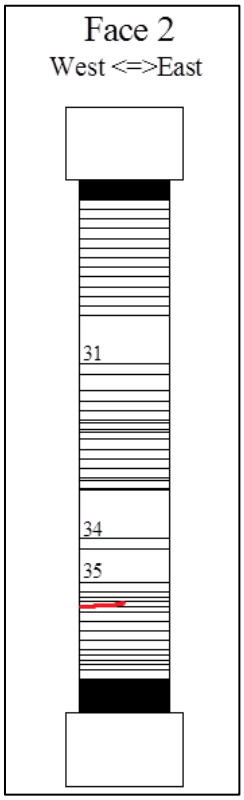

Figure 4. 16 cracking pattern of Grid-shape strengthened specimen and its corresponding position

Afraid of ruining the load cell, which is responsible to measure the applied lateral load, due to exceeding its capacity limit, a decision has been made to stop the test at cycle 6. The complete hysteresis-loop diagram of the test specimen relating the lateral load against the horizontal displacement is shown in Figure 4.17.

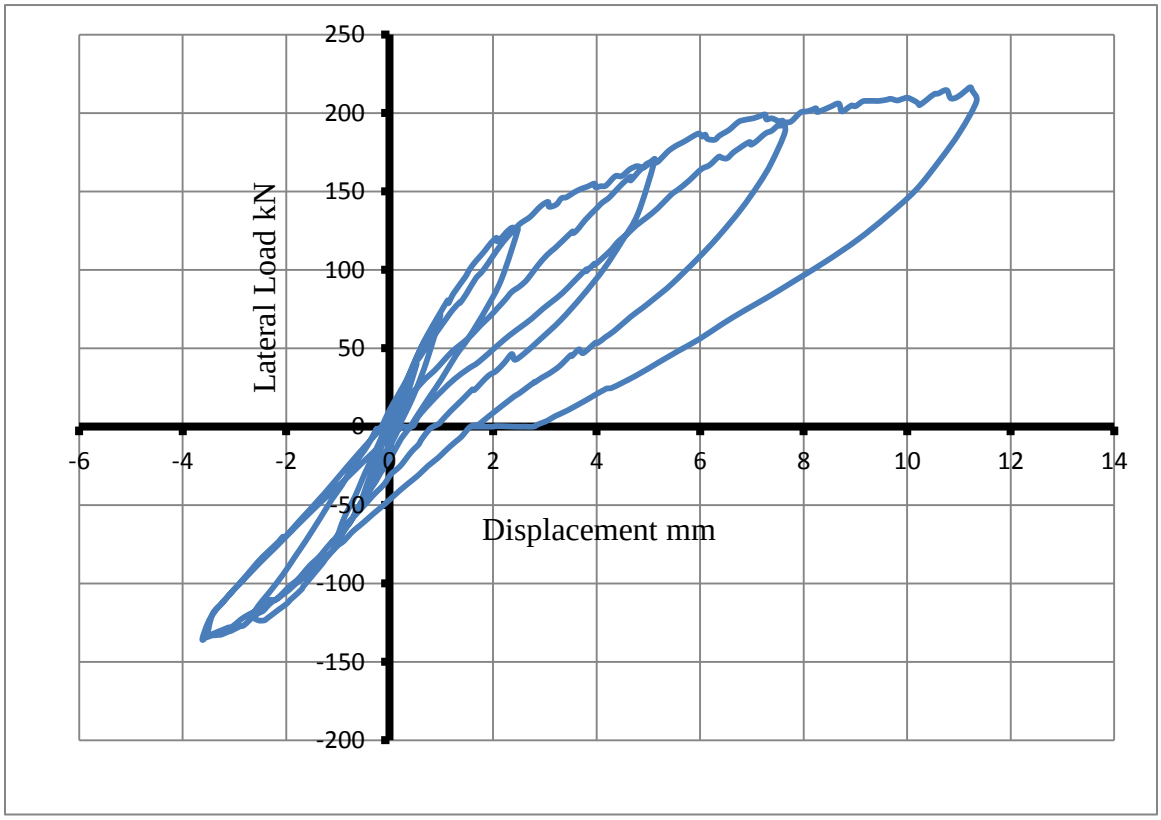

Figure 4. 17 The Lateral Force-Deformation Hysteresis Loop Diagram for Grid-shape strengthened specimen

According to Figure 4.17, it can be observed that the lateral force-deformation curve was increasing linearly up to certain limit confirming that there is a negligible permanent deformation at the first three cycles. After cycle 3, it can be noticed that the lateral-force deformation curve development was stiffer and increased in a constant rate. Also, it can be noted that this specimen did not experience pronounced permanent deformation during all cycles in contrast to the X-shape strengthened specimen. Furthermore, it is evident that the lateral strength was highly developed compared with the other specimen disregard of the slight difference of the axial stress exerted between the two specimens. Finally, it can be observed from this loop diagram that the dissipated energy was a little more compared to X-shape specimen due to invisible cracks happened within the area covered by the CFRP sheets.

4.5 Results Discussion

According to the cyclic test results observed and recorded, it is proved that the quasistatic loading approach is practically effective in terms of capturing the damage evolution and measuring the attained forces and displacements throughout the test.

Regarding the unstrengthened specimen, the rocking failure is first inspected in the lower corners of the specimen due the high tensile stress created in that spot. This tensile stresses are credited to the lateral load accompanying with the constant axial load applied on that specimen. This loading combination produces internal stresses which are responsible to initiate the cracking, specifically in the lime mortar due to its low capacity. Consequently, the unstrengthened specimen is dominated first by the rocking failure. To continue the test and get a shear failure mode, a strip of CFRP was wrapped along the whole first course in order to avoid excessive rocking in the specimen. After that, as the

lateral load increased, the created internal stresses induced to initiate cracking, especially in the head and bed joints due to its weakness introducing the staggered head and bed joints failure, then with increasing the lateral load, the masonry units start to suffer from the cracks initiated within their bodies. These cracks are forming approximately in diagonal shape because the principal stresses resulting from the internal stresses approach nearly to 45º.

Furthermore, it can be observed that there is a strong relationship between the first splitting of the joint from the masonry unit and first noticed stiffness degradation in the hysteresis-loop diagram. This phenomenon could point out to the vital role of the joint in the masonry system when subjected to the seismic loading.

After investigating the unstrengthened specimen experimentally, it is cleared that it is suffered from the low capacity of the sandstone wall materials made of when subjected to cyclic loading. Regarding this deficiency in the masonry specimen, the CFRP was proposed as a strengthening material because it is well-known for its high tensile capacity.

From testing the CFRP strengthened specimens, it was noticed that two factors are governed their behaviors. First factor is the lateral strength which enhanced significantly. Regarding this factor, it was reported that the maximum lateral strength attained during the test for X-shape and Grid-shape strengthened specimens was 18.7% and 48.8% more than the unstrengthened specimen, respectively which confirms the primary purpose of the CFRP strengthening technique. Second factor is the bonding strength between the CFRP and the specimen substrate which considers as the most critical point in the

strengthening technique. In this study, no pronounced debonding was noticed except ineffective delamination occurred at the lower course of the specimen.

In accordance to the cyclic behavior of the X-shape strengthened specimen resulted experimentally, it was observed that there was a permanent deformation, especially appeared at the last cycle as shown previously in Figure 4.14. This is attributed to continuing the test by applying the lateral displacement levels only in the pushing direction beyond cycle 4 due to exceeding the capacity limitation in the pulling direction. As a result, excessive rocking behavior controlled the specimen response showing permanent deformation visibly observed. Hence, the test was stopped at the end of the cycle 6 in order to avoid overturning of the specimen regarding safety requirements. This resulting rocking behavior taken place due in part to the CFRP strengthening technique which promotes the specimen to act as a one body.

No observed cracks and failure mode within the grid-shape strengthened specimen could be attributed to the advantage gained from the overlapping of the horizontal CFRP strips over the vertical ones. This overlapping prevents the development of cracks and debonding, especially in the critical locations. However, it was concluded that this layout is not feasibly economical due to high consumption of CFRP strips.

CHAPTER 5

FINITE ELEMENT MODELING ANALYSIS OF SANDSTONE MASONRY WALL SPECIMENS

5.1 Introduction

The FEM analysis is considered as a practical tool to assess the behavior of URM structures subjected to in-plane loading without experimentally testing them. Regarding the vital role of this method, a number of available commercial FE software have become more popular these days in modeling such structures having complex geometry and boundary conditions.

In this aspect, a three dimensional model of the tested specimens has been developed using ABAQUS environment package. ABAQUS, which is a SIMULIA - Dassault Systèmes product, offers a great facility and varied options to simulate these specimens using the accurate model. This developed model were subjected to the same loading protocol exerted in the full-scale cyclic test, then a comparative study was carried out between the experimental results with modeling one in order to validate the generated model. Consequently, it can be used in conducting many simulating tests with different scenarios. It has also to be mentioned that a non-linear FEM analysis has been conducted on the unstrengthened specimen and those strengthened using CFRP as well in order to simulate their behavior against cyclic loading and illustrate the strengthening role

performed by CFRP. This analysis was based on a concrete plastic damage (CDP) model which is incorporated in ABAQUS.

In this chapter, forming the model step by step has been highlighted. Additionally, the FEM analysis results including stress and plastic strain contours are presented. Also, the generated lateral load-displacement hysteresis loop diagrams are displayed and compared with that experimentally obtained.

5.2 Model Creation

Applying a micro analysis approach, a three dimensional model was created for the tested specimens in which sandstone and lime mortar were modeled as continuum solid elements while CFRP laminate as continuum shell element. This approach offers a great opportunity to capture the cracks within lime mortar and sandstone separately.

First, All the parts forming the model was defined geometrically following their typical dimensions and then they were assembled in order resembling the actual specimen as shown in Figure 5.1.

In this model, an explicit analysis approach was adopted because it guarantees much more stable and good results when compared to standard static analysis. The quasi-static loading, which is the loading approach executed in the cyclic test, can be performed using explicit analysis specifically when the vibration period of the structure does not exceed the loading time. As a result, a Frequency analysis has been conducted for the sandstone masonry specimen to find the natural period of vibration of the specimen related to the axial and lateral vibration mode. For insuring that the quasi-static analysis was achieved,

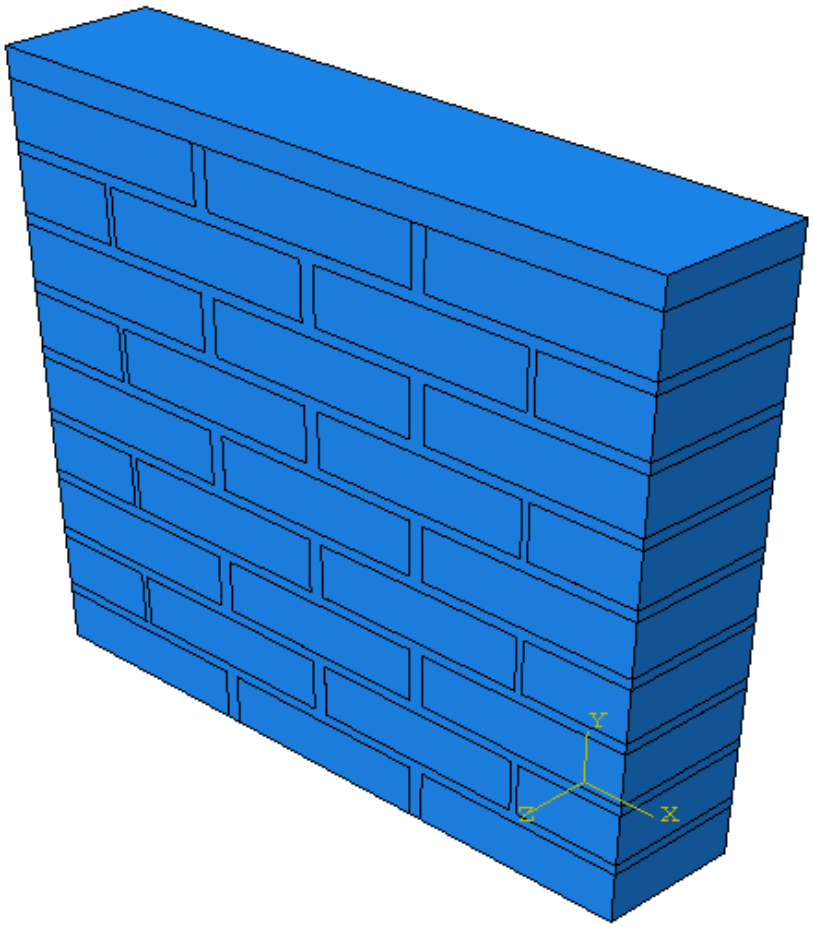

Figure 5. 1 The assembled model of the test specimen

the lower limit of loading time was set to be at least three times the natural vibration period of the specimen. Frequency analysis results regarding the mode of vibration and the associated frequency and natural period of the specimen are listed in Table 5.1. Furthermore, it can be seen that the axial natural vibration period is associated with the 6th mode (Figure 5.2) and the lateral natural vibration period is associated with 3th mode (Figure 5.3). According to Table 5.1, it is evident that the vibration period of each vibration mode was less than one second. Consequently, the step time adopted in ABAQUS model has been set to equal one second for both axial and lateral loading step.

Table 5. 1 Mode of vibrations and natural frequencies and period associated with each vibration mode

Mode of Vibration	Frequency HZ	Vibration Period Sec
1	61.45	0.016273
2	152.42	0.006561
3	203.15	0.004922
4	355.69	0.002811
5	489.93	0.002041
6	505.27	0.001979
7	560.58	0.001784
8	608.45	0.001644
9	809.17	0.001236
10	883.24	0.001132
11	932.1	0.001073
12	989.26	0.001011
13	1126.3	0.000888
14	1277.8	0.000783
15	1279.6	0.000781

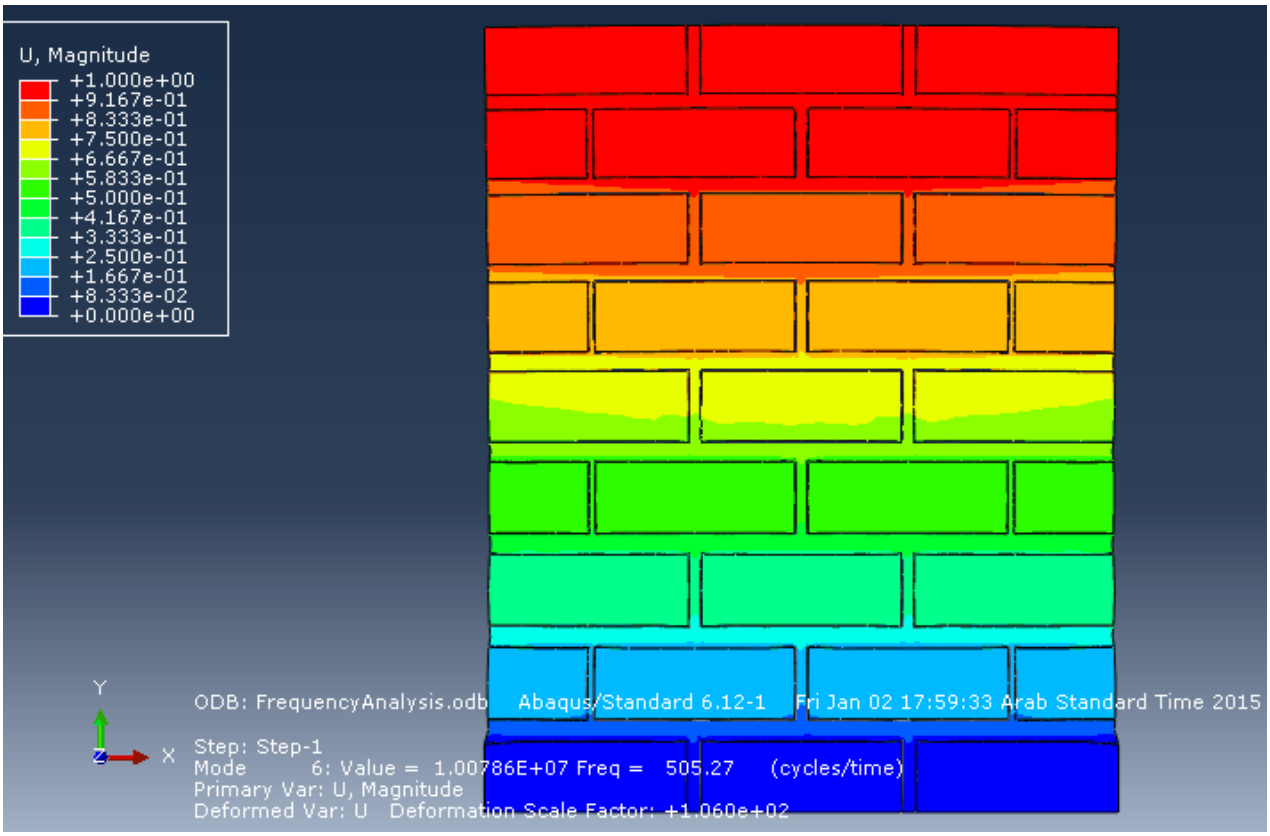

Figure 5. 2 6th mode of vibration (vertical vibration)

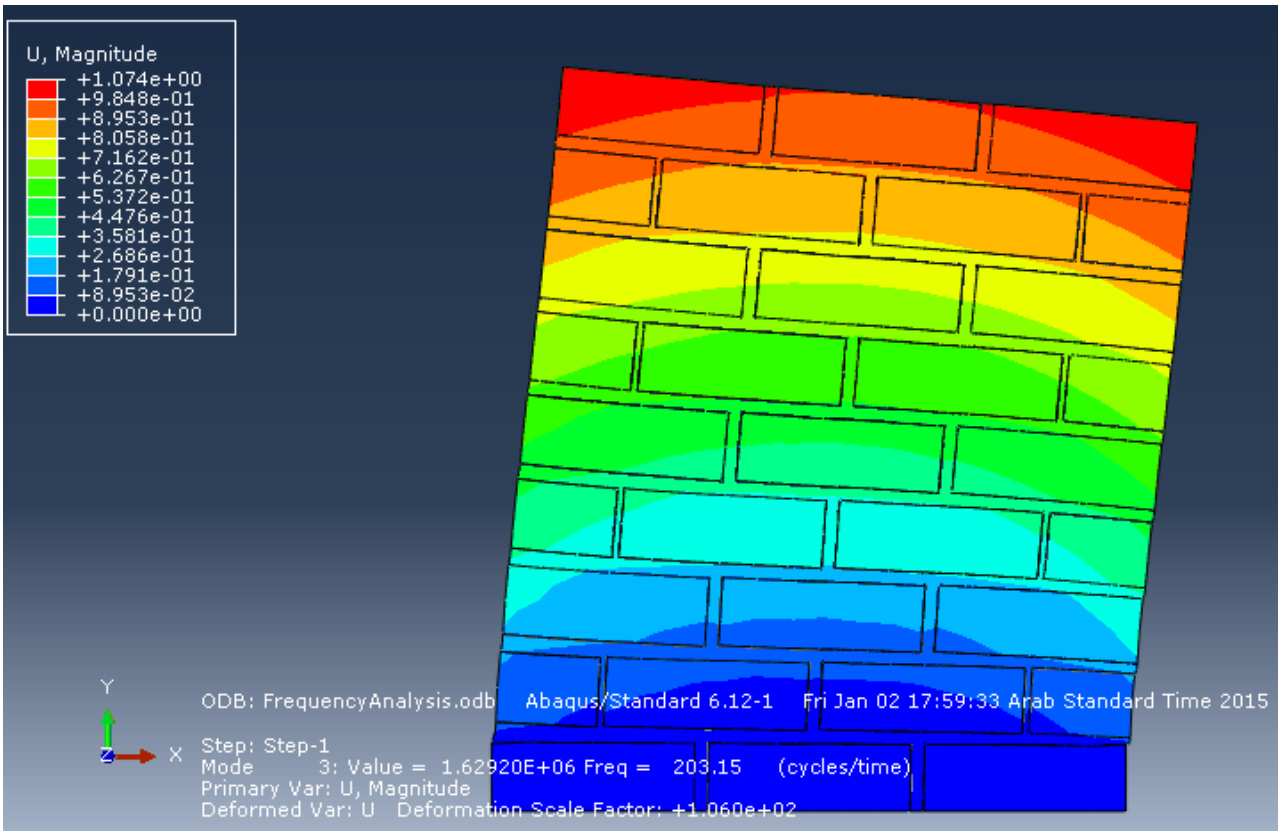

Figure 5. 3 3th mode of vibration (Lateral vibration)

5.3 Material Properties

The adopted CDP model in ABAQUS requires specific material properties and parameters in order to run the model. While some parameters were assumed to be default values given by ABAQUS, the others were obtained from actual experimental tests carried out on sandstone and lime mortar samples [24]. Compressive and tension behavior of both sandstone and lime mortar in the plastic range is shown in Figure 5.4 and Figure 5.5, respectively.

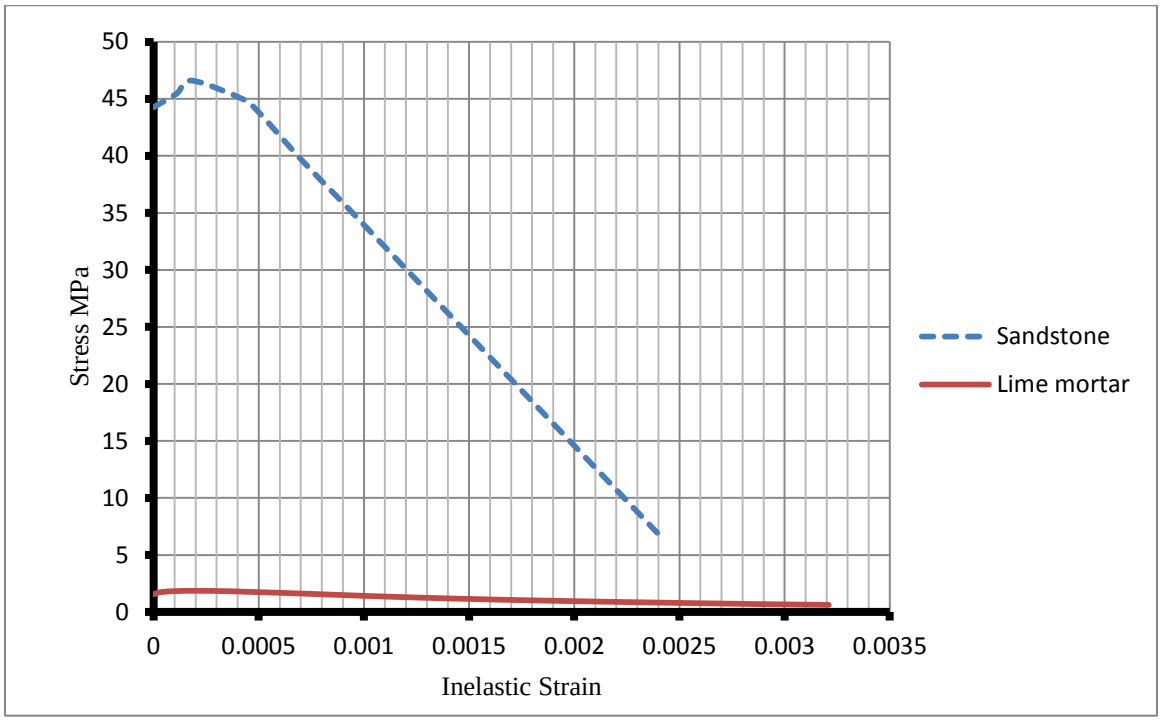

Figure 5. 4 Compressive behavior in plastic zone

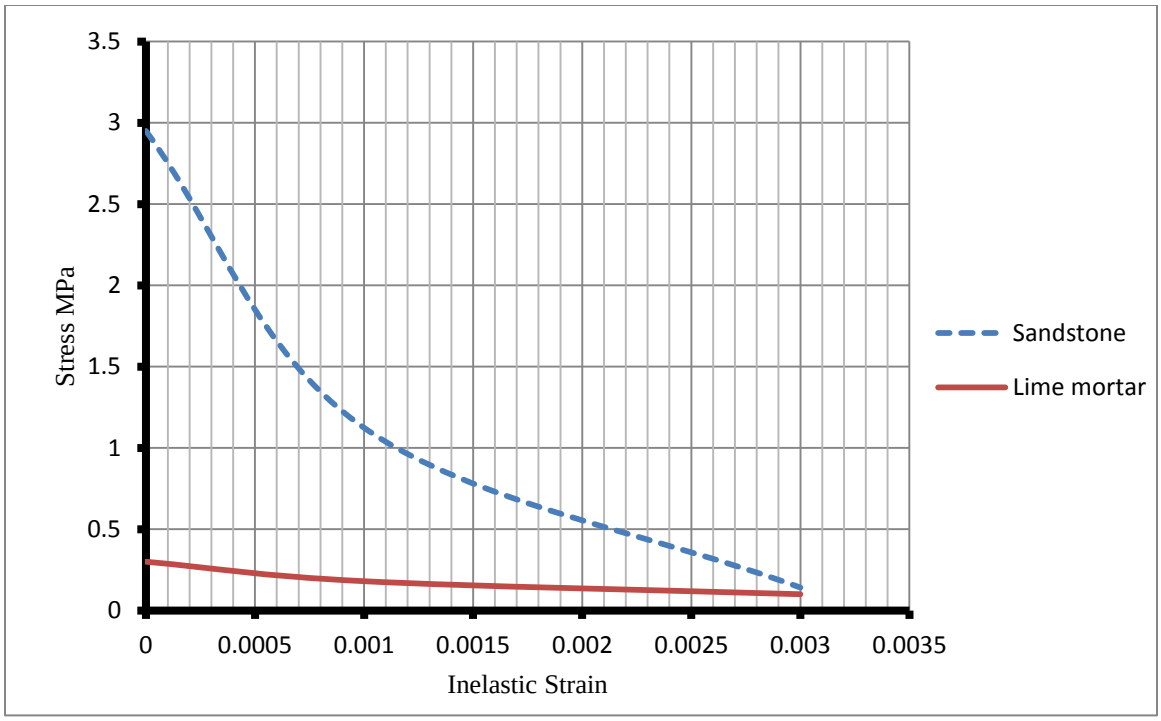

Figure 5. 5 Tension behavior in plastic zone

Summary of parameters used as input data in CDP model for sandstone and lime mortar materials are listed in Table 5.2 and Table 5.3, respectively.

Table 5. 2 CDP Model Parameters of Sandstone Material

Mass Density (Tone/mm³)	Young's Modulus (MPa)	Poisson's Ratio	Dilation Angle ψ (Degree)	Eccentricity ε	f_{b0}/f_{c0}	K
2.26E-009	36,440	0.3	36	0.1	1.16	0.67

Table 5. 3 CDP Model Parameters of Lime Mortar Material

Mass Density (Tone/mm³)	Young's Modulus (MPa)	Poisson's Ratio	Dilation Angle ψ (Degree)	Eccentricity ε	f_{b0}/f_{c0}	K
1.6E-009	2100	0.25	36	0.1	1.16	0.67

Regarding CFRP laminate, one layer of CFRP laminate of 1mm thickness and 200mm width was placed on both sides with the designated patterns. Properties of CFRP laminate input in the model were based on Data sheet of SIKA Company attached with the supplying CFRP [15]. Table 5.4 highlights the elastic properties of CFRP material used in the model.

Table 5. 4 Elastic Properties of CFRP

Mass Density (Tone/mm^3)	Young modulus (MPa)	Ultimate tensile strength (MPa)	Elongation at break (%)
1.76E-009	28,000	350	1.8

After defining all the materials with their designated properties, they were assigned to their specified sections. Regarding sections, both sandstone and lime mortar parts were modeled as a homogeneous section while CFRP parts were modeled as a composite section. In this context, an emphasis has been placed on the consistency of the fiber orientation angle in order to simulate the real behavior of the CFRP laminate correctly.

5.4 Boundary Conditions and Loading

Defining the boundary condition correctly is essential to simulate the real one in the experimental test set-up. As previously mentioned in chapter 3, the test specimen was fixed on U-base steel beam connected firmly to the ground floor area in order to avoid displacing in the out of plane direction. Also two L-steel sections were used to keep the specimen from sliding. As a consequence, the model was restrained at the base of the specimen and also at the first course in both left and right side in all directions (U1=0,

U2=0, U3=0) as shown in Figure 5.6. The first restraint was simulating the U-base steel beam function while the latter one was simulating the two L-steel sections.

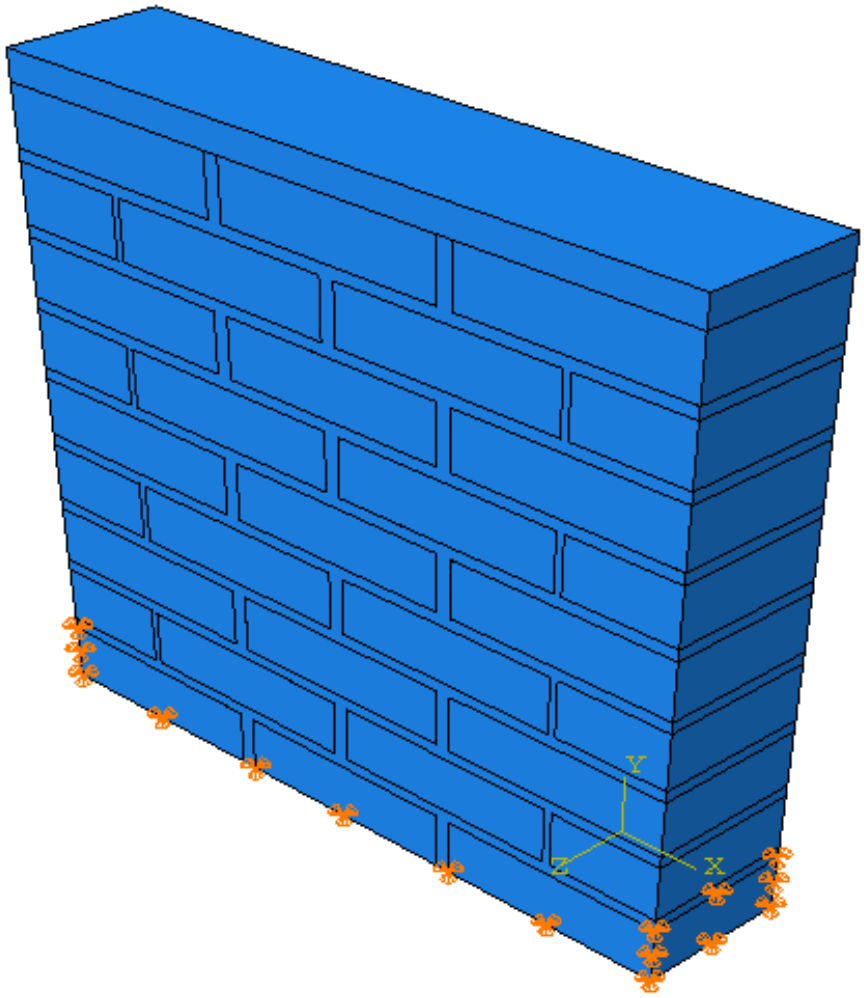

Figure 5. 6 The adopted boundary conditions of the model

The axial loading was applied on the specimen through a steel plate created for the purpose of distributing this load uniformly on the specimen. This axial load was characterized as a force per unit area (pressure) distributed uniformly. Firstly, it was defined in the axial loading step to increase in a regular pace until it reached to the required pressure and then it was defined to keep constant in the lateral loading step

simulating the loading protocol adopted in the cyclic test. Also, the lateral loading was achieved by imposing maximum displacement recorded in the experimental tests on the upper surface of the steel plate. This lateral load was characterized as a displacement control type. It was defined to start exerting the required displacement in the lateral loading step. Regarding the computational time and cost, the lateral loading was implemented initially in a monotonic mode several times until verifying the model correctly. After that, it was implemented in a cyclic mode following the same order adopted experimentally. Figure 5.7 shows the loading system applied on the model.

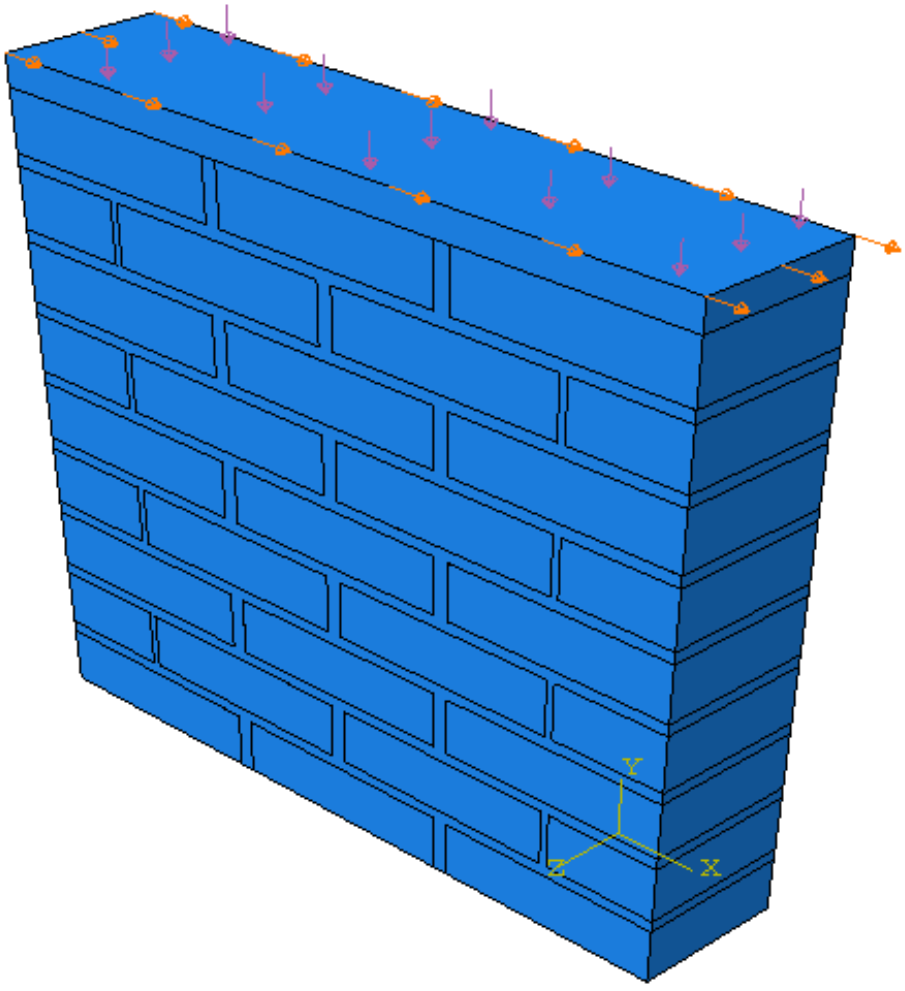

Figure 5. 7 The loading system applied on the model

5.5 Interaction and Meshing Procedure

Defining interaction contact between the different parts forming the model is highly important in order to simulate the real contact behavior of the model's parts correctly. In that aspect, the tangential and normal contact between sandstone and lime mortar elements was assumed to be governed through friction of coefficient value 0.7. In addition, the cohesive behavior property was assumed to control the interaction between the CFRP strips and the targeted specimen surface covered by. Finally, the interaction between the steel plate and the upper surface of the wall was assumed to be perfect bond to facilitate the loading transfer as explained in section 5.4.

After defining all the parameters and properties needed to build the model, it was meshed into elements of different types and shapes. Each part of the model has its own meshing element type and shape. According to the meshing size, these parts were meshed separately into suitable size where reasonable results can be achieved. Table 5.5 summarizes the meshing elements properties.

Table 5. 5 Meshing Element Properties

Part	Element Shape	Meshing Element Designation	Element Description
Sandstone	Hex	C3D8R	8-node linear brick, reduced integration
Lime Mortar	Hex	C3D8R	8-node linear brick, reduced integration
CFRP	Quad dominated	S4R	A 4-node doubly curved thin or thick shell, reduced integration
Steel Plate	Hex	C3D8R	8-node linear brick, reduced integration

5.6 FEM Analysis Results of Test Specimens

The simulated specimens were subjected to combination of axial as well as lateral loading in the same order done in the actual cyclic test. The axial load was characterized as a force per unit area while the lateral load was characterized as a displacement control type. In all FE models, a horizontal displacement of 10.2mm was the maximum displacement exerted. On the other hand, the axial load varied depending on the specimen type as described before in Table 3.7. FEM analysis results regarding stresses, plastic strains and cyclic response of FE models are displayed in the following subsections.

5.6.1 Unstrengthened Model

In the beginning, a static analysis was carried out several times until the model was verified as previously explained in section 5.4. This verification was based on the resulted force-deformation curve compared with that experimentally recorded. For the experimental cyclic hysteresis loop, an envelope was made by taking the maximum at each displacement level. The comparison between the envelope of the experimental result and that resulted from the static analysis is shown in Figure 5.8.

It can be observed from the figure shown below that there is a good agreement between the experimental results and the FEM static analysis. As a result, a dynamic analysis can be performed on this verified model following the same order adopted experimentally.

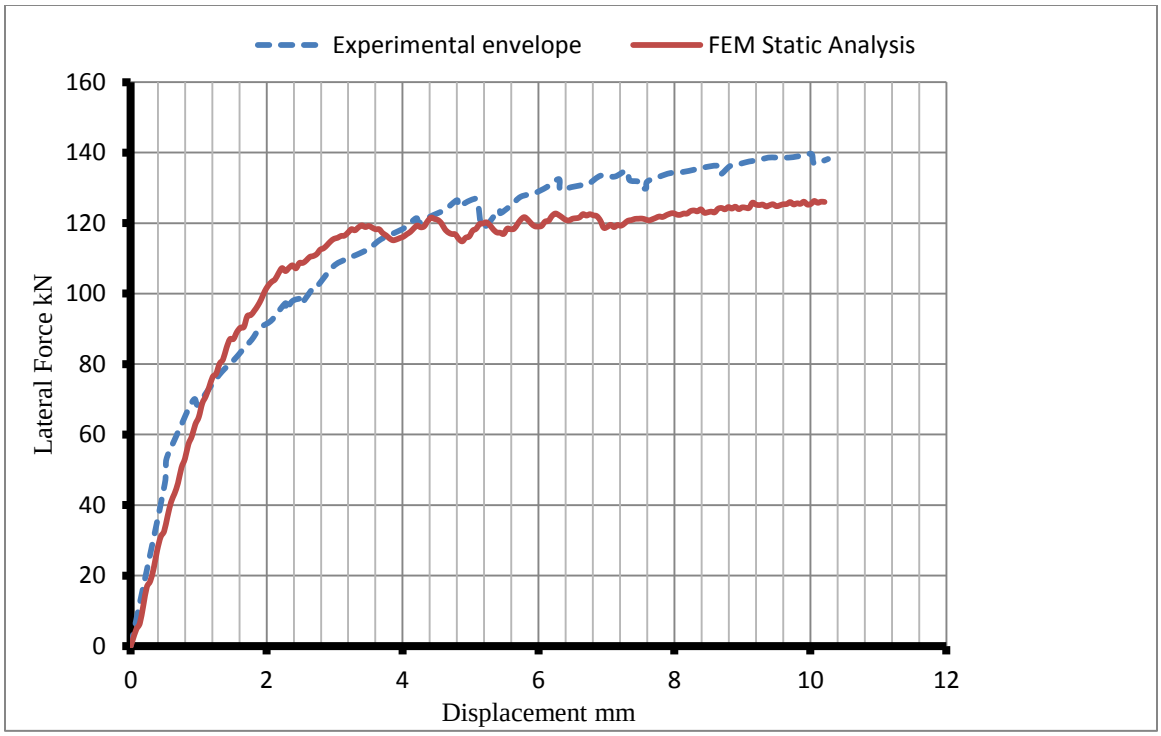

Figure 5. 8 Comparison of Force-Deformation Curve (Control Specimen)

Figures 5.9 and 5.10 illustrate the initiation of cracking pattern and failure mode developed within the specimen body by showing the maximum principal plastic strain with different levels.

According to these figures shown below, it is evident that almost exact failure mode and approximate cracking pattern was achieved from the FEM analysis when compared to the experimental result except in the tension diagonal path due to the limitation of the hydraulic jack capacity in the pull direction.

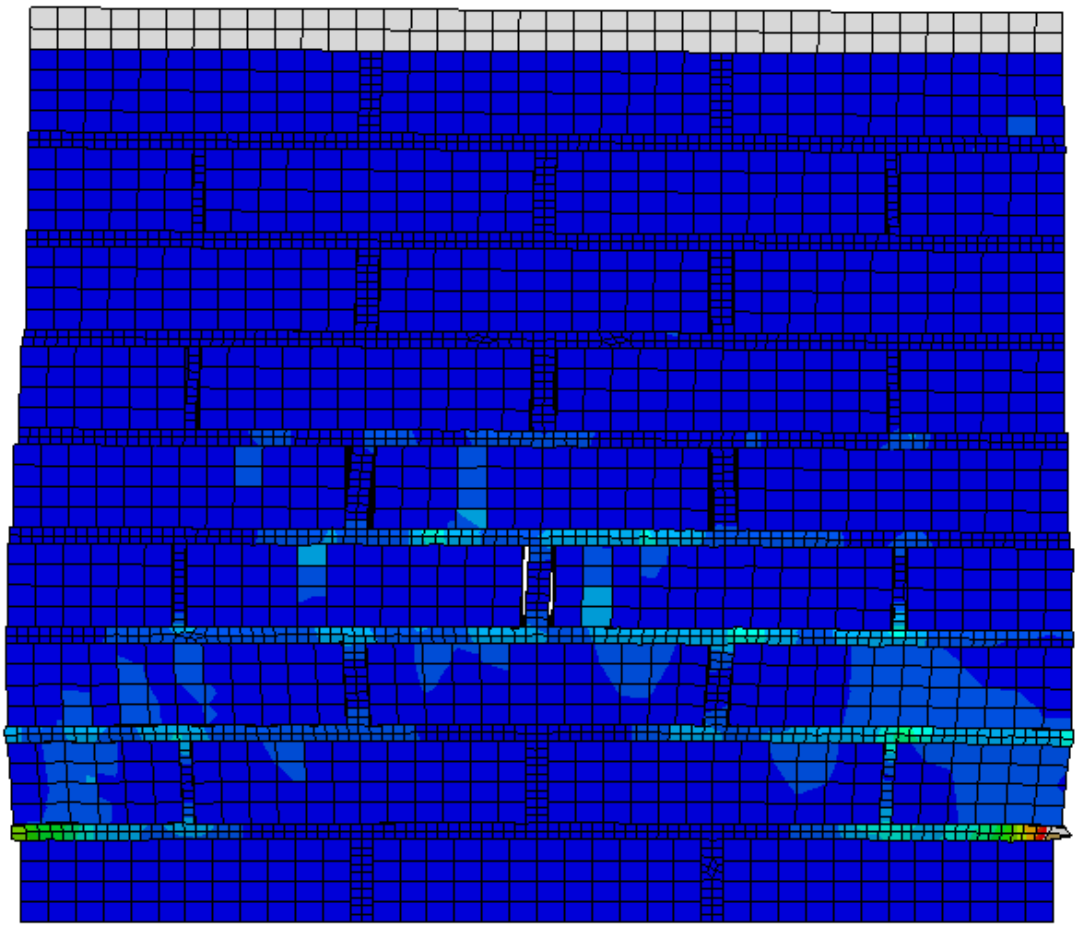

Figure 5. 9 Cracking pattern and Failure mode in the specimen model after dynamic analysis (large plastic strain range)

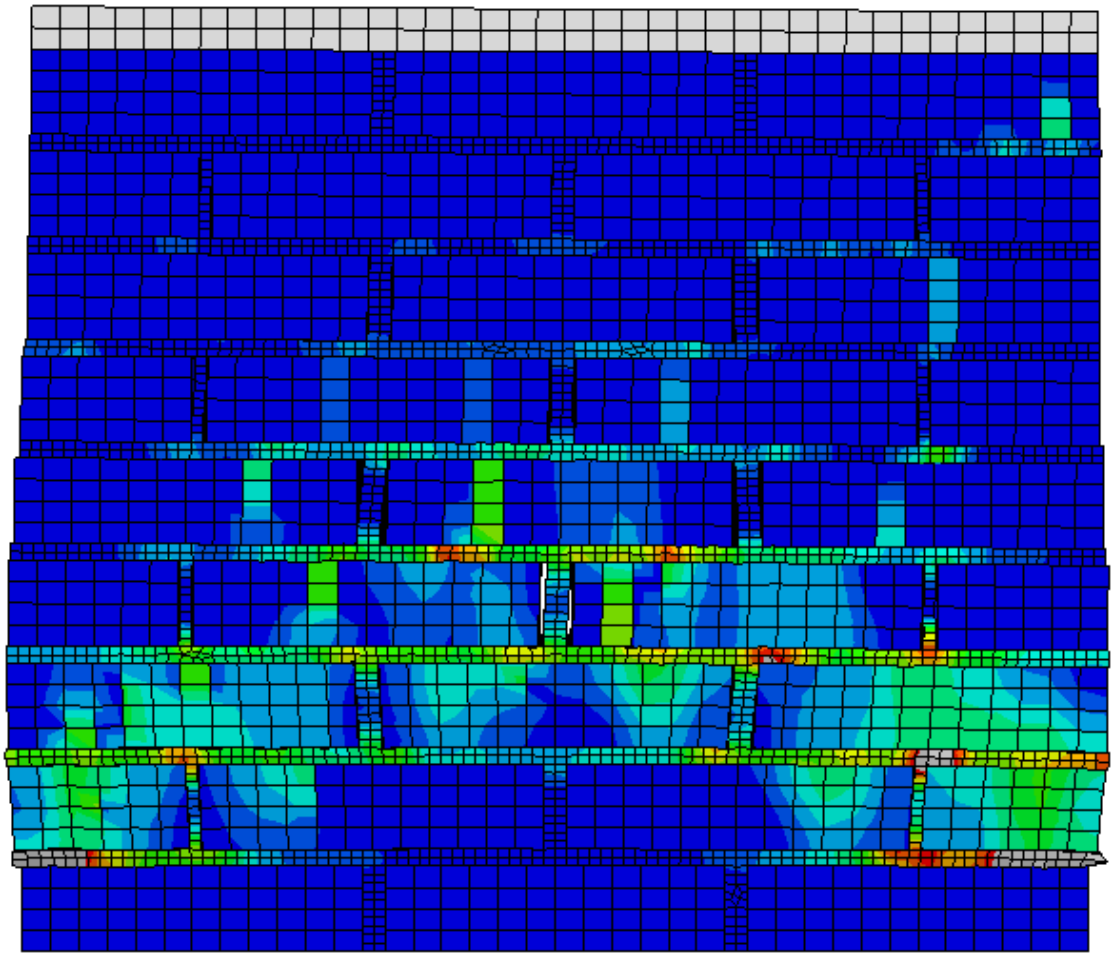

Figure 5. 10 Cracking pattern and Failure mode in the specimen model after dynamic analysis (Low plastic strain range)

Regarding the stress distribution, Fig 5.11 shows the maximum principle stress contour within the specimen body for the second cycle (push). It can be observed that the maximum stress follow a diagonal path in which the cracks formed perpendicular to this path.

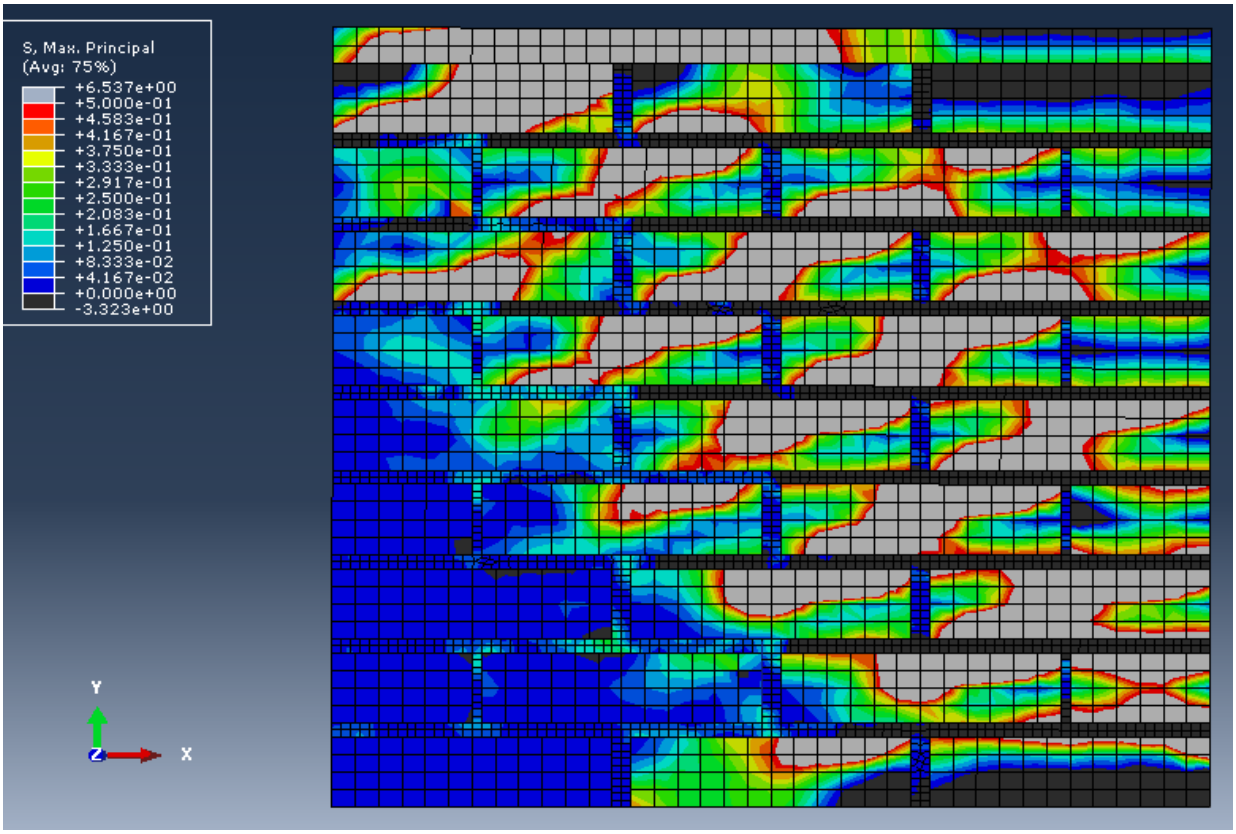

Figure 5. 11 Max principle Stress contour in the second cycle (push)

The response of the model after performing the dynamic analysis can be described by producing the hysteresis loop diagram of the relation between the lateral load and the horizontal displacement and comparing with the experimental one as shown in Figure 5.12

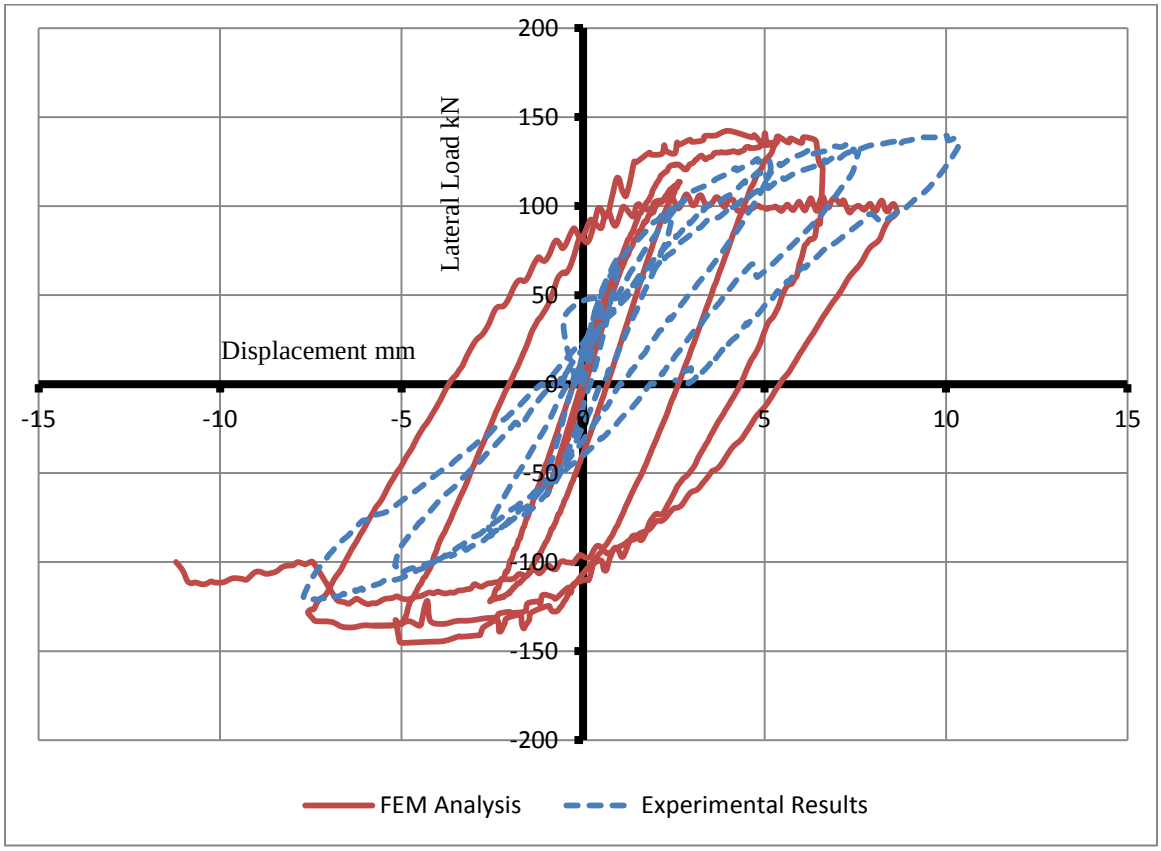

Figure 5. 12 The Lateral Force-Deformation Hysteresis Loop Diagram for Unstrengthened specimen

According to this figure, FEM analysis predicted stronger response in the first three cycles compared to the experimental results. However, FEM analysis predicted less strength after cycle 3 compared to the experimental result, specifically in pushing direction while it matched well in pulling direction. Furthermore, it can be observed starting from cycle 4 that FEM analysis curve experienced a large deformation and high energy dissipation, specifically in pushing direction indicating that the cracks starts to initiate. This matched very well with the experimental observations. As a result, the FEM analysis response is satisfactorily reasonable to simulate the unstrengthened specimen.

5.6.2 X-Shape Strengthened Model

In the beginning, a static analysis was carried out several times until the model was verified taking into consideration the contact behavior between CFRP and masonry parts. This verification was based on the resulted force-deformation curve compared with that experimentally recorded. For the experimental cyclic hysteresis loop, an envelope was made by taking the maximum at each displacement level. The comparison between the envelope of the experimental result and that result from the static analysis is shown in Figure 5.13.

It can be observed from the figure shown below that there is a good agreement between the experimental results and the FEM static analysis. As a result, dynamic analysis can be performed on this verified model following the same order adopted experimentally.

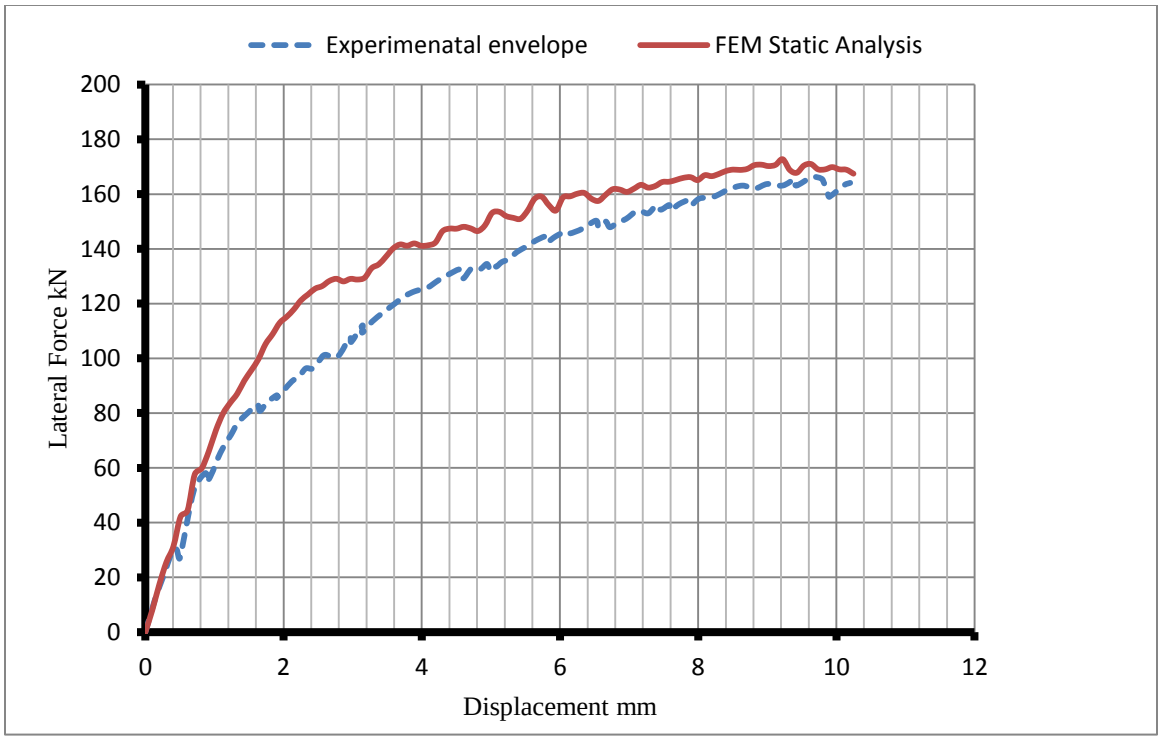

Figure 5. 13 Comparison of Force-Deformation Curve (X-shape CFRP Strengthened Specimen)

Figure 5.14 illustrates the initiation of cracking pattern developed within the specimen body by showing the maximum principal plastic strain. This figure proved what experimentally observed that the cracking pattern developed mainly along the lower course of the specimen, specifically at the bottom corners. Furthermore, it was observed that there is an excessive damage in the middle of the specimen, specifically in the lime mortar which is hidden by CFRP. The observed crack in the right bottom corner which is responsible of the CFRP fracture resulted in the test was confirmed numerically as shown on Figure 5.15.

According to these figures shown below, it is evident that almost exact cracking pattern was achieved from the FEM analysis when compared to the experimental result except at the middle of the specimen. In accordance to the damage resulted from the FEM analysis, it can be proved that the rocking behavior controls the specimen response due to the integral behavior of the specimen gained from the CFRP strengthening.

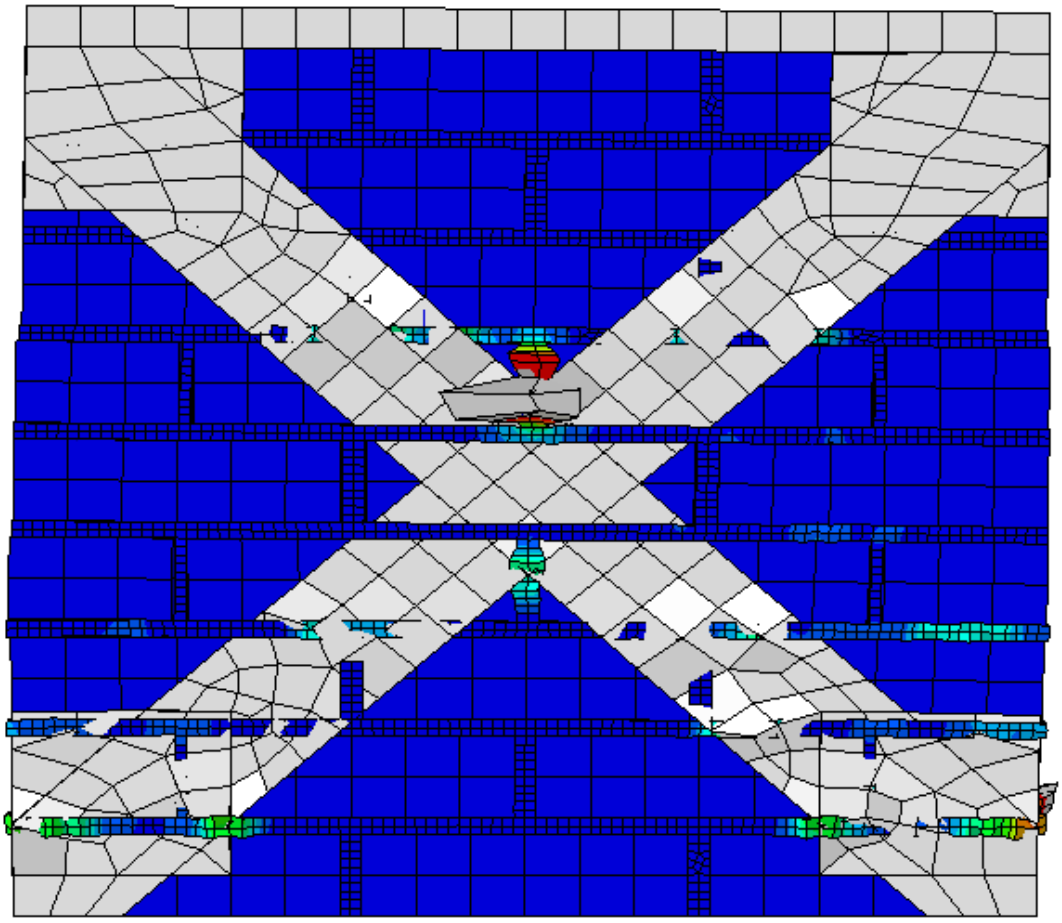

Figure 5. 14 Cracking pattern in the specimen model after dynamic analysis

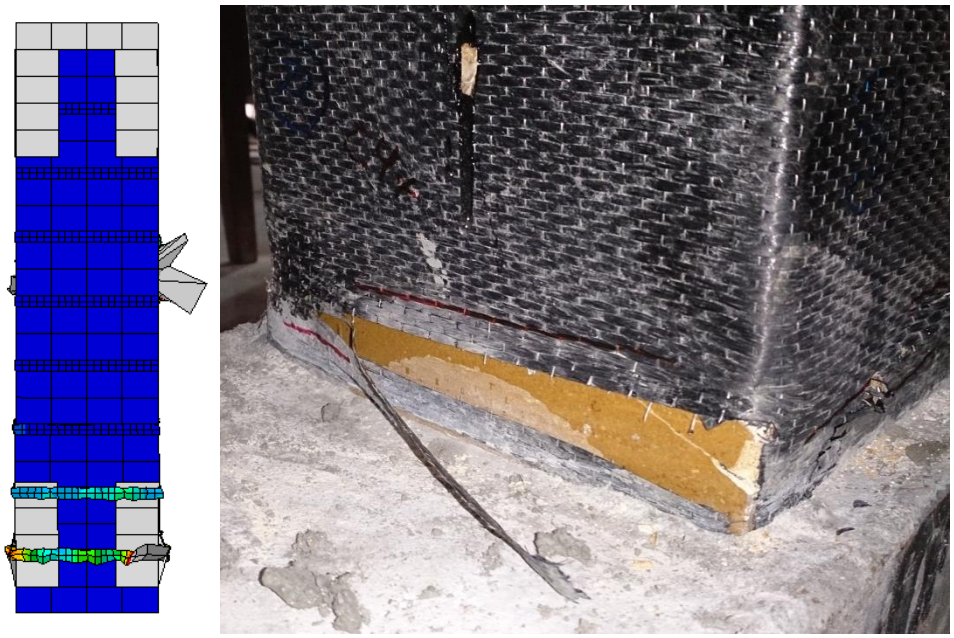

Figure 5. 15 Cracking pattern in the specimen model after dynamic analysis compared with experimental results

Regarding the stress distribution, Fig 5.16 shows the maximum principle stress contour within the specimen body for the second cycle (push). It can be observed that the X-shape strengthening technique successfully minimize the flow of the maximum stress in a diagonal path in contrast to the unstrengthened specimen model so as a significant reduction in cracking initiation can take place within the model, especially in the sandstone units.

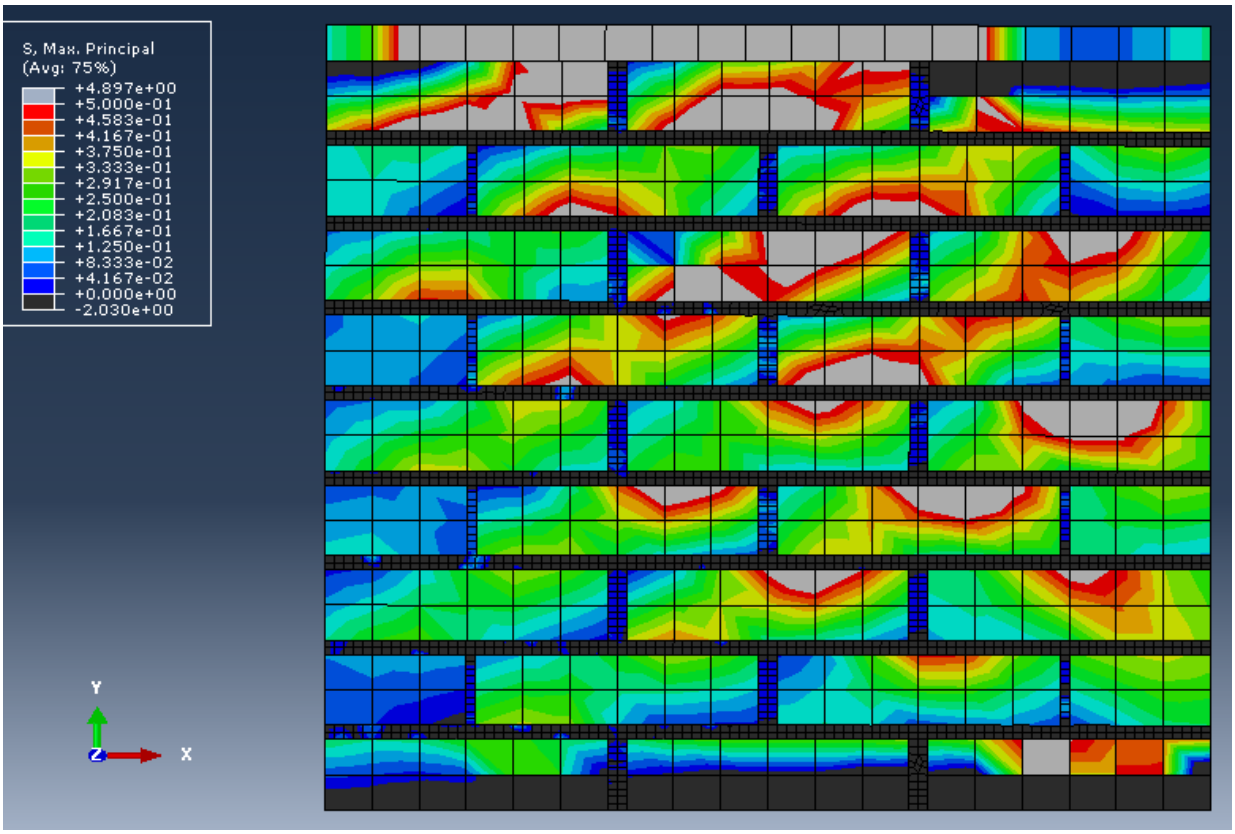

Figure 5. 16 Max principle Stress contour in the second cycle (push)

The response of the model after performing the dynamic analysis can be described by producing the hysteresis loop diagram of the relation between the lateral load and the horizontal displacement and comparing with the experimental one as shown in Figure 5.17.

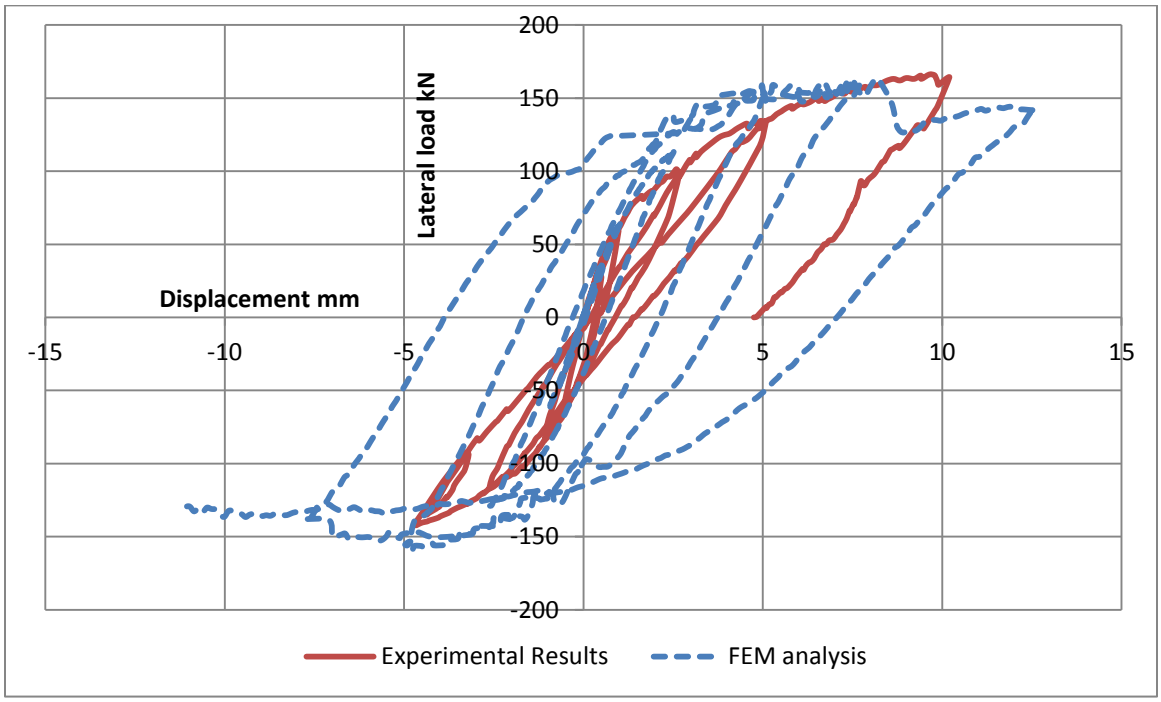

Figure 5. 17 The Lateral Force-Deformation Hysteresis Loop Diagram for X-Shape Strengthened specimen

According to this figure, FEM analysis satisfactorily agrees with the experimental results except at the end of the last cycle when the lateral strength dropped by 22% in the pushing direction while it approximately matches in the pulling direction. Regarding the pushing direction, the analytical hysteresis loop diagram matches very well with the experimental one in terms of lateral strength and permanent deformation in all cycles except the last two cycles which confirms the domination of the rocking behavior.

Furthermore, it can be observed that the energy in the last cycle was dissipated more than the previous cycles thus conforming to the experimental results.

5.6.3 Grid-Shape Strengthened Model

In the beginning, a static analysis was carried out several times until the model was verified taking into consideration the contact behavior between CFRP and masonry parts. This verification was based on the resulted force-deformation curve compared with that experimentally recorded. For the experimental cyclic hysteresis loop, an envelope was made by taking the maximum at each displacement level. The comparison between the envelope of the experimental result and that result from the static analysis is shown in Figure 5.18.

It can be observed from the figure shown below that there is a good agreement between the experimental results and the FEM static analysis. As a result, dynamic analysis can be performed on this verified model following the same order adopted experimentally.

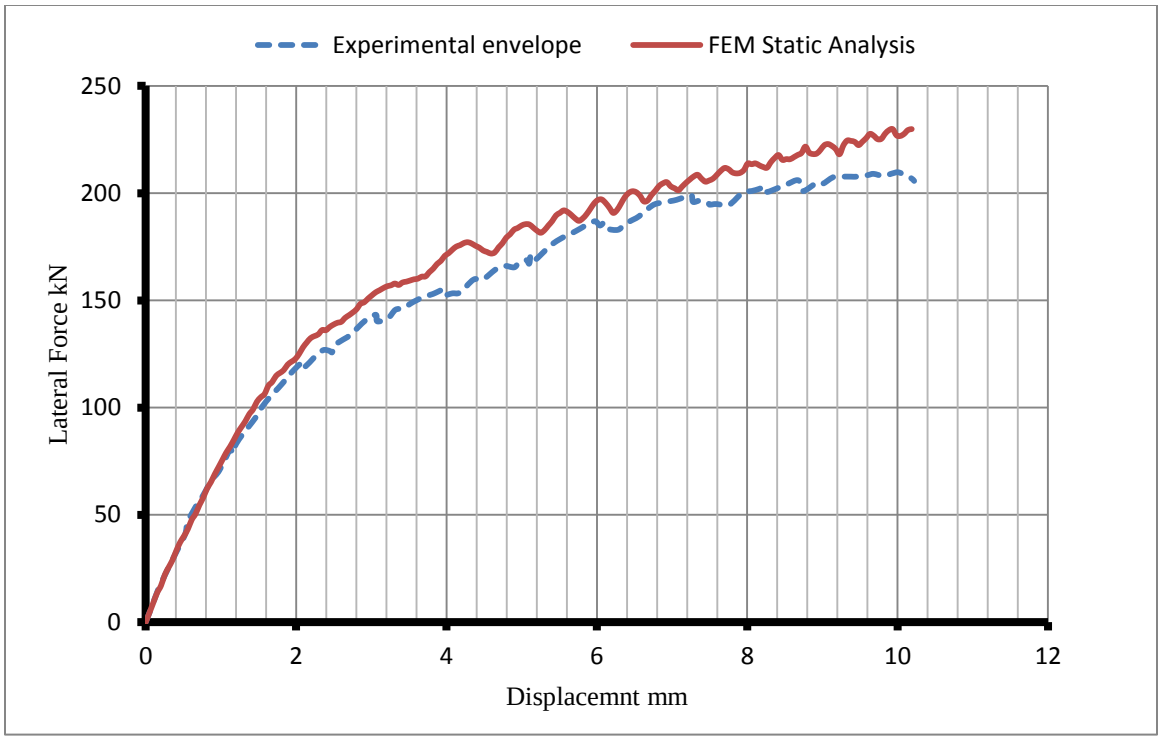

Figure 5. 18 Comparison of Force-Deformation Curve (Grid-shape CFRP Strengthened Specimen)

Figure 5.19 illustrates the initiation of cracking pattern developed within the specimen body by showing the maximum principal plastic strain. This figure proved what experimentally observed that the cracking pattern developed within the area covered by CFRP sheets, specifically in the lime mortar elements. Furthermore, the observed tiny crack in the right bottom corner resulted in the test was confirmed numerically as shown on Figure 5.20.

According to these figures shown below, it is evident that almost exact cracking pattern was achieved from the FEM analysis when compared to the experimental result. Also, it is proved that no failure happened in the masonry units due to the integral behavior of the specimen gained from the CFRP strengthening.

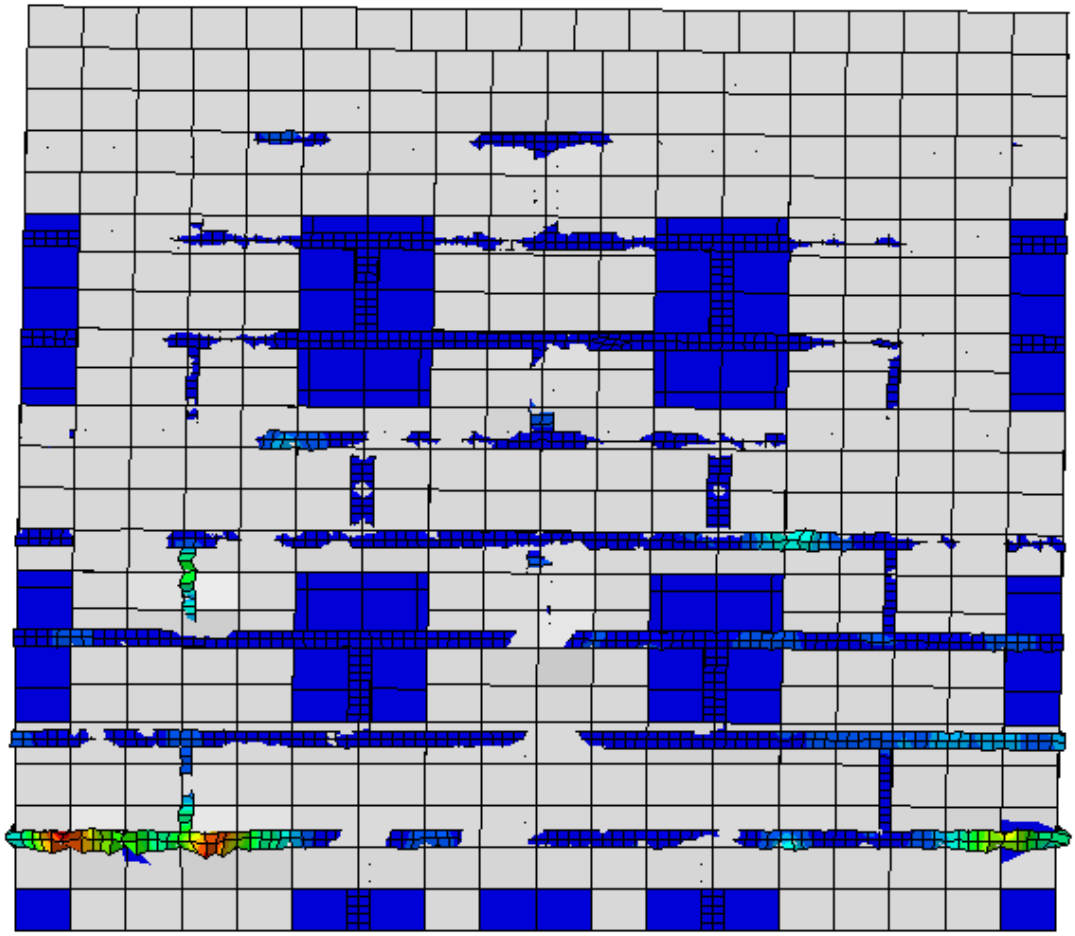

Figure 5. 19 Cracking pattern in the specimen model after dynamic analysis

Figure 5. 20 Cracking pattern in the specimen model after dynamic analysis compared with experimental results

Regarding the stress distribution, Fig 5.21 shows the maximum principle stress contour within the specimen body for the second cycle (push). It can be observed that the grid-shape strengthening technique successfully minimize the flow of the maximum stress in a diagonal path in contrast to the unstrengthened specimen model so as a significant reduction in cracking initiation can take place within the model.

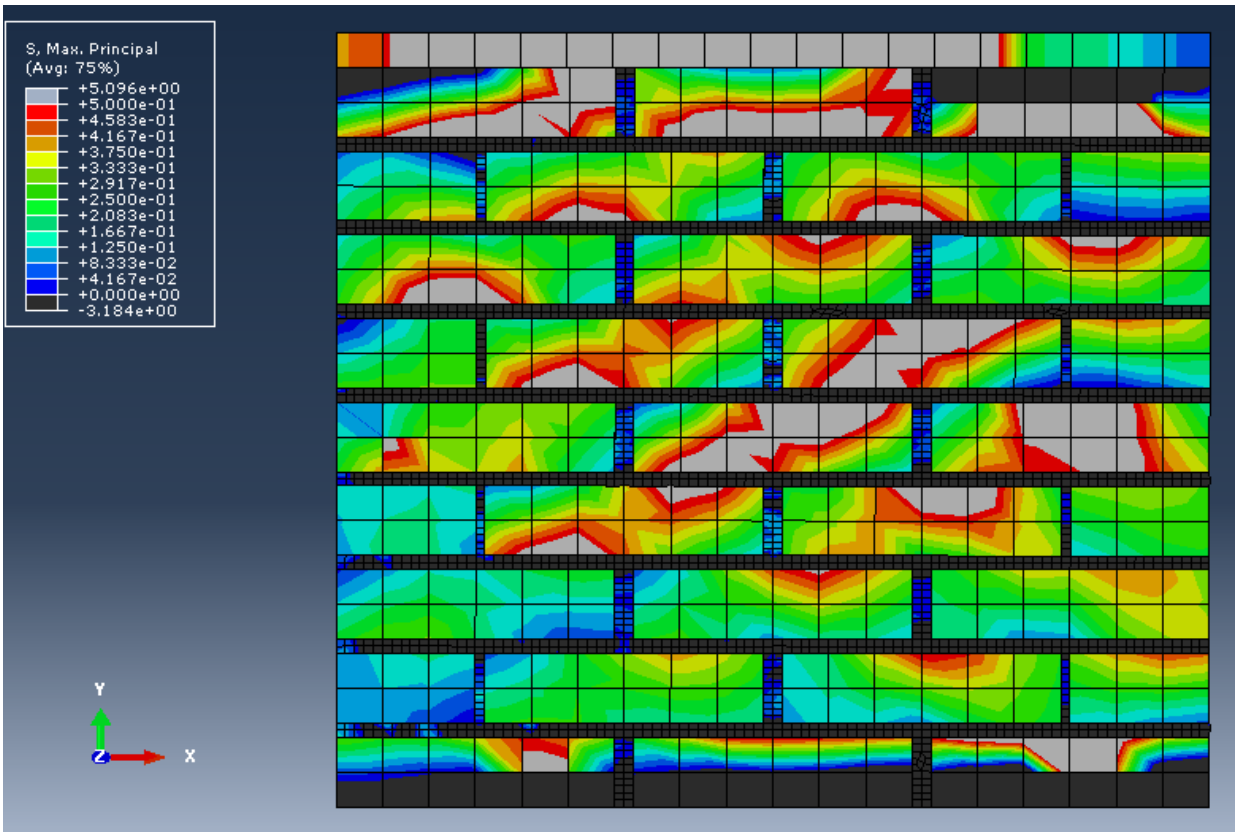

Figure 5. 21 Max principle Stress contour in the second cycle (push)

The response of the model after performing the dynamic analysis can be described by producing the hysteresis loop diagram of the relation between the lateral load and the horizontal displacement and comparing with the experimental one as shown in Figure 5.22.

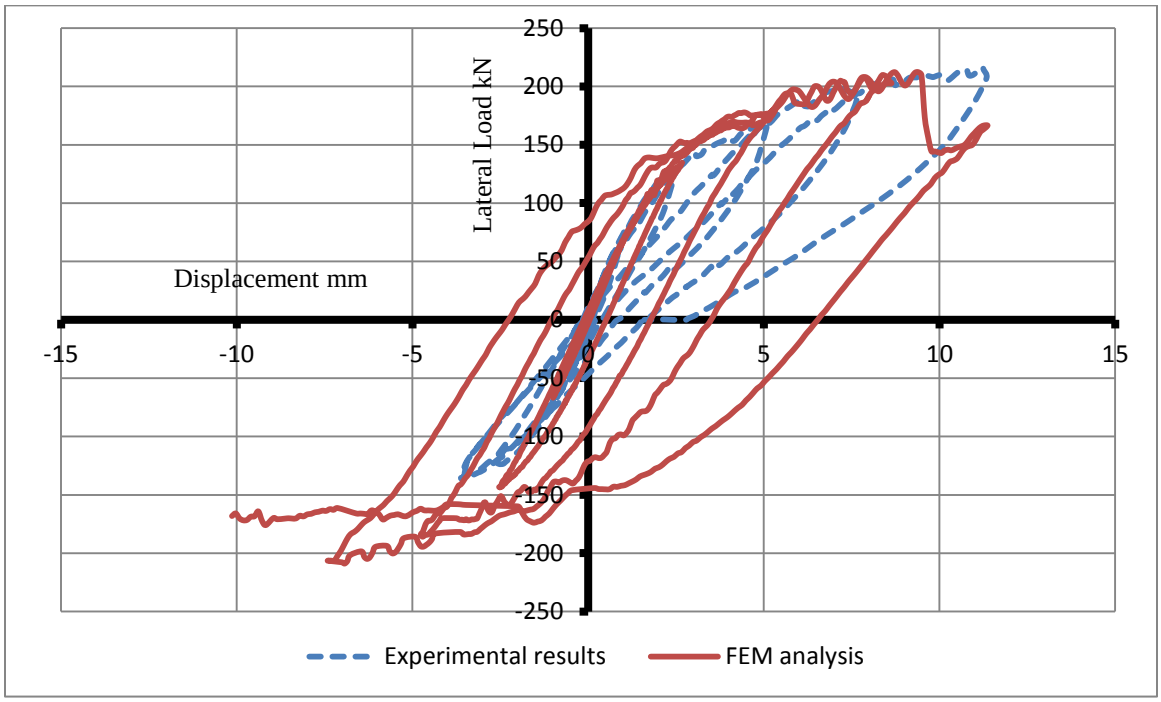

Figure 5. 22 The Lateral Force-Deformation Hysteresis Loop Diagram for Grid-Shape Strengthened specimen

According to this figure, FEM analysis satisfactorily agrees with the experimental results, especially in the pushing direction except at the end of the last cycle when the lateral strength dropped by 31%., while in the pulling direction it is not captured well due the capacity limitation previously mentioned. Regarding the pushing direction, the analytical hysteresis loop diagram matches very well with the experimental one in terms of lateral strength and permanent deformation in all cycles except the last one. Furthermore, it can be observed starting from the cycle 4 that the energy was dissipated more than the previous cycles thus conforming to the experimental results.

5.7 Discussion

The FEM using micro analysis approach has shown good potential for investigating the behavior of the sandstone masonry wall specimens with and without CFRP strengthening. This approach has offered a great opportunity to get a reasonable matching with the main response parameters and failure mode experimentally observed.

The FEM analysis was first performed using static analysis method for several times in order to calibrate the model parameters so that a good agreement with the experimental results can be achieved. The main criterion for validating this model is the lateral load-deformation curve. After validating the model in the monotonic mode, a dynamic analysis was executed so as a full picture of the test specimens' behavior can be investigated when subjected to the same circumstances experienced experimentally.

One of the main challenges encountered during the modeling analysis is the complexity of the model, specifically the huge number of the meshing elements created in the model. Therefore, a machine with normal specification cannot execute the analysis job. Consequently, HPC (High Performance Computing) service, which offered form the ITC, KFUPM, was utilized to carry out the FEM analysis jobs.

For unstrengthened specimen model, it can be seen that the cracking pattern and failure mode in both the test and the analysis were matched satisfactorily as shown in Figure 5.23. However, diagonal cracking in the pull direction is not observed experimentally due to the capacity limitation of the hydraulic jack in that direction.

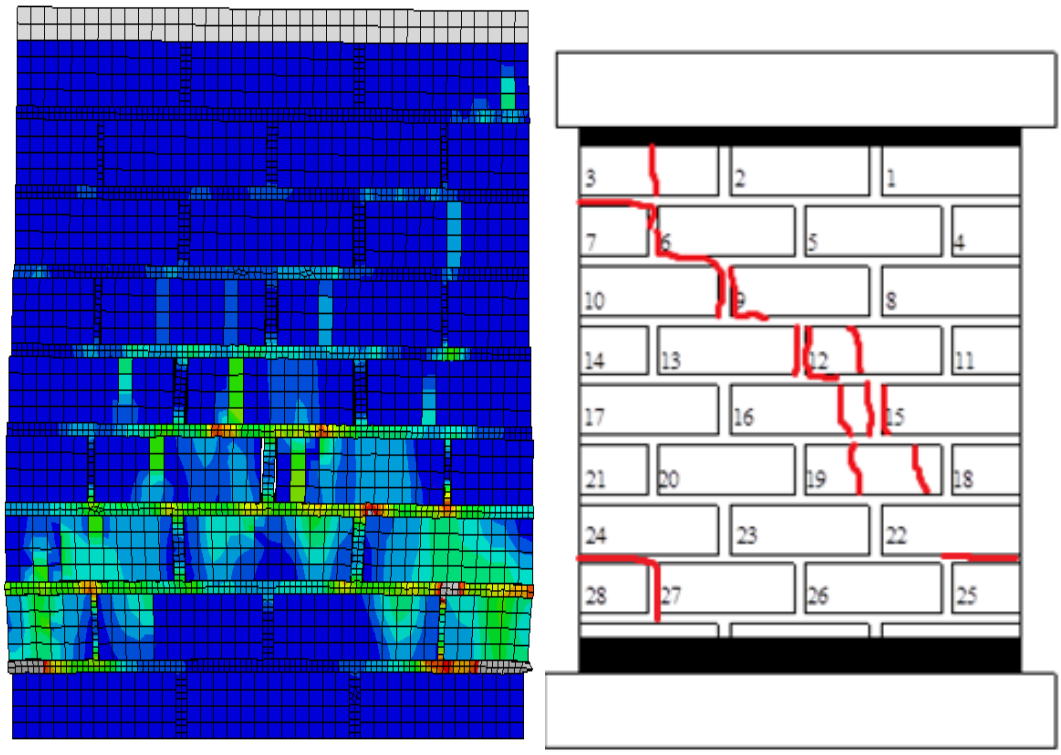

Figure 5. 23 Cracking pattern obtained from analysis and test for unstrengthened specimen

Regarding the lateral load-deformation hysteresis loop diagram resulted from the dynamic analysis; it can be found that the FEM hysteresis loop behaved in a stiff trend compared to the experimental one in almost all cycles. This can be attributed to the fact that the bond between the sandstone and lime mortar was assumed to be a perfect bond in the model. On the other hand, this bond is considered as one of the weaker points in the actual masonry specimen due to the de-bonding occurred between the two materials when subjected to cyclic loading as shown in Figures 5.24 and 5.25. As a result, this de-bonding forced the lateral stiffness to reduce in the actual specimen.

Figure 5. 24 Debonding between sandstone and lime mortar

Figure 5. 25 Debonding between sandstone and lime mortar

It has also to be mentioned that the de-bonding might happened in the masonry specimen due to the poor workmanship, especially placing the lime mortar correctly during the specimen construction.

Regarding the strengthened specimens, it was noticed that the cracking patterns can be captured with reasonable accuracy when compared with the experimental results as described previously. In addition, FEM analysis using ABAQUS environment package provide beneficial tool to track the cracks initiation developed behind the CFRP sheets.

According to the FEM analysis of the strengthened models, stress distribution of the CFRP strips S11, which their directions match with the CRRP fiber direction can be

displayed for both X-shape and Grid-shape strengthened models as shown in Figures 5.26-5.29.

It can be observed from Figures 5.26 and 5.27 that the tensile stresses in the x-shape strengthened model are highly concentrated at the lower part of one of the diagonal strips depending on whether it is on the pushing or pulling mode. Similarly, it can be found in the grid-shape strengthened model. However, compressive stresses can be found in the grid strips in contrast to the diagonal ones. These tensile stresses are responsible of reducing the effect of the excessive rocking phenomenon on the strengthened specimens.

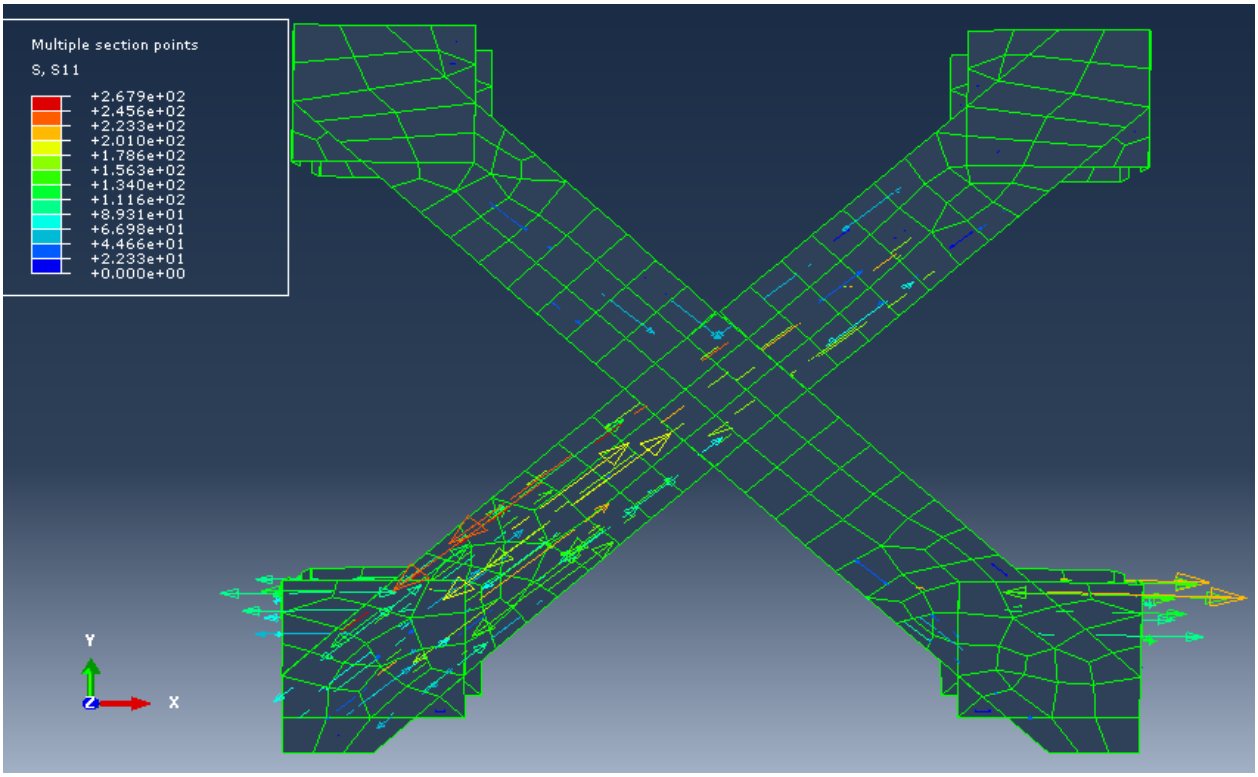

Figure 5. 26 Stress distribution (S11) in the CFRP strips during pushing cycle

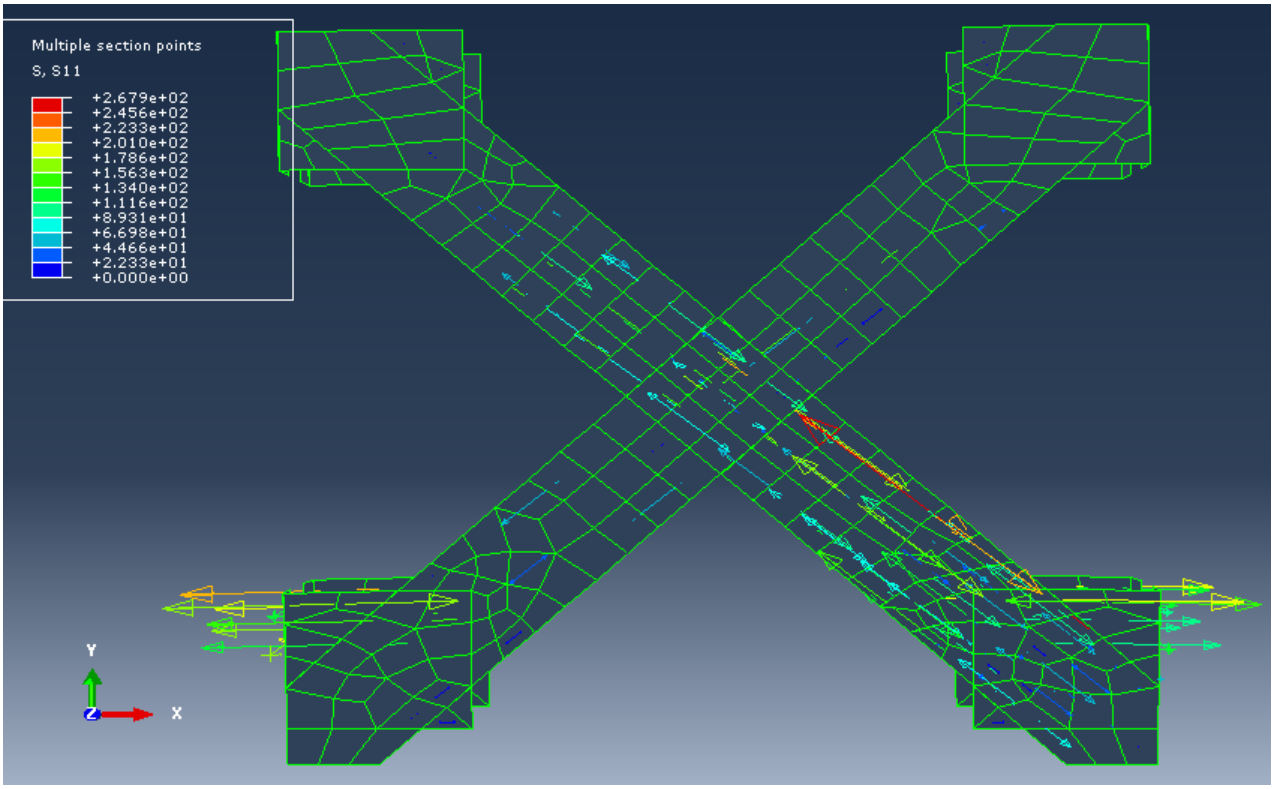

Figure 5. 27 Stress distribution (S11) in the CFRP strips during pulling cycle

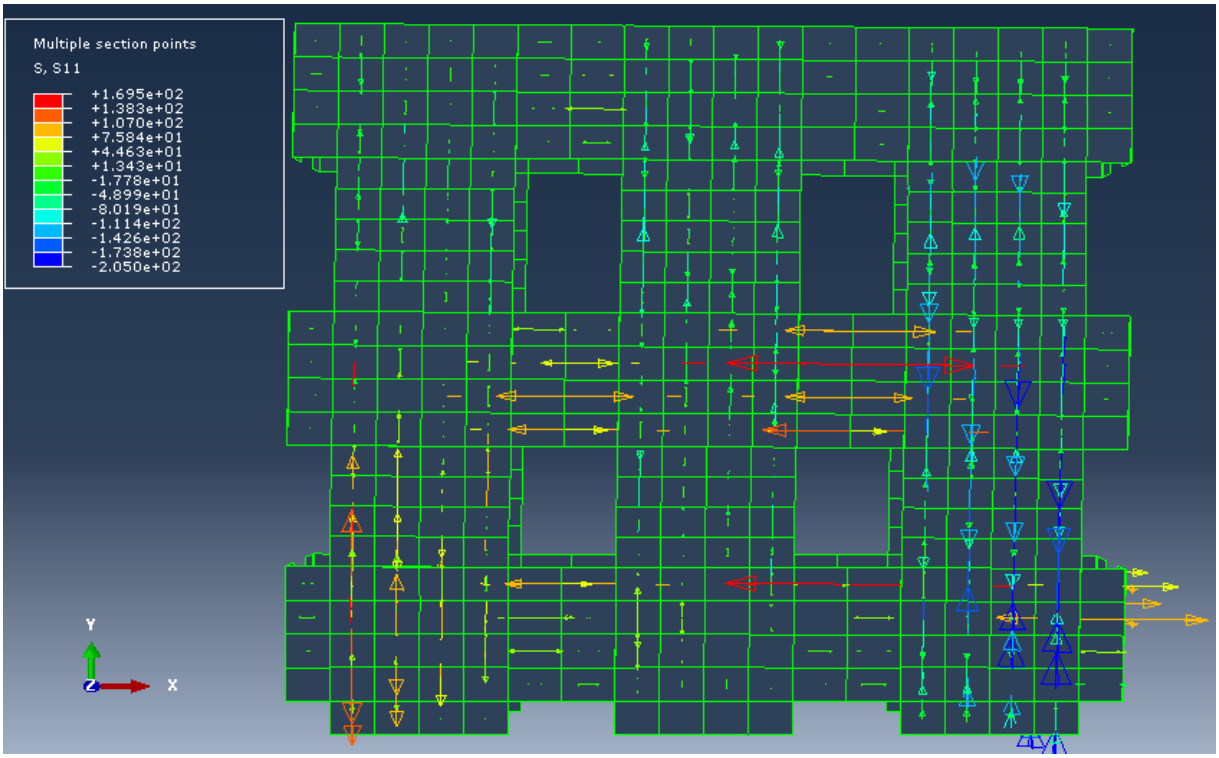

Figure 5. 28 Stress distribution (S11) in the CFRP strips during pushing cycle

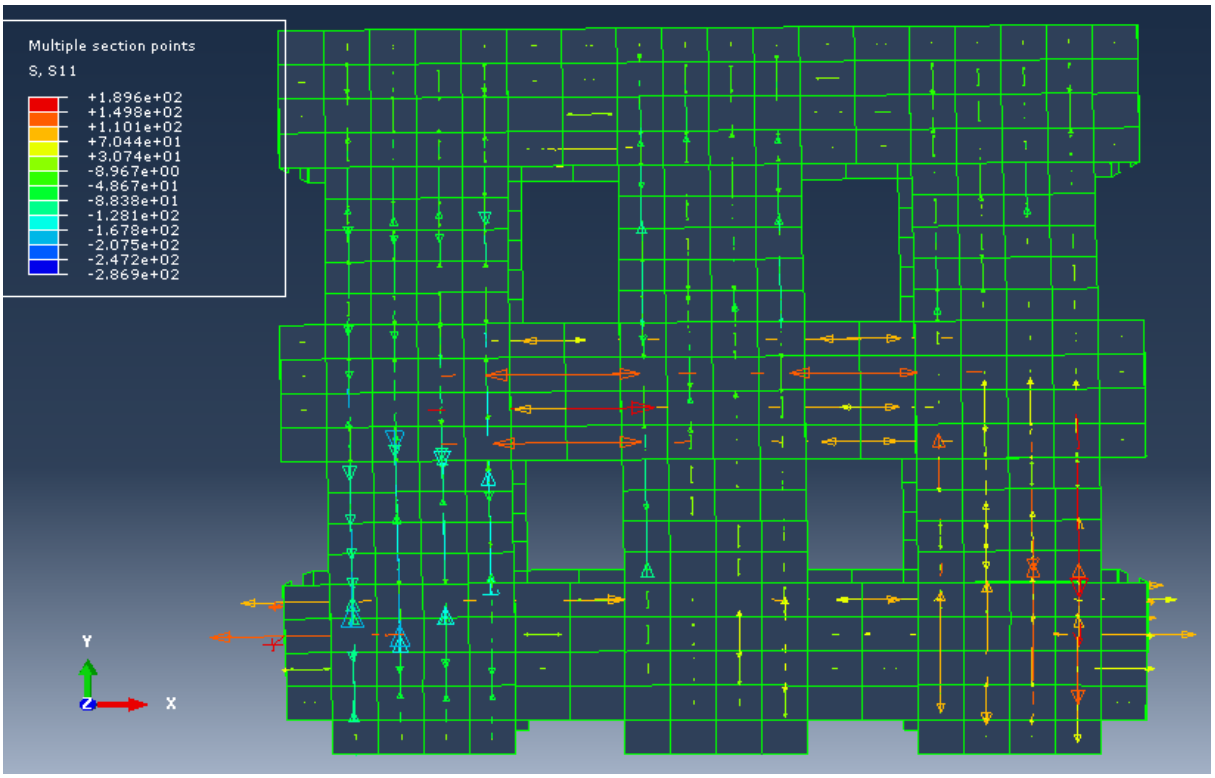

Figure 5. 29 Stress distribution (S11) in the CFRP strips during pulling cycle

CHAPTER 6

CONCLUSION AND RECOMMENDATION

Most of the heritage buildings in Saudi Arabia are poorly performed when subjected to low or moderate earthquake events. Since these buildings were constructed mainly of sandstone URM walls, extensive investigation was carried out to gain knowledge about the performance of such buildings subjected to seismic loading. CFRP sheets were proposed to utilize as a retrofitting material due to its vital function in enhancing the lateral resistance of URM buildings. In the current research project, the cyclic behavior of full scale sandstone masonry wall specimens strengthened with different CFRP patterns has been experimentally investigated. Also, a finite element modeling of theses specimens has been developed in order to simulate their real behavior when subjected to the same circumstances during the cyclic test.

In the experimental phase, three full-scale sandstone block masonry walls were constructed; one of them was un-strengthened one (control) while the others were strengthened with CFRP with different configurations. These walls were subjected to cyclic lateral load applied incrementally under a constant axial load. Before that, a characterization of materials used in the masonry wall and the masonry wall itself have been done by carrying out number of auxiliary tests in order to get some mechanical properties of such materials. As a result, it can be used as input data in the modeling aspect.

In the modeling phase, finite element modeling was carried out in order to get a full knowledge of how the sandstone masonry wall will perform when subjected to cyclic simulation. FEM of Masonry wall retrofitted with different configurations were conducted in the ABAQUS environment using a Plastic-Damage model developed by Lubliner et al (1989) [12] and further expanded by Lee and Fenves (1998) [13].

6.1 Conclusions

The following conclusions can be drawn based on the present research project reported in this thesis:

- From materials characterization, it can be concluded that the compressive behavior of the sandstone material is quite strong while its behavior in tension is not good enough to withstand the tensile stresses. For this reason, CFRP was used as tensile reinforcement in this study. Regarding lime mortar, both compressive and tension behavior is very weak when compared to sandstone material.
- It was clearly noted that the unstrengthened specimen experienced deficient cyclic behavior in terms of stiffness decay, high dissipated energy and appearance of pronounced cracking causing failure in combined patterns of rocking and staggered head and bed joint modes.
- For CFRP strengthened specimens, an increase in lateral strength was evident in comparison to the unstrengthened one. In addition, less energy was dissipated which conforms that no pronounced cracks arose during the test. Finally, the combined failure modes observed in the URM were eliminated due to the integral behavior of the wall as a result of the CFRP strengthening.

- It was observed that no debonding was observed between CFRP and the test specimens during the cyclic loading except at the bottom corners due to high stresses concentrated there and lack of suitable anchorage. This no debonding can be attributed to the high strength epoxy used in attaching the CFRP sheets to the masonry specimen substrate.
- Based on the data obtained from the cyclic test, the grid-strengthened specimen attained more lateral strength and stiffer behavior compared to the diagonal strengthened one. However, the grid-pattern used more CFRP because it covered 84% of the surface area of the wall as compared to the 56% of the area in X-shape case.
- It can be concluded that using CFRP as a strengthening material enhances the concerned parameters which govern the masonry wall behavior. Consequently, CFRP strengthening has been shown to be reliable and effective option in rehabilitation and strengthening the URM.
- According to modeling aspect, CDP model implemented in ABAQUS has proved that the sandstone masonry wall specimens can be effectively simulated when subjected to cyclic loading if the material properties and CDP parameters are correctly obtained. However, this cannot be achieved without making use of the micro analysis approach adopted for both sandstone and lime mortar.
- The static analysis results can be considered as an indicating index of the overall behavior of the masonry specimen model disregard of using the dynamic analysis which consumes much time and cost in modeling computation aspect.

- FEM analysis results reveal a good matching with the experimental results in terms of the lateral force-deformation hysteresis loop diagram. Also, the cracking pattern and failure mode are captured with reasonable accuracy using the CDP model. This good agreement with the experimental results motivates us to consider the FEM as a vital tool to predict the behavior of retrofitted and non-retrofitted masonry structures subjected to cyclic loading notwithstanding complexity of geometry and boundary conditions.
- Regarding the FEM analysis results of the strengthened models, CFRP sheets has confirmed that they play an important role in preventing premature failure driven by rocking and separation of the lower course.
- Finally, sandstone masonry structures can be safely constructed in areas prone to seismic zones if they were strengthened properly with CFRP which has proved its effectiveness experimentally and analytically. However, a final coating with a plaster of similar color to the original stone wall would be necessary to preserve the aesthetic value

6.2 Recommendations for Future Work

During experimental and analytical investigation conducted in the present research project, many recommendations have arisen on the research deck whish some of them are listed as a recommended future work:

- Compression test conducted on masonry prisms is highly recommended to be executed on larger size in order to get the knowledge on the size effect on the

uniaxial strength of the prisms. Therefore, the axial capacity of full-scale walls can be predicted correctly.

- During experimental phase, cyclic test suffered from the capacity limitation of the loading equipment, specifically in the pulling direction. For this reason, new loading equipment with high capacity should be purchased and installed on the loading frame.
- A new restraining system in the loading frame should be smartly created in which the premature failure representing by rocking can be prevented. As a result, diagonal cracking and staggered head and bead joints failure will be promoted to occur.
- Regarding the strengthening technique, additional cyclic tests should be conducted with reduction on the width of CFRP sheets so as the effect of width reduction on the overall cyclic behavior of the masonry specimens can be examined whether it is feasible or not.
- Out-of-plane behavior of sandstone masonry walls is recommended to be characterized experimentally.
- FEM analysis should be carried out on specimens retrofitted with CFRP. Basically, running this model is quite challenging since the specimen model should be damaged prior to place the CFRP sheets.
- Additional research is required to establish appropriate damage parameters in both compression and tension behavior. Consequently, the CDP model can be improved.

- The existing PC lab in the department should be equipped with super machines so that various changes in the FEM parameters including meshing size, material properties, and interaction criteria can be tested without concerning about the computation time.

References

[1] "USGS." [Online]. Available: http://www.usgs.gov/.

[2] "CATDAT." [Online]. Available: http://earthquake report.com/2013/01/07/damaging-earthquakes-2012-database-report-the-year-in-review/.

[3] "Saudi Geological Survey." [Online]. Available: http://www.sgs.org.sa/Arabic/Pages/default.aspx.

[4] M. ElGawady and P. Lestuzzi, "A review of conventional seismic retrofitting techniques for URM," in 13th International Brick and Block masonry conference, pp. 1–10, 2004.

[5] M. ElGawady, P. Lestuzzi, and M. Badoux, "A review of retrofitting of unreinforced masonry walls using composites," Proc., 4th Int. conference on advanced composite materials in bridges and structures., pp. 1–8, 2004.

[6] M. Tomaževič, I. Klemenc, and P. Weiss, "Seismic upgrading of old masonry buildings by seismic isolation and CFRP laminates: A shaking-table study of reduced scale models," in Bulletin of Earthquake Engineering, vol. 7, pp. 293–321, 2009.

[7] H. Santa-Maria, G. Duarte, and A. Garib, "Experimental Investigation of Masonry Panels Externally Strengthened With CFRP Laminates and Fabric Subjected To in-Plane Shear Load," in 13 th World Conference on Earthquake Engineering, no. 1627, 2004.

[8] M. Saatcioglu, F. Serrato, and S. Foo, "Seismic Performance of Masonry Infill Walls Retrofitted With CFRP Sheets," ACI Spec. Publ., vol. Vol. 1, no. No. 230, pp. 341–354, 2005.

[9] N. G. Shrive, "The use of fibre reinforced polymers to improve seismic resistance of masonry," in Construction and Building Materials, vol. 20, pp. 269–277, 2006.

[10] M. ElGawady, P. Lestuzzi, and M. Badoux, "Aseismic retrofitting of unreinforced masonry walls using FRP," Compos. Part B Eng., vol. 37, pp. 148–162, 2005.

[11] J. Gergely, J. Vandergrift, and D. Young, "CFRP Retrofit of Masonry Walls," no. 1998, pp. 1–8, 1999.

[12] A. Mosallam and S. Banerjee, “Enhancement in in-plane shear capacity of unreinforced masonry (URM) walls strengthened with fiber reinforced polymer composites,” Compos. Part B Eng., vol. 42, pp. 1657–1670, 2011.

[13] T. Triantafillou, and C. Antonopoulos, “Design of concrete flexural members strengthened in shear with FRP,” J. Compos. Constr., vol. 4, no. November, pp. 198–205, 2000.

[14] S. Chuang, Y. Zhuge, T. Wong, and L. Peters, “Seismic retrofitting of unreinforced masonry walls by FRP strips,” in Pacific conference on Earthquake Engineering, pp. 1–8, 2003.

[15] T. Zhao, J. Xie, and H. Li, “Strengthening of cracked concrete block masonry walls using continuous carbon fiber sheet,” in 9th North American masonry conference, pp. 156–67, 2003.

[16] G. Vasconcelos and P. B. Lourenço, “In-Plane Experimental Behavior of Stone Masonry Walls under Cyclic Loading,” J. Struct. Eng., vol. 135, no. October, pp. 1269–1277, 2009.

[17] G. Marcari, G. Manfredi, A. Prota, and M. Pecce, “In-plane shear performance of masonry panels strengthened with FRP,” Composites Part B: Engineering 38.7: 887-901 2007.

[18] C. Demir, “Seismic Behavior of Historical Stone Masonry Multi-Leaf Walls,” PhD Dissertation. Turkey: Istanbul Technical University (ITU), 2012.

[19] B. Al-Gohi, “An Experimental and Numerical Study of Retrofitted Masonry Walls under Cyclic Loading,” PhD Dissertation. Dhahran, Saudi Arabia: King Fahd University of Petroleum & Minerals (KFUPM), 2013.

[20] P. Gerardin, M., Negro, “The European Laboratory for Structural Assessment (ELSA) and its Role for the Validation of European Seismic Codes,” in Proceedings of EuroConference on Global Change and Catastrophe Risk Management: Earthquake Risks in Europe, 2000.

[21] G. Vasconcelos, “Experimental Investigations on the Mechanics of Stone Masonry: Characterization of Granites and Behaviour of Ancient Masonry Shear Walls”, PhD dissertation. Portugal: University of Minho; 2005.

[22] G. Edgell, and B. Haseltine, “Building mortar for low rise housing: Recommendations, problems and solutions,” *British Masonry Society*, 2005.

[23] B. Al-Gohi, C. Demir, A. Ilki, M. Baluch, and M. Rahman, "Assessing Seismic Vulnerability of Unreinforced Masonry Walls Using Elasto-Plastic Damage

Model." Seismic Evaluation and Rehabilitation of Structures. Springer International Publishing, 95-114, 2014.

[24] J. Lubliner, J. Oliver, S. Oller, and E. Onate, "A plastic-damage model for concrete." International Journal of solids and structures 25.3: 299-326, 1989.

[25] J. Lee, and G. Fenves, "Plastic-damage model for cyclic loading of concrete structures." Journal of engineering mechanics, 124(8), 892-900, 1998.

[26] ABAQUS (Version 6.13-1) [FEA software]. Vélizy-Villacoublay, France, SIMULIA - Dassault Systèmes.

[27] Sikadur®, Saudi Arabia, Product Data Sheet.

Vitae

Name	Amr Abubaker Mohammed Barahim
Nationality	Yemeni
Date of Birth	2/21/1986
Email	barahim123@gmail.com – g201102410@kfupm.edu.sa
Address	Al-wahda neighborhood-Dar saad – Aden –Yemen
Academic Background	M.S in Civil Engineering, King Fahd University of Petroleum and Minerals (KFUPM), Dhahran, Saudi Arabia B.S in Civil Engineering, University of Aden, Aden,Yemen